NRL Memorandum Report 5521

Turbulent Wake of a Submerged Flat Plate

A. L. COOPER

Fluid Dynamics Branch
Marine Technology Division

April 11, 1985

NAVAL RESEARCH LABORATORY
Washington, D.C.

SECURITY CLASSIFICATION OF THIS PAGE

REPORT DOCUMENTATION PAGE

1a. REPORT SECURITY CLASSIFICATION UNCLASSIFIED	1b. RESTRICTIVE MARKINGS
2a. SECURITY CLASSIFICATION AUTHORITY	3. DISTRIBUTION / AVAILABILITY OF REPORT Approved for public release; distribution unlimited.
2b. DECLASSIFICATION / DOWNGRADING SCHEDULE	
4. PERFORMING ORGANIZATION REPORT NUMBER(S) NRL Memorandum Report 5521	5. MONITORING ORGANIZATION REPORT NUMBER(S)
6a. NAME OF PERFORMING ORGANIZATION Naval Research Laboratory 6b. OFFICE SYMBOL (If applicable) Code 5841	7a. NAME OF MONITORING ORGANIZATION Office of Naval Research
6c. ADDRESS (City, State, and ZIP Code) Washington, DC 20375-5000	7b. ADDRESS (City, State, and ZIP Code) Arlington, VA 22217
8a. NAME OF FUNDING / SPONSORING ORGANIZATION Office of Naval Research 8b. OFFICE SYMBOL (If applicable)	9. PROCUREMENT INSTRUMENT IDENTIFICATION NUMBER
8c. ADDRESS (City, State, and ZIP Code) Arlington, VA 22217	10. SOURCE OF FUNDING NUMBERS PROGRAM ELEMENT NO. 61153N; PROJECT NO.; TASK NO. RR023 01-41; WORK UNIT ACCESSION NO. DN280-006
11. TITLE (Include Security Classification) Turbulent Wake of a Submerged Flat Plate	
12. PERSONAL AUTHOR(S) Cooper, A.L.	
13a. TYPE OF REPORT Interim 13b. TIME COVERED FROM 11/81 TO 11/84	14. DATE OF REPORT (Year, Month, Day) 1985 April 11 15. PAGE COUNT 98
16. SUPPLEMENTARY NOTATION	

17 COSATI CODES			18. SUBJECT TERMS (Continue on reverse if necessary and identify by block number)
FIELD	GROUP	SUB-GROUP	x Turbulence modeling; Wake; Free surface; k-ϵ model (Continues)

19. ABSTRACT (Continue on reverse if necessary and identify by block number)

The turbulent wake of a two-dimensional, submerged flat plate is calculated by means of a parabolic, two-equation, k-ϵ model. The general turbulence model considered involves standard k and ϵ equations and possesses the capability for free-surface proximity effect terms through an algebraic stress model for the Reynolds stress equation. This type of model along with an enhanced Dirichlet type boundary condition for the dissipation at the free surface has been successful in applications to open channel flow but is found to be unsatisfactory for the submerged wake application. Both the proximity terms and the enhanced dissipation boundary condition lead to reduced wake drag when compared with recent experiments. A standard k-ϵ eddy viscosity model with adjusted model parameters and symmetric boundary conditions at the free-surface best describes the wake application. Model parameter sets for application to deep and shallow submerged wakes are optimized by comparing the predictions with the recent experiments of Swean and Keramidas. A parameter set with enhanced ϵ diffusivity and retarded k diffusivity seems to provide best agreement with the (Continues)

20. DISTRIBUTION / AVAILABILITY OF ABSTRACT ☒ UNCLASSIFIED/UNLIMITED ☐ SAME AS RPT ☐ DTIC USERS	21. ABSTRACT SECURITY CLASSIFICATION UNCLASSIFIED
22a. NAME OF RESPONSIBLE INDIVIDUAL A. L. Cooper	22b. TELEPHONE (Include Area Code) (202) 767-2904 22c. OFFICE SYMBOL Code 5841

DD FORM 1473, 84 MAR 83 APR edition may be used until exhausted.
All other editions are obsolete.

SECURITY CLASSIFICATION OF THIS PAGE

18. SUBJECT TERMS (Continued)

Eddy viscosity
Free surface boundary conditions
Algebraic stress model
Fluid mechanics

19. ABSTRACT (Continued)

experimental profiles. The systematic wake drift toward the free-surface which has been observed experimentally is not predicted although excellent agreement is obtained when the predicted profiles are shifted in accordance with the experimental drift observations.

CONTENTS

TURBULENT WAKE OF A SUBMERGED FLAT PLATE

I. INTRODUCTION

In order to characterize turbulence in a dynamic situation at least two local scales are necessary, a turbulence length scale and a turbulence velocity scale. This, of course, does not uniquely define the turbulent state but will provide sufficient detail to characterize the flow field averages: average velocity, momentum flux, etc. For practical calculations one is often satisfied with a description of the average motion. This is especially true when we consider the impracticality of determining the instantaneous fields which would result from direct simulation of the Navier-Stokes equations for flow fields which are non-trivial. For problems which involve the evolution of a momentum wake in the vicinity of a free surface, the computational domain is extensive and we are therefore required by necessity to formulate the problem in such a way as to make any numerical approach practical. That is to say, we hopefully seek a formulation which is "parabolic" so that each point in the domain need be calculated only once and the "solution" can be generated by a marching procedure through the computational domain. We would like to eliminate any extensive iteration.

The recent work of Skop (1), which is based upon a matched asymptotic analysis of the Navier-Stokes equations at large Reynolds number, provides

Manuscript approved December 9, 1984.

us with a conceptual framework in which to imbed our formulation. This work has established the parabolic nature of the momentum wake as the inner solution to the problem which is matched to the well known outer solution providing the Kelvin wake. In consistency with this we seek a turbulence model which is also parabolic and which can be conveniently joined to the parabolic averaged momentum equation to define the unknown Reynolds stresses.

While there is no guarantee that a more detailed turbulence model will provide a better description than a simpler one, we begin with the assumption that at least a two equation turbulence model is required for this application. This is based on the fact that we need to describe at least the local turbulence velocity and local turbulence length scale as indicated earlier. The choice of a turbulence model is dictated by a number of factors including ease and cost of implementation as well as scientific issues involving the physics and accuracy. The latter issues are difficult to assess because turbulence is so ill understood. One can hope to shed light on that question only after numerical predictions are compared with experiment and often only for the specific applications where this is done.

Turbulence modeling is plagued by the truncation problem. The effects of turbulence upon an average flow field is at the most fundamental level due to the interaction of the Reynolds stresses, $-\rho\overline{u_i u_j}$ (second-order correlation) in the averaged momentum equation. The evolution equation for the Reynolds stress involves third order correlations such as $\overline{u_i u_j u_k}$ and other unknown correlations like $\overline{pu_{i,j}}$ (pressure-strain correlation). Due to the existence of the nonlinear inertial term in the Navier-Stokes equations, evolution equations for correlations at each order always involve higher

order correlations. This approach is therefore non-convergent as the number of unknown correlations always exceeds the number of evolution equations. This divergent procedure must be truncated at some level otherwise the system becomes hopelessly complicated without any guarantee of improved accuracy or an ability to generate solutions. The customary procedure is to truncate the system at some order and to model the higher order correlations in terms of lower moments.

Conventional eddy viscosity formulations fall into this class. Here, the unknown Reynolds stresses in the Navier-Stokes equations are assumed to be proportional to the mean strain rate with the eddy viscosity the proportionality factor. The turbulent flow is thereby modeled as an equivalent laminar flow. The eddy viscosity represents an enhanced viscosity to simulate the stronger turbulent diffusion processes. The eddy viscosity so defined is either selected to be some representative constant or to vary throughout the flow field according to flow field geometry and/or the dynamics of the turbulence as determined from some modeled turbulence evolution equations. One approach which has seen wide application is the two-equation k-ε model where evolution equations for k, the turbulence kinetic energy, and ε, the turbulence dissipation are solved along with the mean momentum equation. The eddy viscosity is then taken as some function of k and ε. The most common form is

$$\nu_t = C_\mu \frac{k^2}{\varepsilon}, \tag{1.1}$$

where ν_t is the turbulent eddy viscosity and C_μ is a constant typically taken equal to 0.09. With k and ε determined throughout the flow

field, ν_t is generated by means of the distribution of the average turbulence quantities k and ε which are hopefully in balance with the dynamical situation in question.

The earliest applications for eddy viscosity were ad hoc with the existence of an eddy viscosity assumed as an ansatz and values of ν_t prescribed. More formal justifications for an eddy viscosity and the prescription given above as in equation (1.1) will be established later in this paper. An additional complexity exists in the present application, where a free surface forms one boundary of the computational domain. It is therefore necessary not only to adequately characterize the turbulence in the bulk flow but also to characterize the turbulent interaction with the free surface. We must recognize the possibiity that it may be necessary to model the turbulence somewhat differently in the vicinity of the free surface boundary. We expect, however, that at remote locations relative to the free surface "standard" turbulence modeling will prevail. The free surface interaction will require free-surface boundary conditions for all computed turbulence quantities and, possibly, proximity effects. That is, there could exist a surface layer where the model or the model coefficients are modified from those in the bulk flow.

Very little work is available on the problem of turbulent flow interaction with free surfaces. That work which is available seems to be concentrated in the chemical engineering community where the emphasis is on mass transfer through interfaces, i.e. surface renewal (2), (3). Here we find a number of visual experiments which provide some insight into the interaction of turbulent eddies with a free surface and accompanying analyses which support the conjecture of the existence of an interaction layer.

Recently Komori et al (5) have made some detailed measurements of the normal components of the Reynolds stress in the immediate proximity of a free surface. These results are more detailed and somewhat contrast earlier experiments (4) as interpreted by Naot and Rodi (6). Current evidence indicates that in the vicinity of a free surface the normal fluctuations are damped while the lateral fluctuations are enhanced. The enhancement of lateral fluctuations is consistent with conservation of turbulent kinetic energy at the interface. Naot and Rodi (6) and Hossain (7) have introduced modifications for the k-ϵ turbulence model by means of an algebraic stress model for the Reynolds stress with free surface proximity effects similar to those developed by Shir (8) for wall proximity and a free surface boundary condition for the dissipation, ϵ. A similar model was used by Celik et al (9). These models have been successfully applied to open channel flow. Comparison of predictions and experiments for open channel flow has been good. In particular the expected behavior of the effective eddy viscosity near the free surface (14) is simulated well. Application to open channels with side walls correctly simulates the secondary motions observed experimentally and predicts the observed submergence of the maximum velocity point below the free surface (10).

While open channel flows differ considerably from the present application of turbulent momentum wakes, these are to the writer's knowledge the only applications of turbulence modeling involving free surface effects. Based on the relative success of these former applications, in this note we will develop this particular model to assess its applicability to the wake decay problem in the vicinity of a free surface. While other turbulence models may have also had wide application and comparison with

experiment for different applications, the inclusion of free surface effects seems to be confined to Naot and Rodi (6), Hossain (7) and Celik et al (9), all utilizing similar k-ε turbulence models with an algebraic stress model to simulate free surface proximity effects.

Although differences exist throughout the literature, turbulence models are usually classified in terms of the number of differential equations which are utilized to describe the turbulence quantitites. An extensive review of turbulence modeling has been provided by Rodi (14). From what has been discussed earlier in this paper we consider that the minimum level of description for an arbitrary flow to require at least two equations. This is because of the need to describe the variation of a turbulence velocity scale and a turbulence length scale. It should be emphasized here however that the particular two equations need not characterize the turbulence velocity and length scales directly. Any two turbulence quantities which can define the local velocity and length scales will do equally as well (14). For example, the k-ε set provides such a situation where the velocity scale $\tilde{u} \sim (\frac{2k}{3})^{1/2}$ and the turbulence length scale $\ell \sim k^{3/2}/\varepsilon$. Recognizing this together with the fact that the effective diffusivity for momentum, etc. scales as (11)

$$\nu_t \sim \tilde{u}\,\ell$$

we recover the well known scaling mentioned earlier, i.e.

$$\nu_t \sim k^2/\varepsilon.$$

Historically, zero- and one-equation models have been applied extensively in the literature. For example, constant eddy viscosity models are considered to be zero-equation models. In these models, a constant value for the eddy viscosity is guessed or selected by a consideration of

the overall application and this eddy viscosity is used throughout the flow field to relate the unknown Reynolds stresses to the mean velocity gradients. The "turbulent" momentum equation is solved in a fashion similar to a laminar flow field with the constant eddy viscosity used throughout to characterize the turbulence. These zero-equation formulations can be expected to have difficulties in situations where large gradients exist. For those applications it is clear that average turbulent quantities cannot accurately describe the local turbulence values. Improvement is to be expected by the use of a one-equation description where either the velocity scale or length scale variation is determined through a differential equation. For applications where both scales vary, both variations are necessary to provide the required interaction with the mean flow field and we can anticipate problems with one equation models there also.

For two-equation models, such as the k-ϵ model, there are two classes of approach. In the earliest applications, the local values of k and ϵ were utilized to define the value of the local eddy viscosity by means of an assumed equation of the form (equation (1.1))

$$\nu_t = C_\mu \, k^2/\epsilon .$$

Then this eddy viscosity was used to relate the Reynolds stresses to the local mean strain rate. This then provides a means of characterizing a local eddy viscosity. However, it has been established that many turbulent flows are too complex to be described by a simple eddy viscosity concept, in particular flows where the turbulence itself is the most important mechanism or where several dynamical effects act simultaneously (12), e.g. shear and buoyancy and possibly for our application where free surface proximity exists. To circumvent these shortcomings, more recent models have included

the evolution equation for the Reynolds stress. This equation, of course, contains many terms and usually results in a model which is of higher order than a two-equation model. However, the inclusion of the Reynolds stress evolution equation provides for the first time a Reynolds stress relaxation time scale which competes with the hydrodynamic time scale of the mean motion (13).

The question of local equilibrium takes on a more meaningful interpretation and further provides some level of detail into such questions as isotropy. In terms of turbulence-free surface interaction effects, while various experimenters may differ in their detailed measurements, there appears to be a consensus of opinion supporting the fact that the interaction produces an anisotropic distribution of turbulent normal stresses (4) (5). In particular those normal to the free surface are damped. The relative enhancement of both transverse components is not as universally accepted.

For the particular application which we are stressing here it would appear that some consequences of the Reynolds stress evolution equation may arise. We do recognize that full inclusion of this equation will vastly increase the computational requirements and will additionally require models for the higher-order turbulence correlations which appear in this equation. In order to take advantage of the former benefit and not be penalized by the latter disadvantage we will adopt an approximate form of the equation which provides an algebraic stress model. Therefore no formidable additional computational requirements will result and yet we will be able to include the additional physics associated with a free surface

interaction, i.e. the anisotropic form of the turbulence normal stresses in the vicinity of the free surface. The model then remains a two-equation model.

It seems, therefore, that to successfully model the problem of turbulent flow in the vicinity of a free surface we must consider several factors. These are the state of the art in turbulence modeling, the physics of free surface-turbulence interactions, the necessity of maintaining control over the required computational times and the advantages of employing a well-established turbulence model. Then we are led in a straightforward manner to select a two-equation k-ϵ turbulence model with an algebraic stress model. This is the particular type of formulation that has been almost exclusively applied to model free surface effects in open channel flow. Its applicability to the submerged wake problem will be addressed below.

II. DEVELOPMENT OF THE EQUATIONS

In this section we will define the concept of Reynolds averaging and then develop from the Navier Stokes equations the exact averaged equations which it provides. These equations also provide a starting point for the generation of the turbulence model equations. To simplify our discussion we will restrict our consideration to incompressible flow. This assumption is certainly consistent with our application. For this case the Navier-Stokes equations are written as

$$\frac{\partial U_i}{\partial t} + U_j \frac{\partial U_i}{\partial x_j} = - \frac{1}{\rho} \frac{\partial P}{\partial x_i} + \nu \frac{\partial^2 U_i}{\partial x_j \partial x_j} . \qquad (2.1)$$

The continuity equation

$$\frac{\partial U_i}{\partial x_i} = 0 \tag{2.2}$$

completes the equation set. Here U_i represents the instantaneous velocity component in the x_i direction, P the instantaneous static pressure, and ν the kinematic viscosity. For a turbulent flow application, these equations cannot be solved exactly for a practical flow situation. In order to proceed, a statistical approach is employed. Toward this end, the following definitions are adopted. All dependent variables are separated into mean and fluctuating components. This was originally suggested by Osborne Reynolds many years ago and the technique to be described below is well known as Reynolds averaging. We therefore take

$$\begin{aligned} U_i &= \overline{U}_i + u_i \\ P &= \overline{P} + p \end{aligned} \tag{2.3}$$

where the mean quantities $\overline{U}_i$ and $\overline{P}$ are defined by the following time averages

$$\overline{U}_i \equiv \frac{1}{t_2 - t_1} \int_{t_1}^{t_2} U_i \, dt \tag{2.4}$$

$$\overline{P} \equiv \frac{1}{t_2 - t_1} \int_{t_1}^{t_2} P \, dt$$

It is important to note here that the averaging time interval $t_2 - t_1$ has to be long compared with the time scale of the turbulent fluctuations and small

compared with the hydrodynamic time or time scale of the mean motion variations. When this procedure of Reynolds averaging is applied to the continuity and Navier-Stokes equations we obtain the Reynolds-averaged forms

$$\frac{\partial \bar{U}_i}{\partial t} + \bar{U}_j \frac{\partial \bar{U}_i}{\partial x_j} = -\frac{1}{\rho}\frac{\partial \bar{P}}{\partial x_j} + \frac{\partial}{\partial x_j}\left(\nu \frac{\partial \bar{U}_i}{\partial x_j} - \overline{u_i u_j}\right) \tag{2.5a}$$

$$\frac{\partial \bar{U}_i}{\partial x_i} = 0 \tag{2.5b}$$

Equation (2.5b) also implies $\frac{\partial u_i}{\partial x_i} = 0$. Note the appearance of the second-order correlation of the fluctuating velocity field $-\rho\ \overline{u_i u_j}$ in the momentum equation. This term characterizes the turbulent transport of momentum and is called the Reynolds stress. It is in fact the appearance of this unknown term which renders the equation set above unsolvable since the number of unknowns exceeds the number of equations. To generate solutions for the above equations, this term must be modeled or expressed in terms of the other variables in the equation. However, we can generate an exact equation for the second order correlation by means of the following procedure. If we subtract the time-averaged momentum equations from the full time-dependent Navier-Stokes equation an equation for the x_i component of the fluctuating momentum results. If this equation is multiplied by the fluctuating velocity u_j and added to the equation resulting from the same procedure with i and j reversed, and the equation is time averaged, we obtain the following equation describing the evolution of $\overline{u_i u_j}$ (27)

$$\frac{\partial \overline{u_i u_j}}{\partial t} + \bar{U}_k \frac{\partial \overline{u_i u_j}}{\partial x_k} = -\frac{\partial}{\partial x_k}\left(\overline{u_k u_i u_j}\right)$$

$$-\frac{1}{\rho}\left(\frac{\partial \overline{u_j p}}{\partial x_i} + \frac{\partial \overline{u_i p}}{\partial x_j}\right) - \overline{u_i u_k}\frac{\partial \bar{U}_j}{\partial x_k} - \overline{u_j u_k}\frac{\partial \bar{U}_i}{\partial x_k}$$

$$+\overline{\frac{p}{\rho}\left(\frac{\partial u_i}{\partial x_j} + \frac{\partial u_j}{\partial x_i}\right)} - 2\nu\,\overline{\frac{\partial u_i}{\partial x_k}\frac{\partial u_j}{\partial x_k}} + \nu\frac{\partial^2 \overline{u_i u_j}}{\partial x_k \partial x_k} \tag{2.6}$$

We note the appearance in this equation of the third-order correlation $\overline{u_i u_j u_k}$ and additional terms which involve the correlation of pressure and velocity fluctuations. For high Reynolds number applications, the last term of the $\overline{u_i u_j}$ equation is usually neglected and henceforth in this development it will be omitted. In short, our ability to characterize the $\overline{u_i u_j}$ equation has not really improved the situation, other unknown correlations have been introduced which have to be characterized before a problem solution can be generated.

It is the task of turbulence modeling to provide a tractable algorithm from this situation. The basic ingredients of turbulence are contained in Equation (2.6). It remains to provide additional information which includes the relevant physics of the particular application in sufficient detail to provide a legitimate and solveable approximation. Turbulence modeling therefore involves the art of approximation while, of course, balancing the real factors of computational time and cost. It is the writer's opinion,

shared by many others, that a "universal" turbulence model does not yet exist. Each application provides for its own optimum model reflecting the economics of the situation as well as the basic physical complications.

The reader should note that upon contraction, the $\overline{u_i u_j}$ equation becomes an equation for the turbulence kinetic energy k, where

$$k \equiv \frac{1}{2} \overline{u_i u_i}$$

Therefore the turbulent kinetic energy equation is obtained as

$$\frac{\partial k}{\partial t} + \bar{U}_k \frac{\partial k}{\partial x_k} = -\overline{u_i u_k} \frac{\partial \bar{U}_i}{\partial x_k} - \frac{\partial}{\partial x_k} \left(\frac{p}{\rho} + \frac{\overline{u_i u_i}}{2} \right) u_k$$

$$- \nu \overline{\frac{\partial u_i}{\partial x_k} \left(\frac{\partial u_i}{\partial x_k} \right)} \qquad (2.7)$$

This k equation or a variation thereof is almost universally used by turbulence modelers as the required evolution equation for the turbulence velocity scale discussed earlier. To complete the most fundamental two-equation description we need additionally an evolution equation for the turbulent length scale. While some variability exists, most models employ an equation for the turbulent energy dissipation, ε (the last term in equation (2.7)) to provide this local information. This represents a legitimate variable since the scaling suggests $\varepsilon \sim k^{3/2}/\ell$. Therefore a combination of k-ε variables enables one to determine the local turbulent

velocity scale, $k^{1/2}$ and the local turbulent length scale $k^{3/2}/\varepsilon$. Furthermore, experience has shown that the use of an ε equation simplifies some of the modeling problems and also simplifies the considerations near walls (15).

An equation must therefore be developed for the dissipation, ε. It is possible to derive an exact equation from the Navier-Stokes equations for the fluctuating vorticity and thereby an equation for ε. However, this equation contains many additional complex correlations whose behavior would require drastic modeling assumptions to be of any use. Therefore the model equation for ε is usually provided somewhat hueristically rather than being derived from first principles.

The modeled form of the ε equation is given as (14)

$$\frac{\partial \varepsilon}{\partial t} + \bar{U}_i \frac{\partial \varepsilon}{\partial x_i} = \frac{\partial}{\partial x_i}\left(\frac{\nu_t}{\sigma_\varepsilon} \frac{\partial \varepsilon}{\partial x_i}\right) + C_{1\varepsilon} \frac{\varepsilon}{k} P - C_{2\varepsilon} \frac{\varepsilon^2}{k}. \tag{2.8}$$

Additionally the modeled form of the k equation is presented as

$$\frac{\partial k}{\partial t} + \bar{U}_i \frac{\partial k}{\partial x_i} = \frac{\partial}{\partial x_i}\left(\frac{\nu_t}{\sigma_k} \frac{\partial k}{\partial x_i}\right) + \nu_t\left(\frac{\partial \bar{U}_i}{\partial x_j} + \frac{\partial \bar{U}_j}{\partial x_i}\right) \frac{\partial \bar{U}_i}{\partial x_j} - \varepsilon \tag{2.9}$$

with $\nu_t = C_\mu \frac{k^2}{\varepsilon}$, $P \equiv -\overline{u_i u_j} \frac{\partial \bar{U}_i}{\partial x_j} = \nu_t \left(\frac{\partial \bar{U}_i}{\partial x_j} + \frac{\partial \bar{U}_j}{\partial x_i} \right) \frac{\partial \bar{U}_i}{\partial x_j}$ and $\varepsilon \equiv \nu \frac{\partial u_i}{\partial x_j} \frac{\partial u_i}{\partial x_j}$.

This k-ε equation set is seen to possess five constants whose specification becomes part of the model. These five constants are C_μ, $C_{1\varepsilon}$, $C_{2\varepsilon}$, σ_ε and σ_k. We note that although an eddy viscosity type formulation has been specified to model the diffusion terms in the k-ε model equations, the specification of the Reynolds stress terms in the momentum equation (2.5) has not yet been made or tied to an eddy viscosity. Many k-ε eddy viscosity models do, in fact, employ the k and ε models given above and utilize ν_t given above as an eddy viscosity to define the Reynolds stresses. This is the standard k-ε model. The characterization of the Reynolds stresses will in general arise from a consideration of the $\overline{u_i u_j}$ equation given above. Additional model constants may be introduced at this stage and, most importantly, additional physics may be introduced as well. It is at this level where we will introduce the experimentally-observed phenomena of the anistropic turbulence Reynolds stresses in the vicinity of the free surface.

There have been various attempts recorded in the literature to model the Reynolds stress equation and include it in a turbulence model. However, it should be emphasized once again that the inclusion of this equation within a turbulence model greatly complicates the situation and would clearly provide the need for more extensive computation times in an application where the computational domain is already extensive. Experience has shown that higher order modeling techniques do not always represent an improvement over those of lower order. Our consideration of the Reynolds stress equation has been dictated by our desire to incorporate the turbulence-free surface interaction, i.e., the establishment of a free

surface proximity effect and/or the establishment of the necessary free surface boundary condition required. If we could extract this information from the equation without including the full differential equation as part of our computational load, the situation would be ideal.

Just such a compromise could be provided by an algebraic stress model for the Reynolds stress equation. This approach has been applied, in fact, to open channel flow in a number of investigations, e.g. Hossain (7), Naot and Rodi (6) and Celik et al (9).

In Appendix A we discuss the problems of modeling the Reynolds stress equation. Appendix B develops the required algebraic stress equations for the Reynolds stress components including free surface proximity effects.

For the problem under consideration here, the two-dimensional submerged flat plate wake, there is only one important turbulent shear stress component, $\overline{uv}$. This component is approximated by equation (B 21) including free surface proximity effects

$$\overline{uv} = - C_\mu \frac{k^2}{\varepsilon} \frac{1}{\left(1+2\left(\frac{C_1'}{C_1}\right)f\right)\left(1+\frac{3}{2}\left(\frac{C_1'}{C_1}\right)f\right)} \frac{\partial u}{\partial y} \tag{2.10}$$

where f, the free surface proximity term, is given from equation (B.10)

$$f = \frac{1}{\left(\frac{y}{\ell} + C_f\right)^n}, \quad n = 1 \text{ or } 2 \tag{2.11}$$

and ℓ is a local dissipation length scale of the turbulent motion. The geometry is illustrated in Figure 1.

This is seen to represent an eddy viscosity formulation for the turbulent shear stress $-\overline{uv}$ with the effective eddy viscosity a function of distance from the free surface y through the proximity term f. For $f \to 0$, at remote locations from the free surface, we recover the standard eddy viscosity

$$\nu_t \to C_\mu \frac{k^2}{\varepsilon}$$

while as we aproach the free surface $y \to 0$ the effective eddy viscosity is reduced. This is consistant with open channel flow measurements (4). For fixed n (linear or quadratic), the inclusion of free surface proximity effects through an algebraic stress model (Appendix B) is seen to introduce two additional parameters $\left(C_1'/C_1\right)$ and C_f. The decay of the eddy viscosity near the free surface predicted by equation (2.10) seems to be a consequence of modeling the anisotropic normal stress behavior through a Shir (8) type wall proximity function.

The complete turbulence model description is seen to include the k and ε model equations (2.8) and (2.9) with the Reynolds shear stress component given by equation (2.10). These equations are to be solved in conjunction with the mean flow equations (2.5a) and (2.5b). As is typical with high Reynolds number turbulent flow in the absence of walls, the viscous stress can be neglected in equation (2.5a) in comparison with the turbulent stress $\left(-\overline{uv}\right)$.

III. BOUNDARY CONDITIONS

Boundary conditions are necessary for all the dependent variables U, k and ε. These conditions are required at an "initial" plane or upstream boundary and at the lateral boundaries of the domain since the formulation is parabolic and solutions are to be generated by a marching technique. The lateral boundaries are of two types for our application free boundaries and a free surface. At a free boundary, free stream conditions on velocity and turbulence quantities are recovered. Typically this implies that the wake velocity approaches free stream and k and ε vanish. The situation at the free surface is not so clear.

The asymptotic analysis of Skop (1) has provided the proposition that symmetry conditions are to be satisfied by the horizontal velocity at the free surface. We would expect further that the turbulence kinetic energy would also satisfy a symmetry condition here. The experimental evidence (4,5) indicates that at the free surface there occurs a redistribution of the normal stresses $\overline{u^2}$, $\overline{v^2}$, and $\overline{w^2}$, with $\overline{v^2}$ damped by gravity and surface tension and with $\overline{u^2}$ and $\overline{w^2}$ enhanced while preserving the total kinetic energy. This is consistent with a conservative interaction of turbulent eddies with the free surface or a symmetry condition for k.

The boundary condition for ε at the free surface is more complicated. Here we take two alternatives, both of which seem to have some experimental verification. The detailed experiment of Komori et al (5) and their estimated energy budget near the free surface suggest that ε has zero normal gradient near the free surface for open channel flows. This is illustrated in Fig. 2. However the experiments of Ueda et al. (4) indicate that the eddy viscosity is reduced to zero near the free surface. This seems to

require a larger dissipation than that which would result from a symmetry condition for ε and suggests the imposition of an enhanced ε at the free surface. The experiments of Quarmby and Quirk (24) and Hussain and Reynolds (28) for confined flows indicate much higher measured eddy viscosities at the symmetry plane.

Hossain (7), Hossain and Rodi (26), and later Naot and Rodi (16) have suggested that while the dissipation length scale is reduced as we approach a free surface, similar to the behavior near a wall, the effective dissipation length does not go to zero at the free surface but goes instead to some finite limit, ℓ_o. Therefore they propose

$$\varepsilon_s = \frac{k_s^{3/2}}{\ell_o} \tag{3.1}$$

where k_s is the turbulence energy at the surface and ℓ_o is related to the open channel depth D, by

$$\ell_o = 0.07D. \tag{3.2}$$

For application to our far wake problem, we anticipate a similar possibility and suggest that a boundary condition for ε_s be given as

$$\varepsilon_s = \frac{k_s^{3/2}}{Ay_m}, \tag{3.3}$$

where y_m represents the depth of the wake. This is equivalent to defining the effective dissipation length at the free surface as

$$\ell_o = A\, y_m \quad . \tag{3.4}$$

This is in direct analogy with equation (3.2) above for open channels. As a free surface boundary condition for ε, two alternatives are therefore suggested, a symmetry condition for ε or the use of equation (3.3). Both conditions will be utilized in the calculations to be presented in Section IV and their plausibility will be assessed.

IV. NUMERICAL RESULTS AND COMPARISON WITH EXPERIMENT

Above, a k-ε model was developed to describe the behavior of a turbulent wake in the vicinity of a free surface. That model is a variant of the standard k-ε model with the inclusion of an algebraic stress model to describe some of the physics of turbulent eddy-free surface interaction. For two-dimensional flow that model is summarized by standard k and ε transport equations given by (2.8) and (2.9) and an eddy viscosity type formulation for the Reynolds stress component, $\overline{uv}$, given by (2.10). The eddy viscosity defined by (2.10) possesses surface proximity terms f as defined by equation (2.11). Without the surface proximity terms or in the limit as $f \to 0$ we obtain the standard eddy viscosity relation

$$\nu_t = C_\mu \frac{k^2}{\varepsilon} \quad .$$

Additionally two choices are provided for the boundary condition for ε to be applied at the free surface, e.g. symmetry or ε_s as defined from equation (3.3). Symmetry boundary conditions are taken for U and k at the free surface. The model can therefore be viewed as possessing three levels of

complication. At the most fundamental level we have a standard k-ε eddy diffusivity model with symmetry boundary conditions satisfied by all the dependent variables at the free surface. At the second level, a special boundary condition is to be satisfied by ε at the free surface to model the reduction of turbulent length scale there. This boundary condition has previously been successful in modeling open channel flows (2-6). The most complete model has, in addition to the above, a surface proximity effect to model the anisotropic nature of the normal components of the Reynolds stress tensor near the free surface (2-6) as has been observed in a number of experiments. In the numerical results that follow, the parabolic forms of the momentum and k - ε equations have been utilized. This is consistent with the results of Skop (1), for large Reynolds number applications as considered here.

In this section we will attempt to optimize the above model in terms of the proper level and the appropriate free parameters by means of a comparison of the numerical predictions that it provides and the experimental turbulent wake data of Swean and Keramidas (25). They measured the properties of a two-dimensional turbulent wake induced by a flat plate towed beneath the free surface. Measurements were made at several locations downstream of the plate trailing edge. We will concentrate on the first two levels of the model as described above; the standard k-ε model with symmetric boundary conditions and the special boundary condition for ε at the free surface as developed for open channel flows. These two cases will provide insight into the necessary behavior of eddy viscosity in the vicinity of the free surface. Some of the expected consequences of the

surface proximity terms can be determined from the variation of the ε boundary condition as both tend to reduce the near-surface eddy viscosity.

First we discuss the experimental results of Swean and Keramidas. Second we present the results of model parameter variation for the standard k-ε model with full symmetry conditions at the free-surface. Thirdly we will describe the model results associated with the nonsymmetric ε boundary condition. From these results on the ε boundary condition we will then be able to establish the inapplicability of the surface proximity effects for the two-dimensional decaying wake problem.

The two cases above represent an eddy viscosity formulation with ν_t given as

$$\nu_t = C_\mu \frac{k^2}{\varepsilon}$$

For applications to two-dimensional flows, there is only one important Reynolds stress component and it therefore is reasonable to fix C_μ and consider only the variation of the other parameters. In addition to C_μ, the model is seen to contain four free parameters which are σ_ε, σ_k, $C_{1\varepsilon}$ and $C_{2\varepsilon}$. σ_k and σ_ε are recognized as effective turbulent Prandtl numbers governing the diffusion of k and ε respectively. $C_{1\varepsilon}$ and $C_{2\varepsilon}$ are model constants for the dissipation equation, ε. For the purposes of this paper, we will fix C_μ at its universal value of 0.09 and consider only the variation of the other four parameters.

It should be noted at this point that previous applications of this standard k-ε model to an infinite plane wake behind a flat plate by Rodi (14) have provided excellent agreement with the experiments of Chevray

and Kovasznay (30). The comparison is reproduced in Figure 3 to provide some confidence in the standard k-ε model for infinite 2-D wake flow computations. The values for the parameters of Figure 3 are

$$C_\mu = .09,$$
$$\sigma_k = 1.0 ,$$
$$\sigma_\varepsilon = 1.3 ,$$
$$C_{1\varepsilon} = 1.43,$$
$$C_{2\varepsilon} = 1.92.$$

This set of parameters will be referred to as the "reference" values. They have been obtained by an extensive application of the model to a number of types of free turbulent flows. This set of parameters has previously also been successfully applied to many two-dimensional wall boundary layers, duct flows, free shear flows, recirculating flows and to three-dimensional wall boundary layers, confined flows and jets (14).

A. NRL Experiments

In this section we will summarize the experimental results of Swean and Keramidas (25) as these provide our only basis for comparison with model predictions. The plate was 1 m long and the towing speed was .59 ms^{-1} in all cases. Two main experimental cases were investigated for the two-dimensional flat plate wake flow. The first case which is called "finite" corresponds to the translating plate submerged 5 cm below the free surface. Data were collected at four stations downstream of the plate trailing edge. In the second case, the translating plate was 25 cm below

the undisturbed free surface and data were collected at the same four downstream stations of the trailing edge. This case is called the infinite case as the submergence of the plate was sufficiently large so that the wake flow was uninfluenced by the presence of the free surface for the extent of experimental domain considered. These results are therefore expected to be characteristic of an infinite domain two-dimensional flow field.

Figures 4-6 display the experimental profiles obtained by Swean and Keramidas (25) for the infinite case. The variation of mean velocity relative to an observer fixed on the plate, turbulent shear stress and turbulent kinetic energy with depth measured from the undisturbed free surface are displayed at the four stations downstream of the trailing edge. Figures 7-9 display the same variations as measured for the finite case. An obvious difference between the finite and infinite cases is immediately apparent from an examination of these results. The infinite case profiles seem to display a permanent anchor at of the depth of submergence of the plate. That is, the depths of the maximum velocity defect point, zero shear stress point and the central wake minimum of turbulent kinetic energy all appear to be fixed at the original plate submergence depth as we move downstream. Further, these profiles are nearly symmetric about the plate centerline level. This is not the case for the finite experiments. All the experimental results for the finite case display a systematic drift of these above points toward the free surface. That is, in addition to the expected evolution of the profile form, the entire profile appears to migrate toward the free surface. The data at station 1, $x = 5$ cm., already displays a "drift" to within 4.75 cm of the free surface. This type of behavior is indicative of a systematic mean

vertical motion although none was observed experimentally. Except for any local elliptical behavior associated with the free surface proximity or a drastically asymmetric vertical diffusion, this migration is not anticipated until further downstream.

B. Numerical Results

The numerical results to be described have been generated by means of a parabolic Patankar-Spalding (32) code as provided by Rodi (31). This code utilizes a forward marching finite difference procedure. The various turbulence models and boundary conditions described above can be readily included.

In order to gain a direct connection with the experimental data, we utilize as upstream boundary conditions profiles obtained from the actual experimental data at the first experimental station. In this way, we hope to eliminate any consideration of plate free surface interaction upstream and immediately downstream of the trailing edge. We will then be presumably exercising the code in regions where it is most likely to correspond with parabolic behavior. That is, the profiles at $x = 5$ cm have been obtained directly from the measured values at that point. Profiles of mean velocity, turbulence kinetic energy k and dissipation ε are thereby specified at that station. The parabolic Patankar-Spalding code is then utilized to propagate these results downstream in a marching fashion to produce the predicted profiles at the other three experimental stations $x = 23$, 62, 111 cm. This facilitates the comparison of code predictions and experimental observations.

1. Standard model-symmetric boundary conditions.

In this section we will describe the numberical results for the standard k-ε model with full symmetry boundary conditions as applied to the two-dimensional, submerged flat plate problem. We will provide the predictions for the two experimental cases defined above, finite and infinite. In both situations we have found it convenient to vary four of the model parameters in the following way: (1) for fixed values of $C_{1\varepsilon}$ and $C_{2\varepsilon}$ we vary the effective turbulent Prandtl numbers σ_k and σ_ε for the diffusivities of k and ε, (2) for fixed values of σ_ε and σ_k we then vary parameters of the ε equation, $C_{1\varepsilon}$ and $C_{2\varepsilon}$. Lastly, (3), we consider the effects of non-reference values for all four parameters in a few cases. Our main objective here is to gain an appreciation of the sensitivity of the results and structural details of the predicted profiles to the various model parameters so that an optimum parameter set may be selected.

i. Infinite Fluid

The results obtained for the infinite fluid case will now be presented. Figure 10 displays for the reference parameter set the mean velocity as function of distance below the undisturbed free surface for the four x - stations of the experiment. The reader will recall that the x = 5 cm station represents the boundary values derived from experiment which are imposed for the computation. No apparent influence of the free surface on the results is obvious here. As a matter of fact, there is no significant fluid deceleration obvious closer than approximately 18-19 cm below the free-surface or equivalently beyond 6-7 cm above the plate centerline. This is further exemplified in Figure 11 where the velocity profiles are

displayed for the case where the same boundary data were translated to within 7 cm of the free surface. The subsequent velocity profiles are essentially identical. This translated data set was in fact the one utilized by Swean and Keramidas (25) for the computations in their paper. Figures 10 and 11 agree reasonably well with the infinite fluid experiments. This has also been noted by Swean and Keramidas. Therefore we find that the reference parameters do provide a good prediction for the velocity field data in the infinite case.

Anticipating some of the results to be discussed later for the finite fluid case, the parameter set $\sigma_\varepsilon = 2.0$ and $\sigma_k = .75$ with $C_{1\varepsilon}$, $C_{2\varepsilon}$ taken at their reference values will be shown below to provide a good approximation to the finite fluid experimental results. Figure 12 shows the behavior of the velocity field for this parameter set as applied to the infinite fluid boundary data. By means of comparison with the results of the reference parameter set we note that the acceleration of the minimum velocity is only slightly retarded for these parameters while the wake structure spread in the tails of the velocity profiles appears to be enhanced for this case. In the infinite fluid case, the reference parameters appear to describe the experimental measurements more closely. This result will be seen to be at variance with our application to the finite fluid case. This factor will be discussed in more detail later.

The results of applying the same parameter set as in Figure 12 but with the translated boundary data set of Figure 11 is displayed in Figure 13. For these parameters we note there is free surface deceleration (wake drag) obvious at the last x-station, x = 111 cm. The case is not really infinite for this translated boundary data set. Therefore if these parameters were

to be utilized to describe an infinite case, the data set would have to be translated further from the free surface. It is the more rapid spread of the wake tails which is responsible for this situation. This has presumably occurred because of our utilization of an enhanced diffusivity for k and a retarded diffusivity for ε relative to the reference case in our modeling of the diffusion terms in the k and ε equation. This combination is equivalent to an enhanced eddy viscosity ν_t away from the plate centerline.

The reference parameter set seems to do an adequate job in describing the wake decay for the infinite case. This is not surprising when we consider the efforts that have been devoted by many previous investigations to "optimize" this reference set. By definition, the infinite case should not involve any free-surface interaction and hence the reference parameter set which has been obtained from the examination of many flows which do not contain free surfaces should be applicable.

To complete the description for the infinite fluid case, Figures 14-17 display the evolution of the turbulent kinetic energy, k, and the magnitude of the turbulent shear stress for two of the parameter sets; the reference set and the set which is found to be satisfactory for the finite fluid case to be considered next.

ii. Finite Fluid

In this section, we will consider the more interesting simulations of the code; those which have been called finite fluid since the plate submergence is sufficiently small relative to the downstream experimental domain that we expect a significant wake-free surface interaction. As indicated earlier these correspond to the 5 cm submergence case measured by Swean and Keramidas. Once again, the experimental data at the closest

downstream station is utilized to define the upstream boundary values of mean velocity turbulent kinetic energy, k, and dissipation, ε. The boundary conditions at the free surface are taken as symmetry conditions, or vanishing of the normal gradients. The Patankar-Spalding code with k-ε turbulence model is again utilized to numerically propagate the solution to the other downstream experimental stations where a comparison between experimental and numerical predictions can be made.

Figure 18 illustrates the results for the velocity field obtained for the finite boundary data propagated with a turbulence model utilizing the reference parameters. No vertical migration of the maximum velocity defect point is predicted within the downstream domain defined by the experiments. This will be seen to be the result for all parameter sets which will be utilized below. It can be seen by a comparison with Figure 5 that this reference parameter set does not predict the free-surface velocity very well and seems to underestimate the value of maximum velocity defect as compared to experiment at the last station, x = 111 cm.

Figures 19-25 display the resulting velocity field associated with varying σ_ε and σ_k while keeping $C_{1\varepsilon}$ and $C_{2\varepsilon}$ at their reference values. It is interesting to note that over the variation of σ_ε and σ_k considered, the values of the maximum defect velocity are essentially constant. It appears that these parameters preferentially alter the tails of the velocity distributions. With respect to variations of these two parameters the set associated with Figure 19, $\sigma_\varepsilon = 2.0$, $\sigma_k = 0.75$ seems to describe the experimental trends best.

In Figures 26-29, σ_ε and σ_k are returned to their reference values and $C_{1\varepsilon}$ and $C_{2\varepsilon}$ are varied. The results show a very strong sensitivity to

variations in these parameters. The effects of these parameter variations are seen to modify both the maximum velocity defect and free-surface velocity.

Figures 30 and 31 illustrate the evolution of the turbulent kinetic energy, k and shear stress profiles for the reference parameter set. Figure 32 and 33 display the evolution of turbulent kinetic energy and shear stress profiles for the "optimum" finite parameter set. This set seems to model the experiment more closely.

Table I summarizes and compares for all parameter sets considered the behavior of the maximum defect point and free surface velocities associated with the velocity profile evolution. The properties of the experimental profiles are also listed. Parameter set 2 seems to model the experimental profiles best. This is the "optimum" set described above.

2. Standard model - ε boundary condition.

In this section we present the numerical results obtained by the application of the standard k-ε model with symmetry conditions imposed at the free surface for all dependent variables except the dissipation ε. For the boundary condition on ε at the free surface, equation (3.3) is applied for various values of the parameter A. This boundary condition has been applied to both the reference parameter set and the "optimum" set.

Figures 34-43 illustrate the evolution of the velocity profiles, turbulent kinetic energy distribution and turbulent Reynolds stress as a function of the parameter A for each of the two k-ε parameter sets.

The results display for the smaller values of A an enhanced ε near the free surface which tends to reduce k at the free surface and thereby drive

TABLE 1

COMPARISON WITH EXPERIMENT OF THE EVOLUTION OF THE PROPERTIES OF THE VELOCITY PROFILES FOR VARIOUS PARAMETER SETS

CASE	MODEL PARAMETERS $(\sigma_k, \sigma_\varepsilon, C_{1\varepsilon}, C_{2\varepsilon})$	MINIMUM VELOCITY @ (x_2, x_3, x_4)	FREE SURFACE VELOCITY @ (x_2, x_3, x_4)
1	(1.0, 1.287, 1.43, 1.92)	(.67, .78, .832)	(1.00, .996, .972)
2	(.75, 2.00, 1.43, 1.92)	(.67, .774, .83)	(1.00, .986, .96)
3	(1.00, 2.00, 1.43, 1.92)	(.67, .776, .836)	(1.00, .992, .962)
4	(1.00, 1.00, 1.43, 1.92)	(.67, .78, .834)	(1.00, 1.00, .98)
5	(.75, 1.287, 1.43, 1.92)	(.67, .77, .832)	(1.00, .995, .967)
6	(1.287, 1.287, 1.43, 1.92)	(.67, .78, .832)	(1.00, 1.00, .98)
7	(1.00, 1.50, 1.43, 1.92)	(.67, .78, .832)	(1.00, .995, .972)
8	(1.00, 1.75, 1.43, 1.92)	(.67, .778, .834)	(1.00, .993, .964)
9	(1.00, 1.287, 1.43, 1.75)	(.66, .758, .81)	(1.00, .998, .987)
10	(1,00, 1.287, 1.43, 2.25)	(.69, .81, .86)	(1.00, .995, .94)
11	(1.00, 1.287, 1.00, 1.92)	(.70, .83, .88)	(1.00, .976, .922)
12	(1.00, 1.287, 1.75, 1.92)	(.65, .74, .784)	(1.00, 1.00, .993)
Experiment (25)		(.66, .745, .82)	(1.00, .99, .95)

$\nu_t = k^2/\varepsilon$ toward zero. Within the experimental domain this effect appears as a boundary layer concentrated near the free surface which affects the surface velocity without any significant interaction with the maximum defect points. This behavior seems to reduce the predicted deceleration at the free surface. To provide predictions more in agreement with the experiments large values of $A \sim 15$ are needed which actually have the effect of increasing the surface eddy viscosity. This behavior is at variance with that provided by the open channel experiments where best agreement was obtained by reducing the surface eddy viscosity toward zero. The decaying wake seems to require an enhanced eddy viscosity.

It is because of these trends with the ε boundary condition that we did not pursue the results for the free-surface proximity terms $\pi_{ij,s}$ of the algebraic stress model. The effects of including these terms in the eddy viscosity should be similar to those obtained for the smaller values of A since both reduce the eddy viscosity near the free surface.

V. SUMMARY AND CONCLUSIONS

A general two-equation turbulence model has been developed for application to wake studies in the vicinity of free surface. The model includes standard k and ε equations and ability to include surface proximity effects through the use of an algebraic stress model very similar to that previously applied to model open channel flows. The entire problem is cast in a parabolic form which lends itself to a marching procedure in which profiles at any x station may be efficiently propagated downstream.

Numerical results for a turbulent wake induced by a submerged flat plate have been generated and compared with the experiments of Swean and

Keramidas. For pure symmetry boundary conditions for all variables at the free surface, turbulence model parameters have been varied so as to obtain the best overall fit with the experimental data.

The reference parameter set seems to provide a good description of the wake field for the cases of infinite fluid. These are cases where plate submergence is sufficient so that the free surface condition does not interact with the flow field within the finite downstream domain considered. For the finite case, plate submergence sufficiently small so that free surface interaction occurs, the reference parameter set does not adequately describe the wake field. A better description for this finite case is provided by the parameter set

$$C_{\mu} = 0.09,$$
$$\sigma_{\varepsilon} = 2.0,$$
$$\sigma_{k} = 0.75,$$
$$C_{1\varepsilon} = 1.43,$$
$$C_{2\varepsilon} = 1.92.$$

This set differs from the reference set only with respect to the effective Prandtl numbers σ_{ε} and σ_{k} which model the diffusion terms in the k and ε equations. Diffusivity of ε is retarded while diffusivity of k is enhanced relative to the reference set. These changes which are necessary only in the finite case would appear to be associated with free surface proximity effects.

The special boundary condition for ε at the free surface (3.3) which has been found to be desirable for applications to open channel flow was introduced. This enhanced ε boundary condition is necessary to drive the

effective eddy viscosity to zero near the free surface as observations predict for open channel flow. To obtain agreement with the experiments on wake flows this boundary condition has to reduce ε at the free surface in opposition to what is required for open channel flows. This reduced ε at the free surface tends to increase the eddy viscosity at the free surface. Applications of the ε boundary condition which reduce eddy viscosity at the free surface deteriorate the agreement between numerical predictions and experimental velocity profiles.

As a consequence of this behavior for the imposed ε boundary conditions, surface proximity effects within the algebraic stress model were not analyzed any further. Their effect can be shown to be similar to increasing ε at the free surface.

From the results described above, we suggest that a best compromise for a turbulence model for wake decay the vicinity of a free surface to be a standard $k - \varepsilon$ model with a modified parameter set as given above and symmetric boundary conditions for all variables at the free surface. This is in agreement with the proposition of Skop (1). The model does not predict the experimentally observed migration of the wake features toward the free surface within the domain of the experiment for the finite fluid case. More definitive experiments are needed to resolve this behavior. This is particularly important since the predicted velocity profiles with reference parameters provide excellent agreement with the observed profiles if the predictions are shifted vertically in accordance with the measured migration.

VI. REFERENCES

1. R.A. Skop, "The Hydrodynamic Wake of a Surface Ship: Theoretical Foundations", Naval Research Laboratory Report 8833, June 1984. AD-B084 604L

2. V.G. Levich, Physicochemical Hydrodynamics, 2nd ed., Prentice Hall, Englewood Cliffs, N.J., 1962.

3. J.T. Davies, Turbulence Phenomena, Academic Press, New York, 1972.

4. H. Ueda, R. Moller, S. Komori and T. Mizushina", Eddy Diffusivity Near the Free Surface of Open Channel Flow", Int. J. Heat Mass Transfer, Vol. 20, 1127-1136, 1977.

5. S. Komori, H. Ueda, F. Ogino and T. Mizushina, "Turbulence Structure and Transport Mechanism at the Free Surface in an Open Channel Flow", Int. J. Heat Mass Transfer, Vol. 25, 513-521, 1982.

6. D. Naot and W. Rodi, "Calculation of Secondary Currents in Channel Flow", Journal of Hydraulic Division, Proceedings of the ASCE, Vol. 108, No. HY8, 948-968, 1982.

7. M.S. Hossain, "Mathematische Modellierung von turbulenten Auftriebsstromungen", thesis presented to the University of Karlsruhe in 1980 in partial fulfillment of the requirements for the degre of Doctor of Philosophy.

8. C.C. Shir, "A Preliminary Numerical Study of Atmospheric Turbulent Flows in the Idealized Planetary Boundary Layer", Journal of Atmospheric Sciences, Vol. 30, 1327-1339, 1973.

9. I. Celik, M. S. Hossain and W. Rodi, "Modeling of Free-Surface-Proximity Effects on Turbulence", Proceedings of the International Symposium on Refined Modelling of Flows, Paris, Sept. 1982.

10. J. Nikuradse, "Turbulente Stromung in Innern des Nechteckigen Offenen Kanols", Forschungsarbeiten, Heft 281, 36-44, 1926.

11. H. Tennekes and J.L. Lumley, A First Course in Turbulence, M.T.T. Press, Cambridge, 1972.

12. J.L. Lumley, "Turbulence Modeling", J. Appl. Mech., Vol 50, 1097-1103, 1983.

13. C. DuP. Donaldson, "Calculation of Turbulent Shear Flows for Atmospheric and Vortex Motions", AIAA J., Vol. 10, No. 1, 4-12, 1972.

14. W. Rodi, Turbulence Models and their Application in Hydraulics, IAHR, Delft, The Netherlands, 1980.

15. B.E. Launder and D.B. Spalding, "The Numerical Computation of Turbulent Flows", Comp. Methods in Appl. Mech. and Engr., Vol. 3, 269, 1974.

16. D. Naot and W. Rodi, "Interactions of the Turbulent Eddies with Free Surface", MHD-Flow and Turbulence III, edited by H. Branover and A. Yakhot, 1981.

17. J. Rotta, "Statistiche Theorie nichthomogener Turbulenz", Zeitschrift fur Physik, Vol. 129, 547, 1951.

18. B.E. Launder, G.J. Reece and W. Rodi, "Progress in the Development of a Reynolds-Stress Turbulence Closure", J. Fluid Mech., 68, 537-566, 1975.

19. B.J. Daly and F.H. Harlow, "Transport Equations in Turbulence", Phys. of Fluids, Vol. 13, No. 11, 2634, 1970.

20. W. Rodi, "A New Algebraic Relation for Calculating the Reynolds Stesses", Z.AMM, Vol. 56, T219-T221, 1976.

21. W.Rodi, "Examples of Turbulence Models for Incompressible Flows", AIAA Journal, Vol. 20, 872-879, 1982.

22. B.E. Launder, "On the Effects of a Gravitational Field on the Turbulent Transport of Heat and Momentum", J. Fluid Mech., 67, 569-581, 1975.

23. M.M. Gibson and B.E. Launder, "Ground Effect on Pressure Fluctuations in the Atmospheric Boundary Layer", J. Fluid Mech. Vol. 52, 609, 1972.

24. A. Quarmby and R. Quirk,"Measurements of the Radial and Tangential Eddy Diffusivities of Heat and Mass in Turbulent Flow in a Plain Tube", Int. J. of Heat and Mass Transfer, Vol. 15, 2309-2327, 1972.

25. T.F. Swean, Jr. and G.A. Keramidas, "Turbulent Wake of a Flat Plate Near a Free Surface", Proceedings of the Second Int. Conference on Computational Methods and Experimental Measurements, C.A. Brebbia and G.A. Keramidas, June/July, 1984.

26. M.S. Hossain and W. Rodi, "Mathematical Modelling of Vertical Mixing in Stratified Channel Flow", Proceedings, Second Symposium on Stratified Flows, Trondheim, Norway, 1980.

27. J.O. Hinze, Turbulence, 2nd ed., McGraw-Hill Book Co., New York, 1975.

28. A.K.M.F. Hussain and W.C. Reynolds, "Measurements in Fully Developed Turbulent Channel Flow", ASME J. of Fluids Eng., Vol. 97, 568-578, 1975.

29. D. Naot and W. Rodi, "Calculation of Secondary Currents in Channel Flow", Journal of Hydraulic Division, Proceedings of the ASCE, Vol. 108, No. HY8, 948-968, 1982.

30. R. Chevray and L.S.G. Kovasznay, "Turbulence Measurements in the Wake of a Thin Flat Plate", AIAA J., Vol. 7, 1641-1643, 1969.

31. W. Rodi, private communication, 1982.

32. S.V. Patankar and D.B. Spalding, Heat and Mass Transfer in Boundary Layers, Intertext Books, London, 1970.

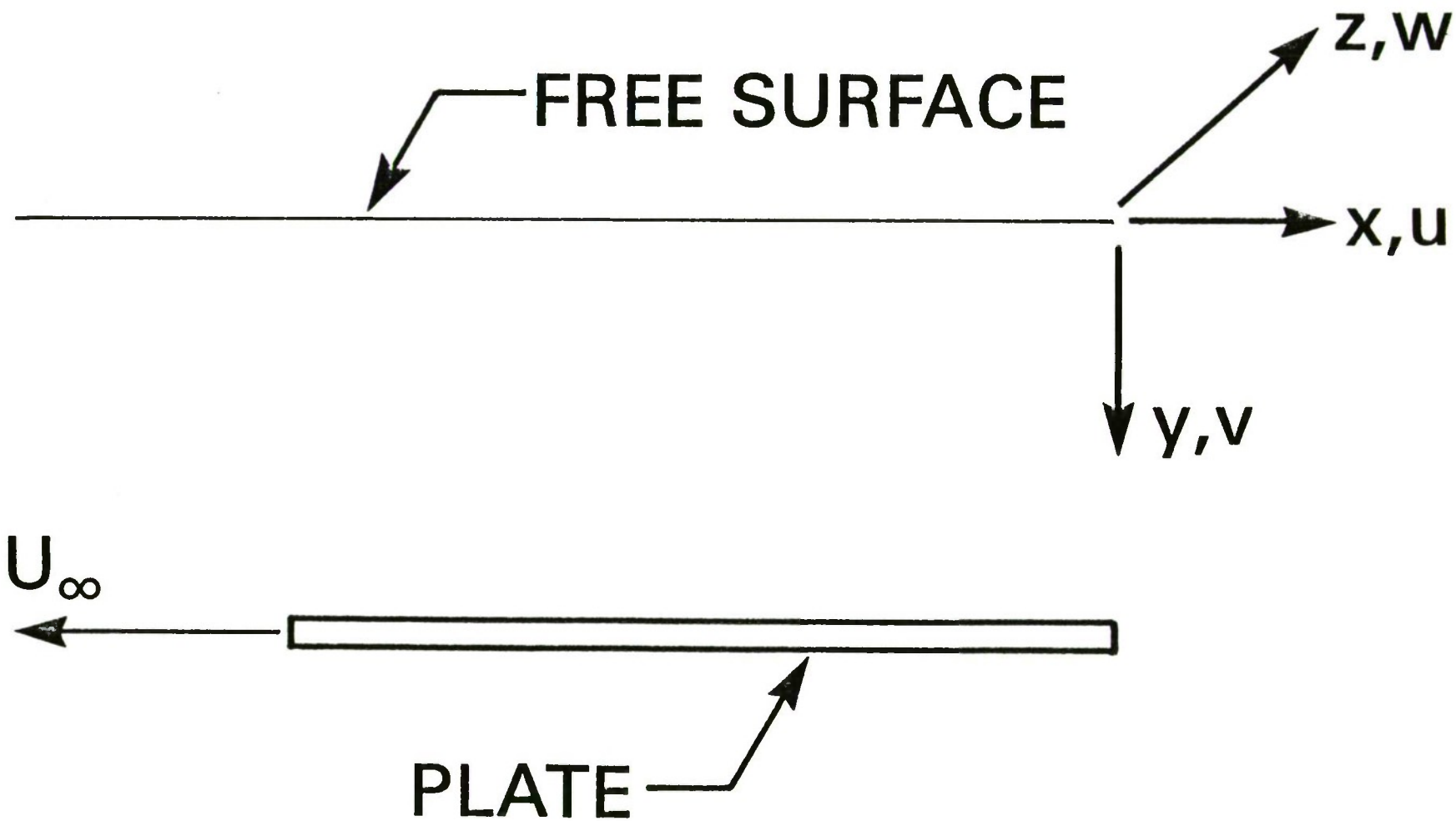

Figure 1 Geometry of the submerged flat plate.

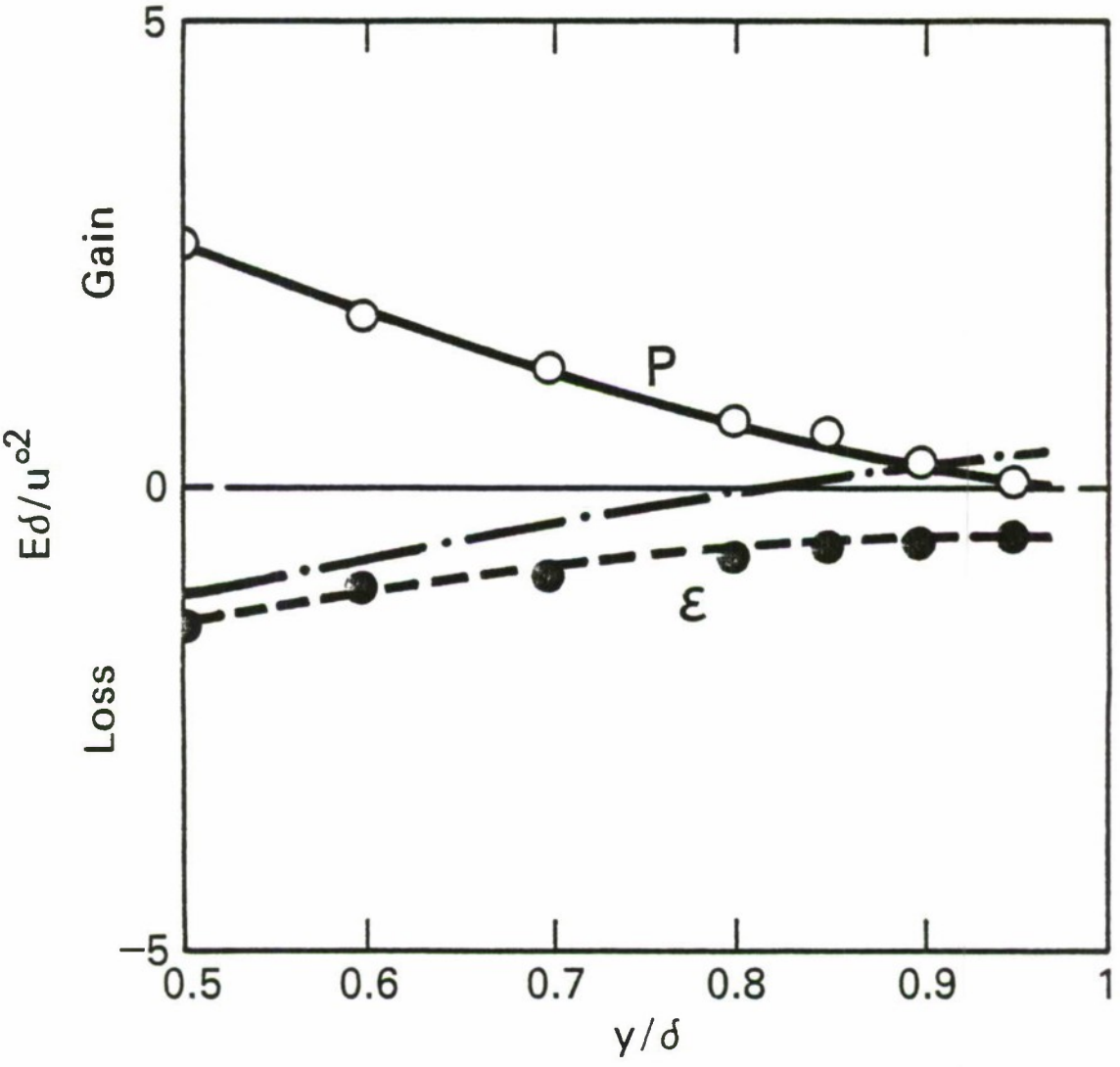

From *Turbulence Structure and Transport Mechanism at The Free Surface in an Open Channel Flow*, figure 3 on p. 515 from the International Journal of Heat and Mass Transfer Vol. 25, No. 4 by Satoru Komori, Hiromasa Ueda and Fumimaru Ogino and Tokuro Mizushina; published by Pergamon Press Copyright © 1982; used by permission.

Figure 2 The budget of the turbulence kinetic energy from the experiments of Komori et al (5).

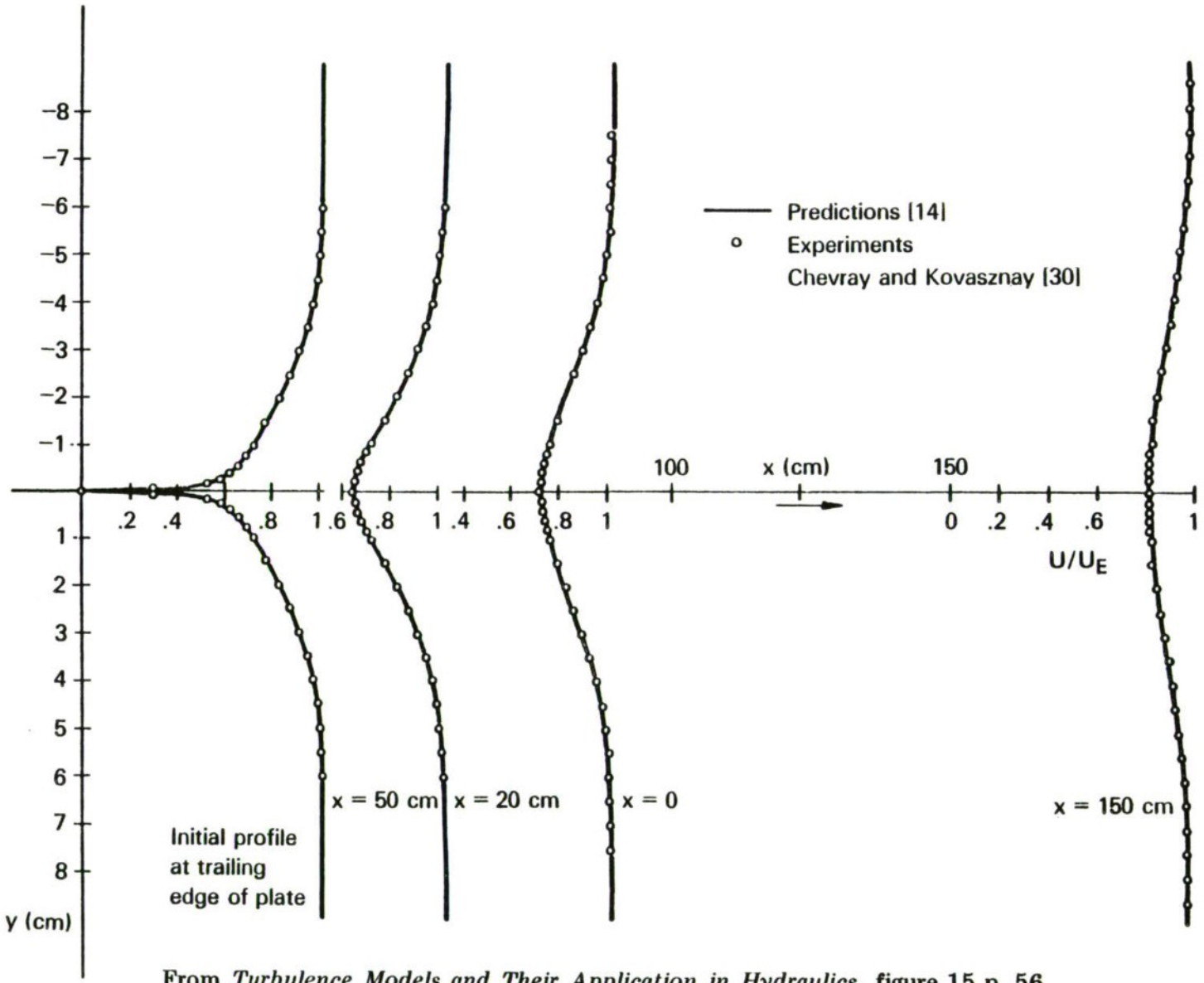

From *Turbulence Models and Their Application in Hydraulics*, figure 15 p. 56 by Wolfgang Rodi, published by International Association for Hydraulic Research Copyright © 1980; used by permission.

Figure 3 Velocity profiles in a plane wake behind a flat plate.

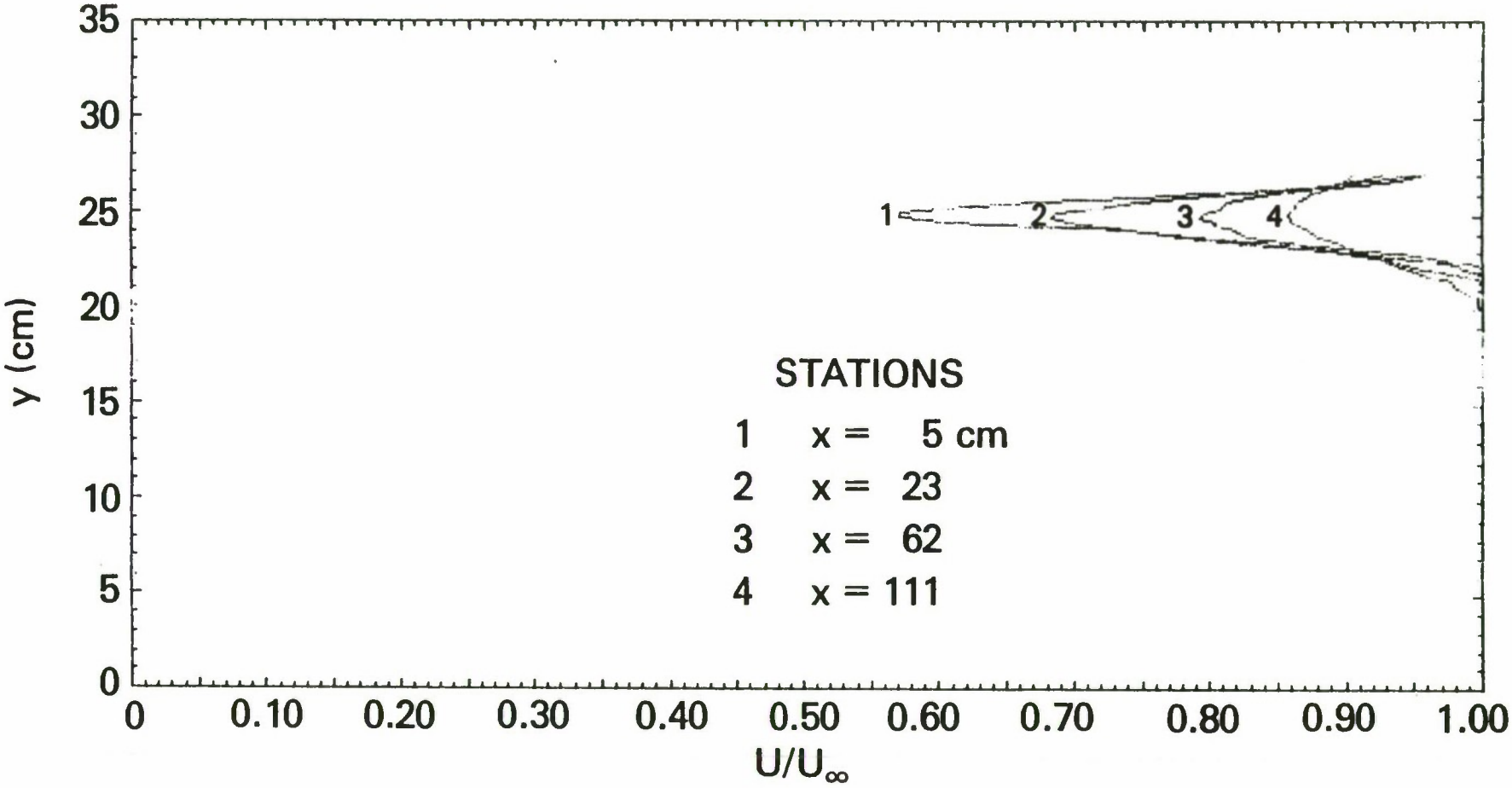

Figure 4 Measured velocity profiles of Swean and Keramidas (25) for the infinite fluid case.

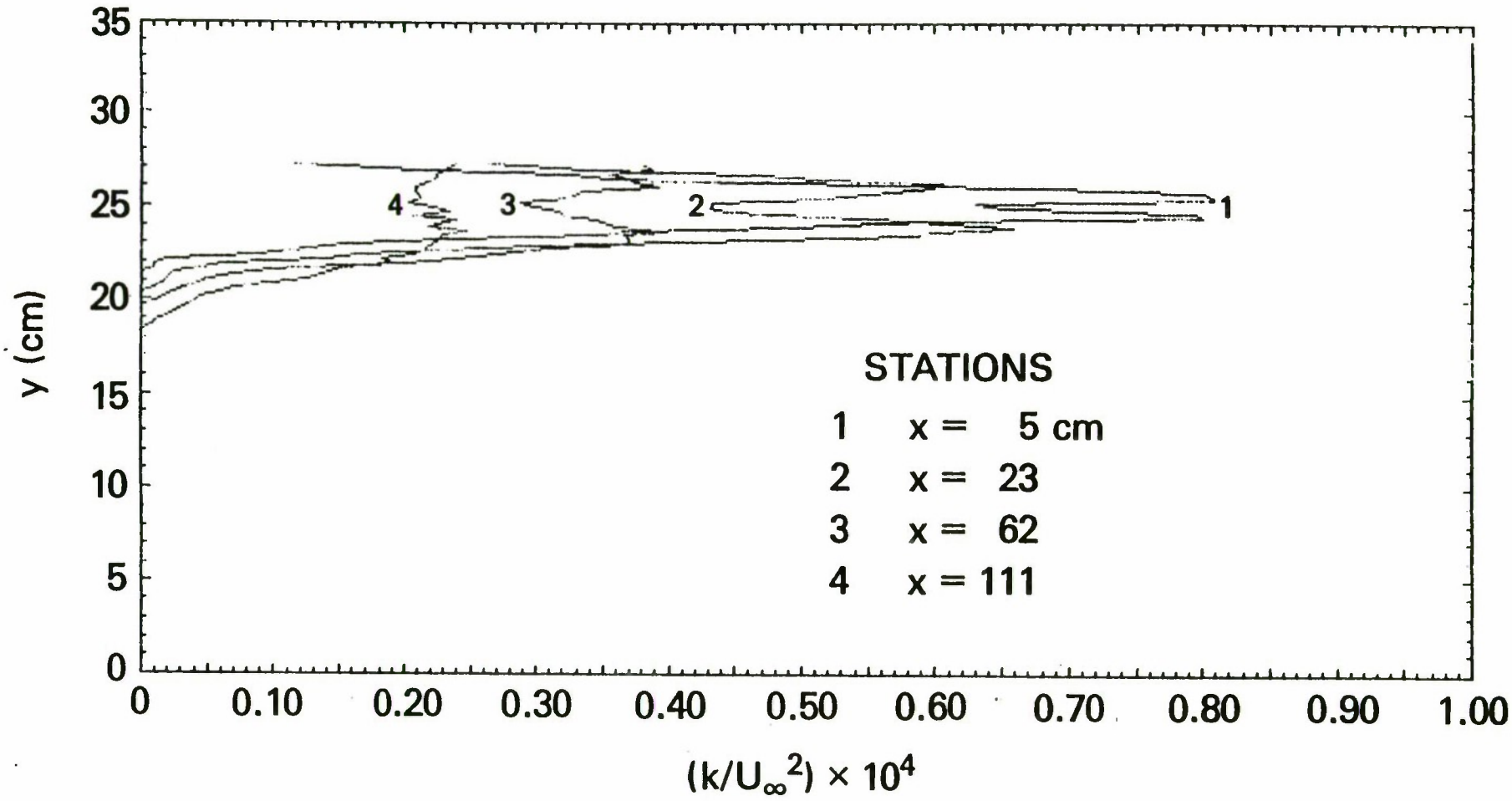

Figure 5 Measured turbulence kinetic energy profiles of Swean and Keramidas (25) for the infinite fluid case.

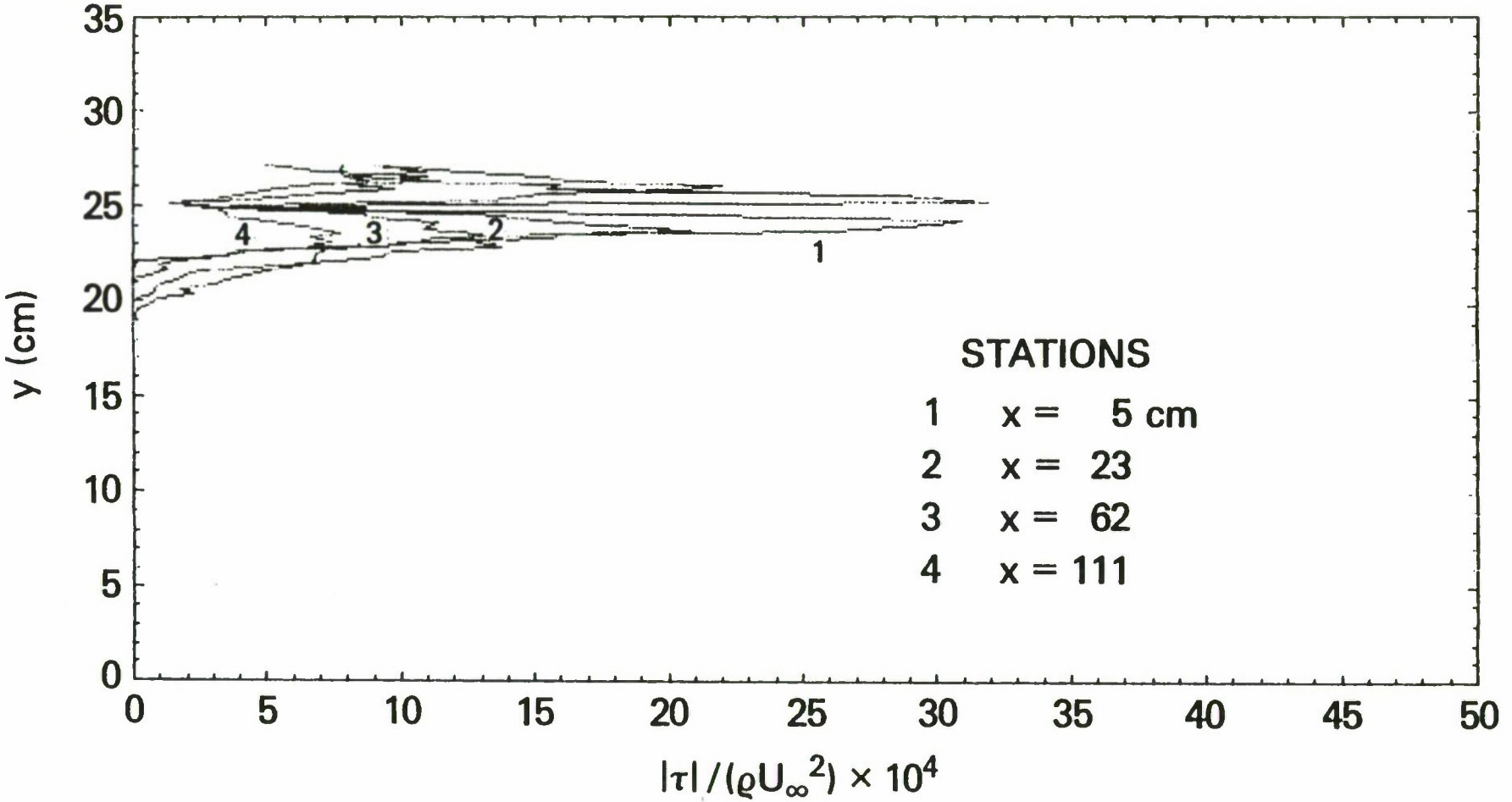

Figure 6 Turbulent shear stress profiles of Swean and Keramidas (25) for the infinite fluid case.

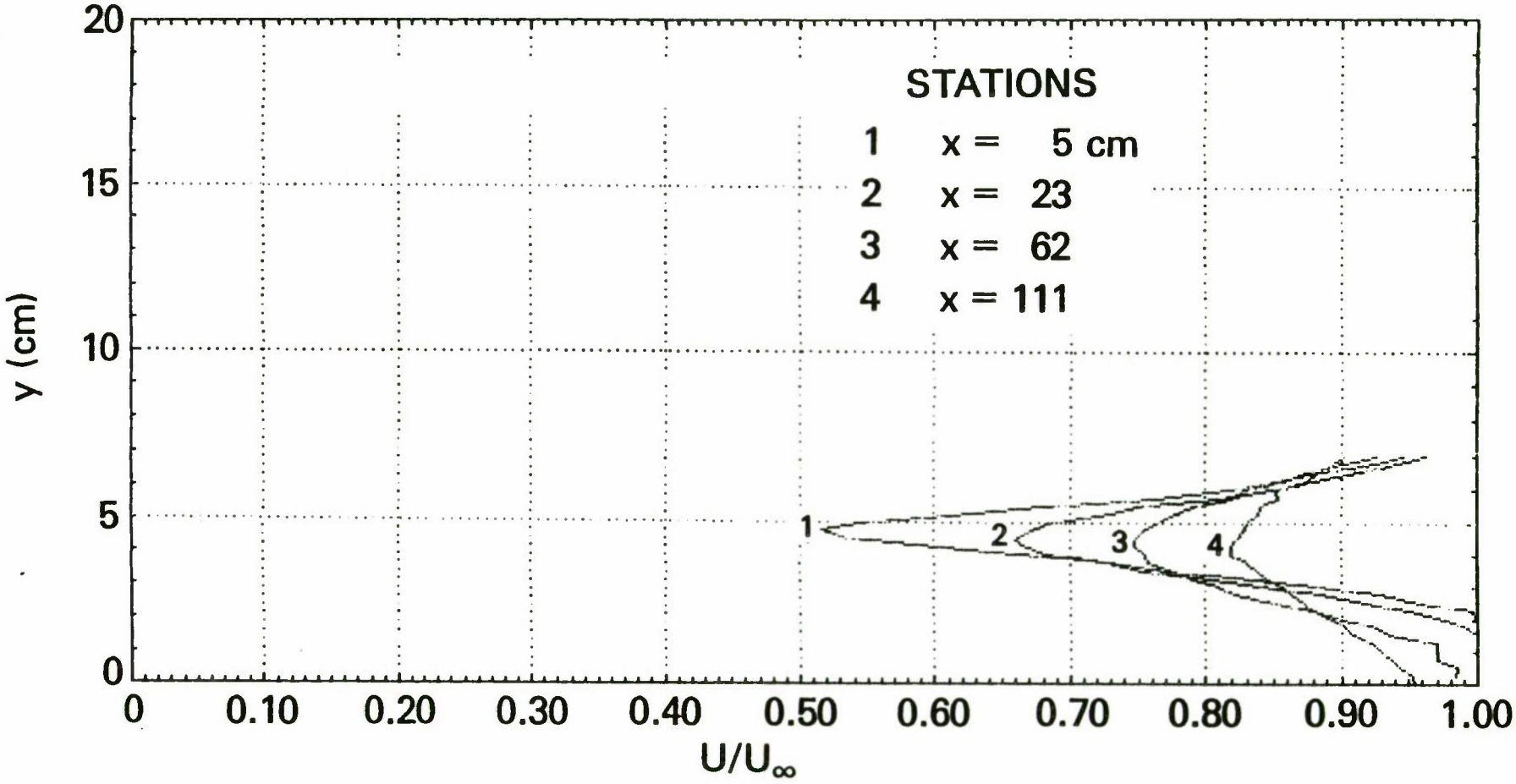

Figure 7 Measured velocity profiles of Swean and Keramidas (25) for the finite fluid case.

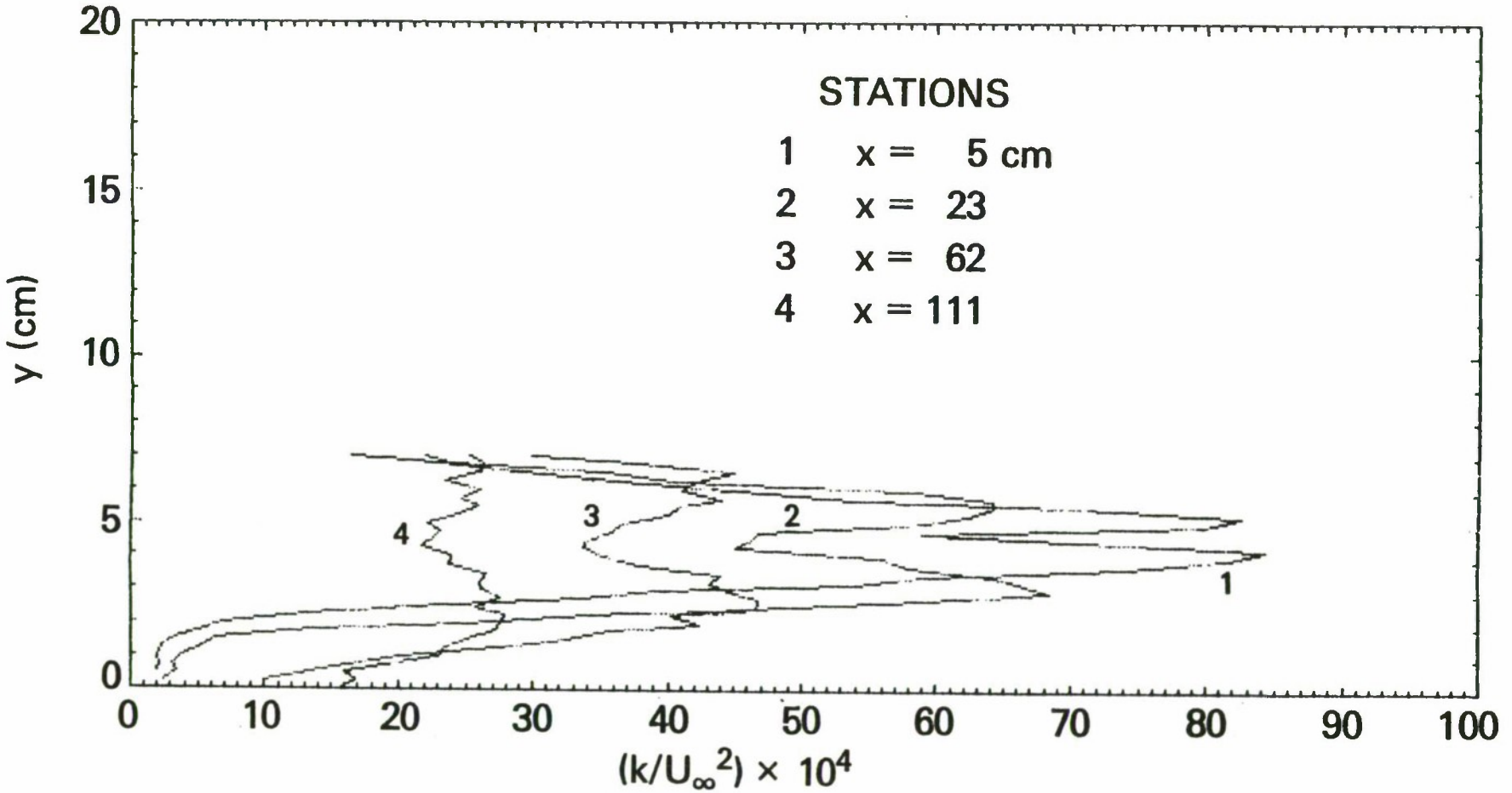

Figure 8 Measured turbulence kinetic energy profiles of Swean and Keramidas (25) for the finite fluid case.

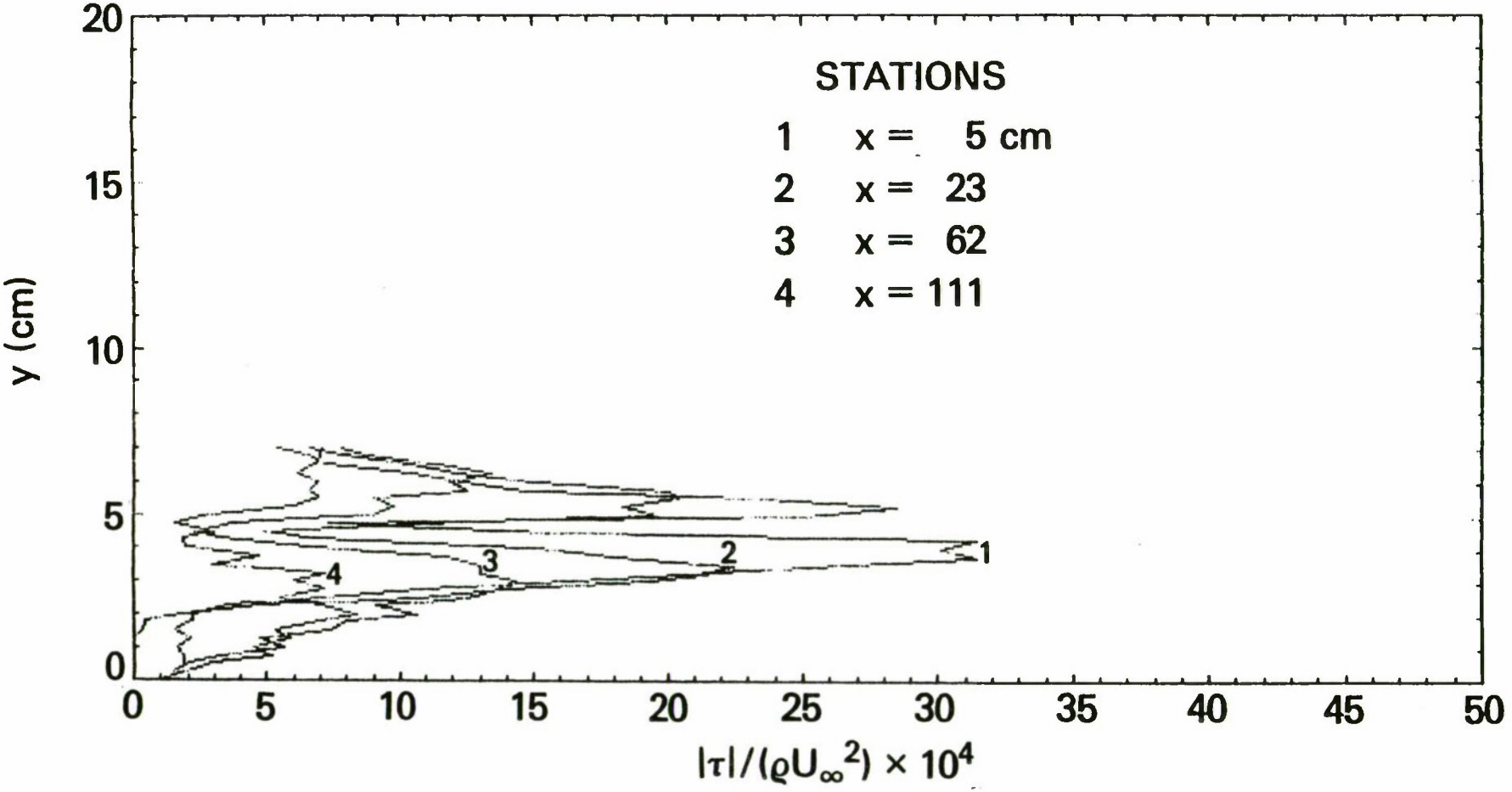

Figure 9 Measured shear stress profiles of Swean and Keramidas (25) for the finite fluid case.

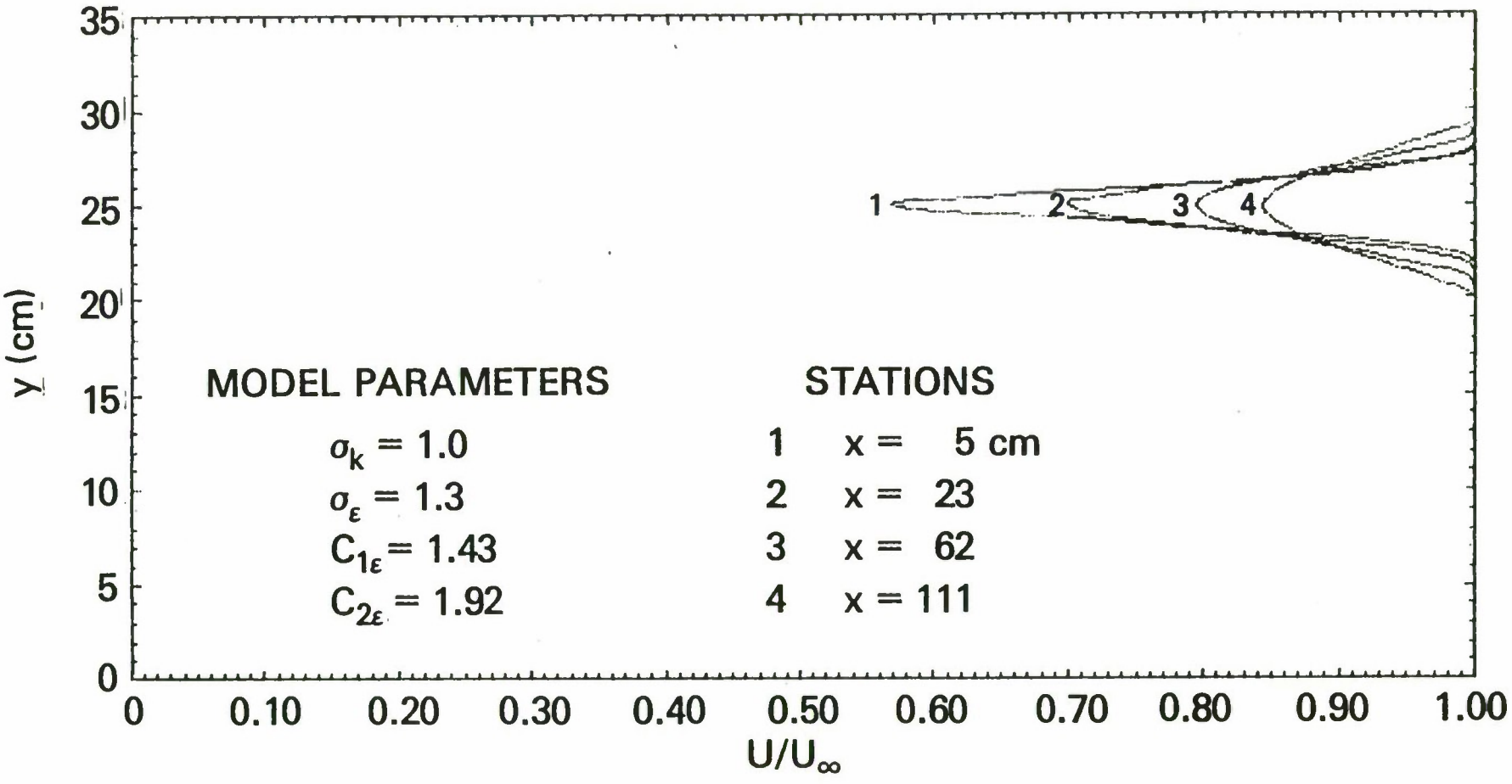

Figure 10 Predicted velocity profiles for infinite fluid with reference parameters.

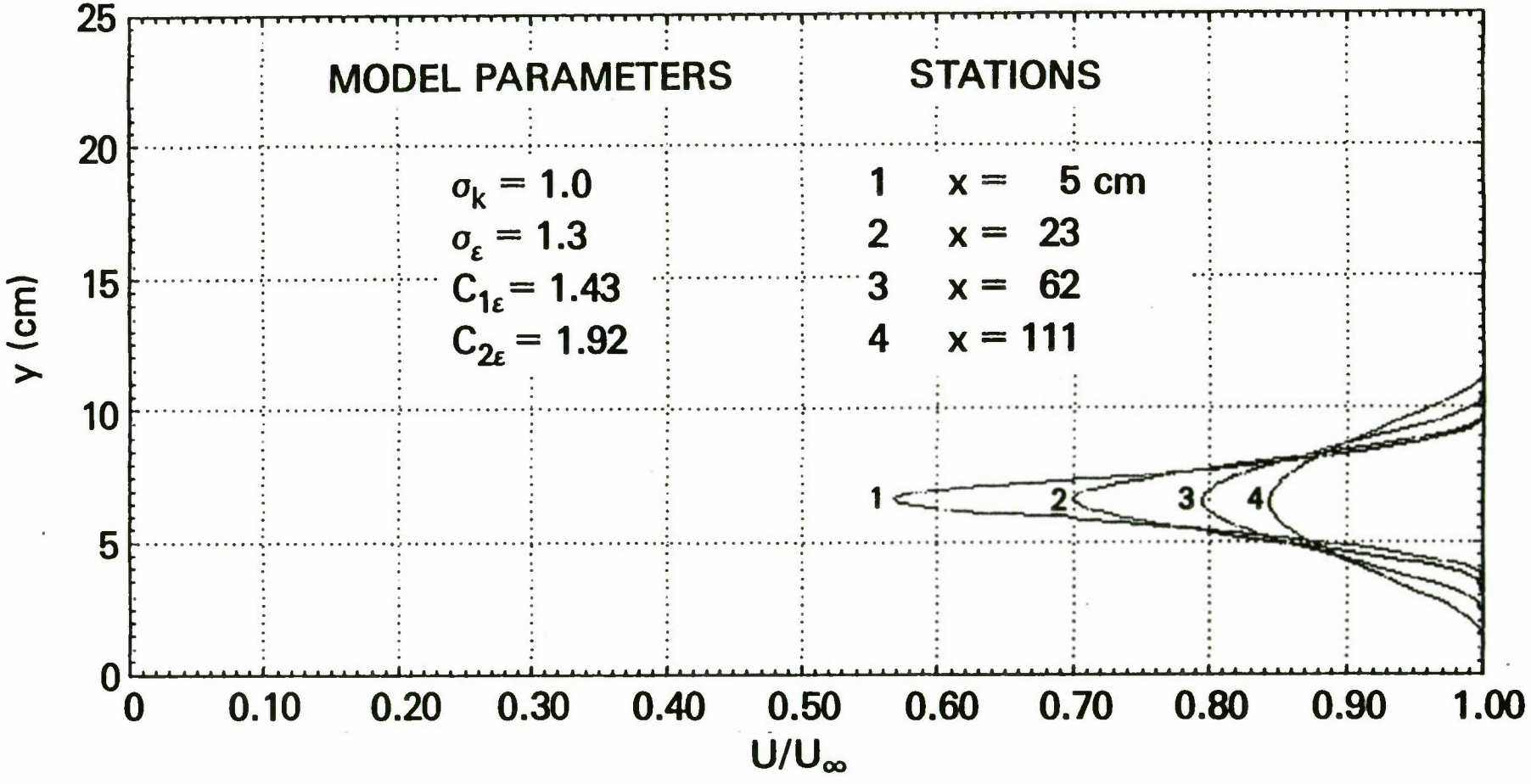

Figure 11 Predicted velocity profiles for displaced infinite fluid with reference parameters.

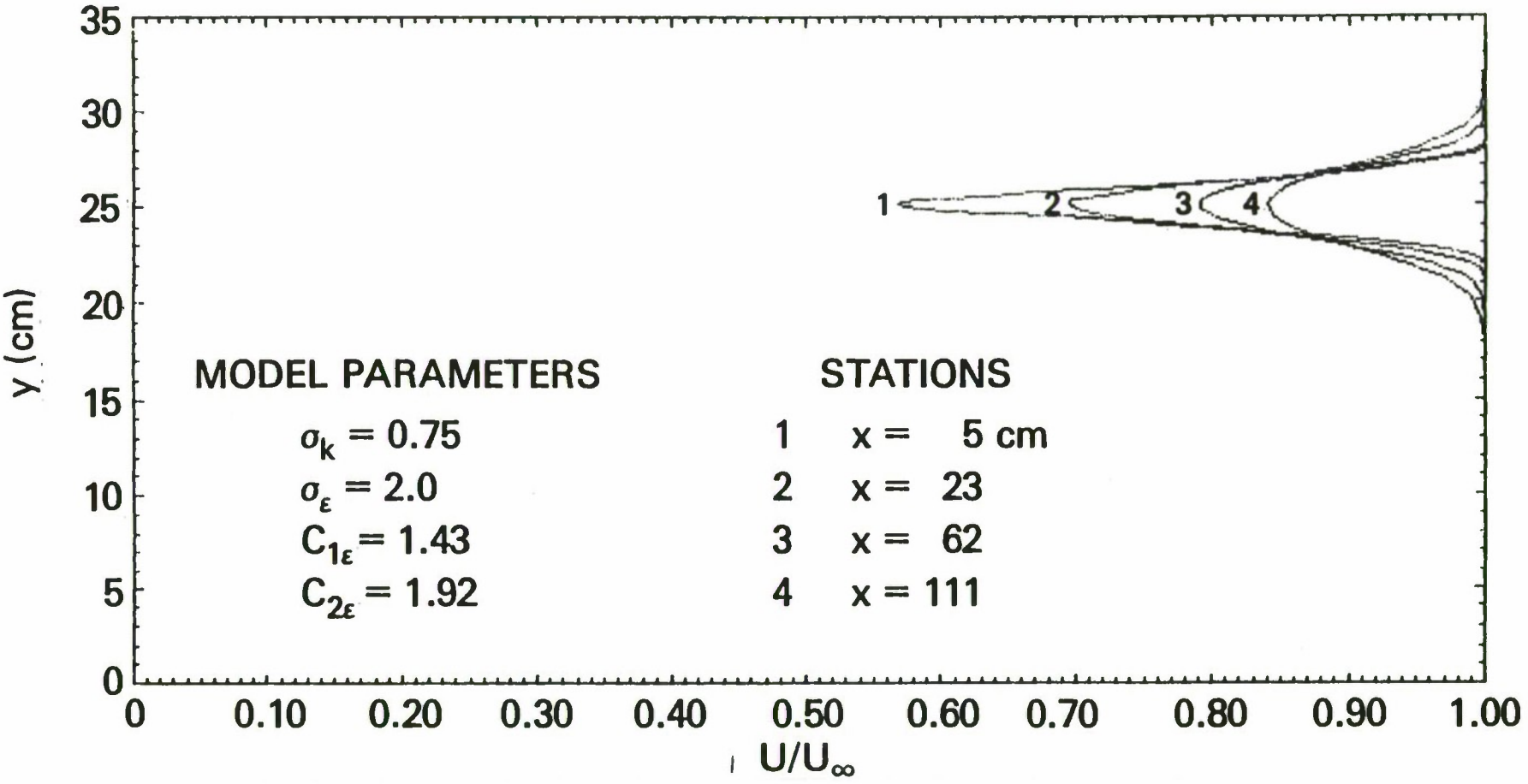

Figure 12 Predicted velocity profiles for infinite fluid with $\sigma_k = .75$ $\sigma_\varepsilon = 2.0$.

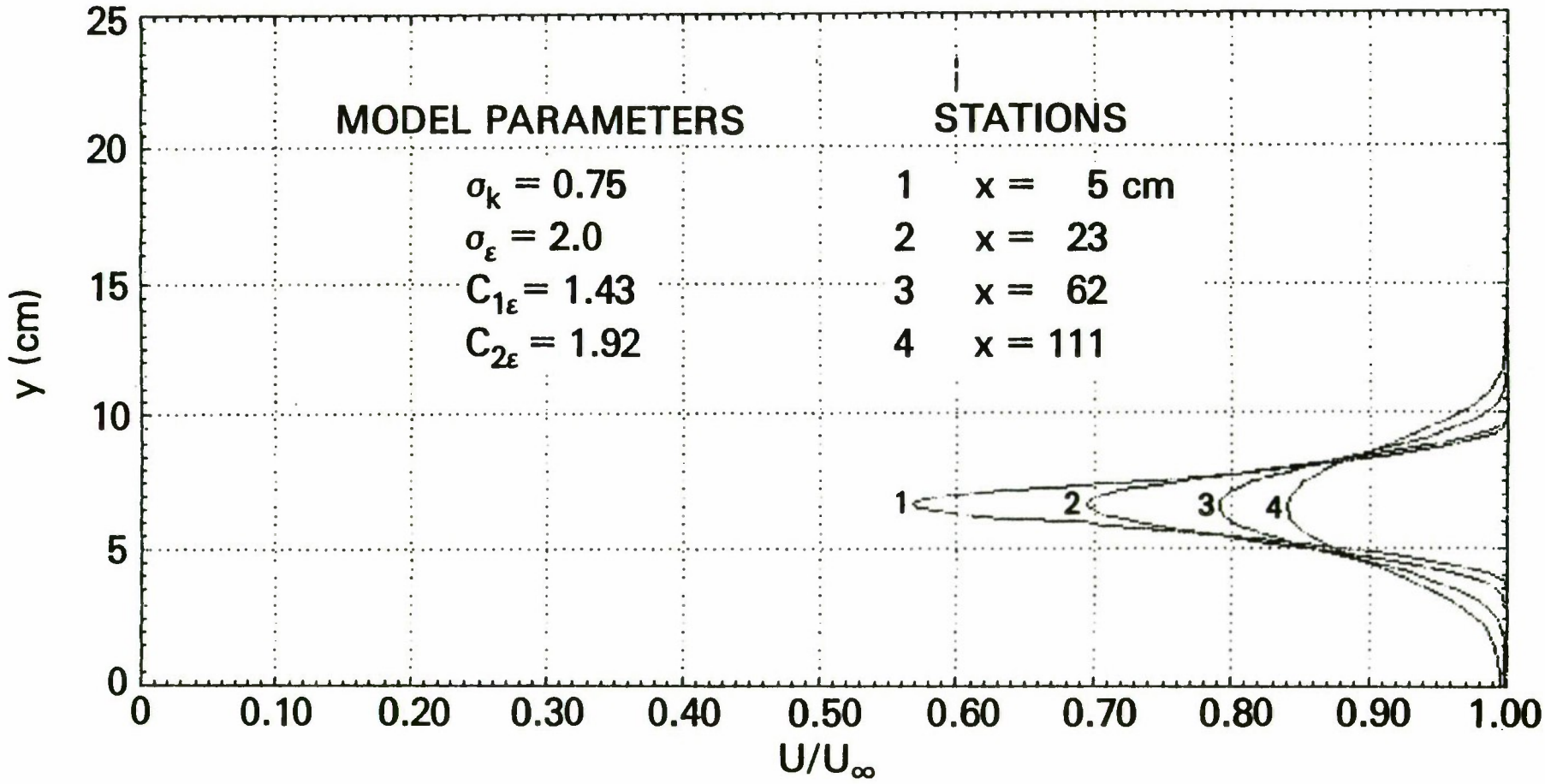

Figure 13 Predicted velocity profiles for displaced infinite fluid with $\sigma_k = .75$ $\sigma_\varepsilon = 2.0$.

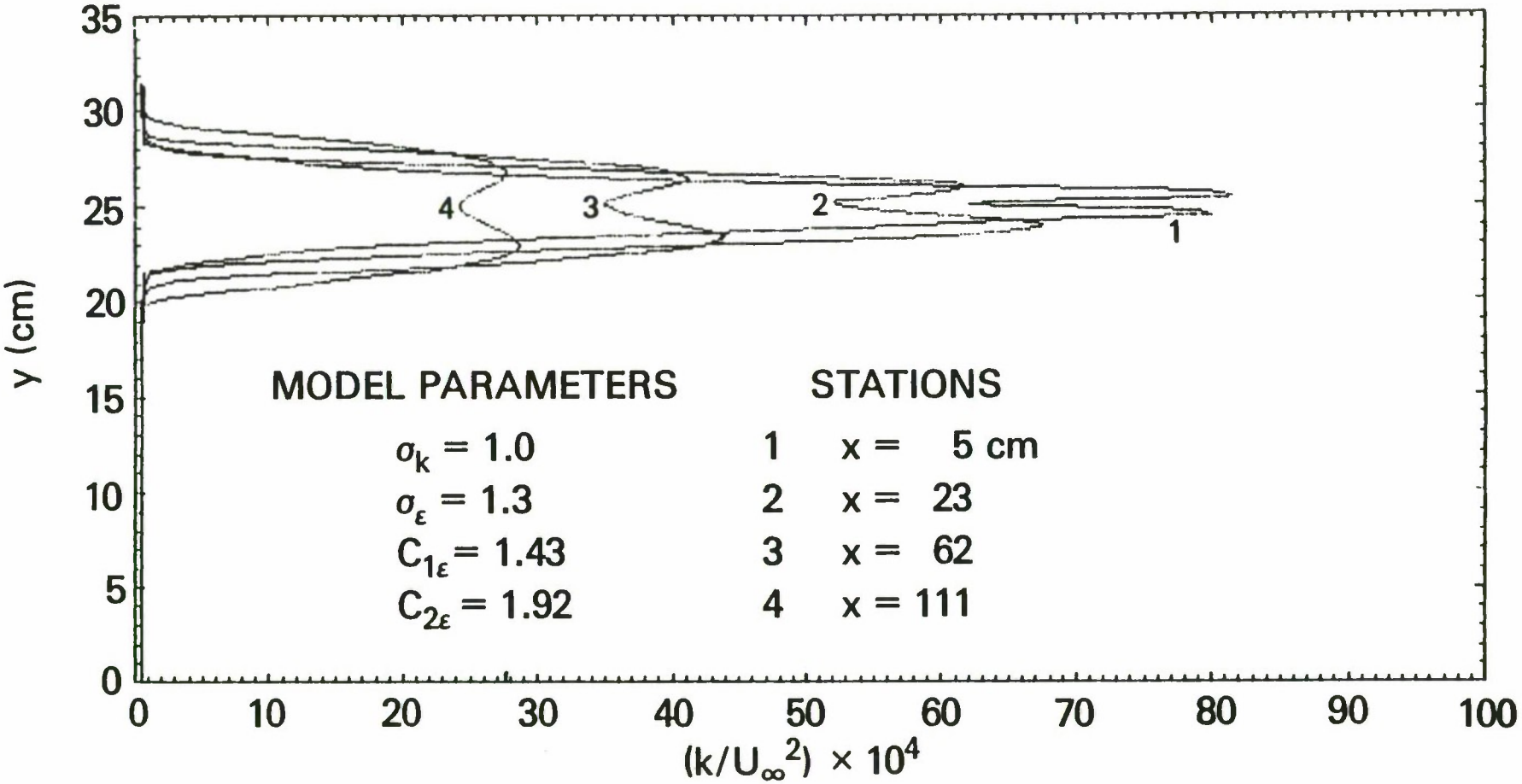

Figure 14 Turbulence kinetic energy profiles for infinite fluid with reference parameters.

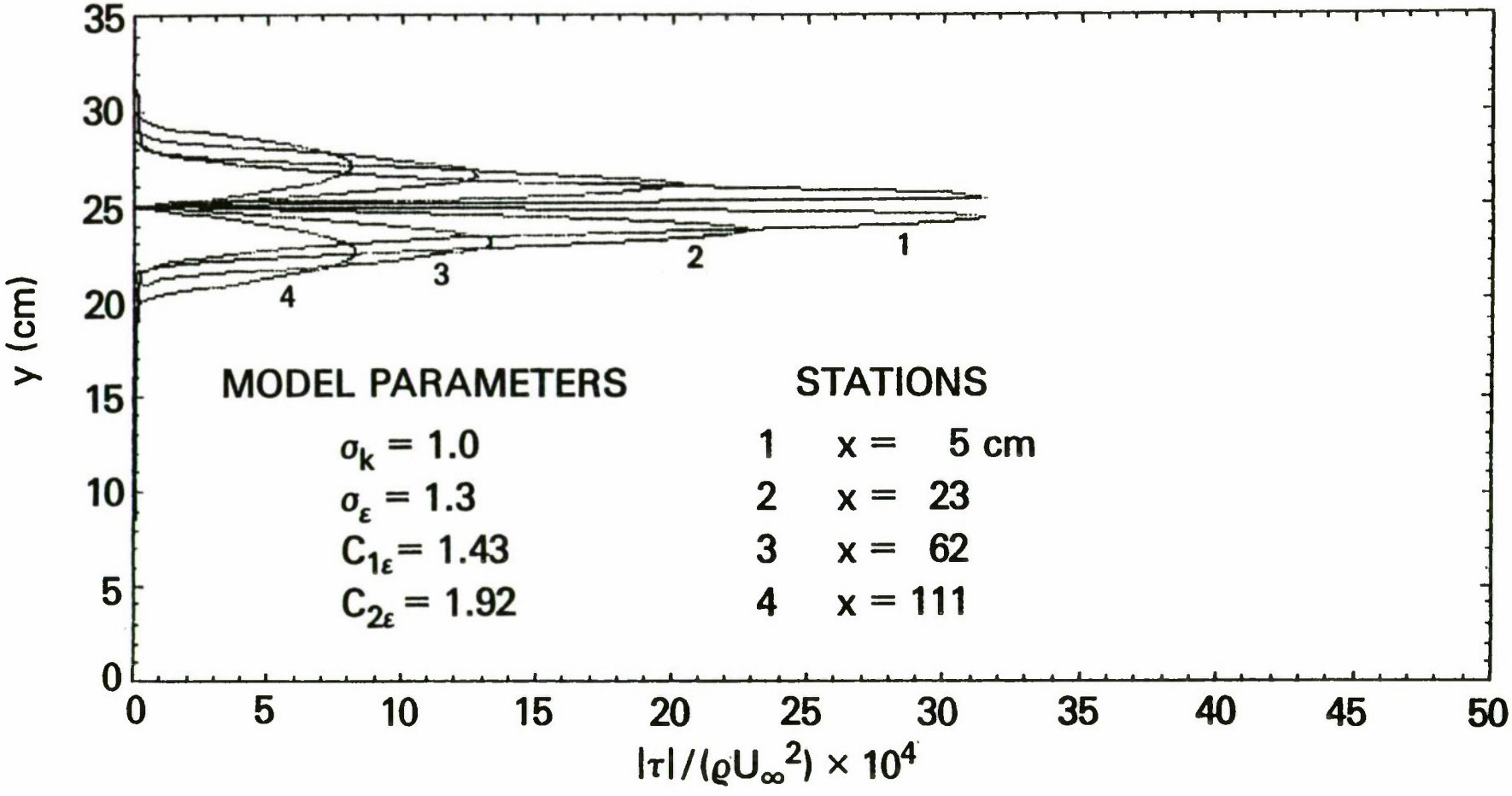

Figure 15 Turbulent shear stress profiles for infinite fluid with reference parameters.

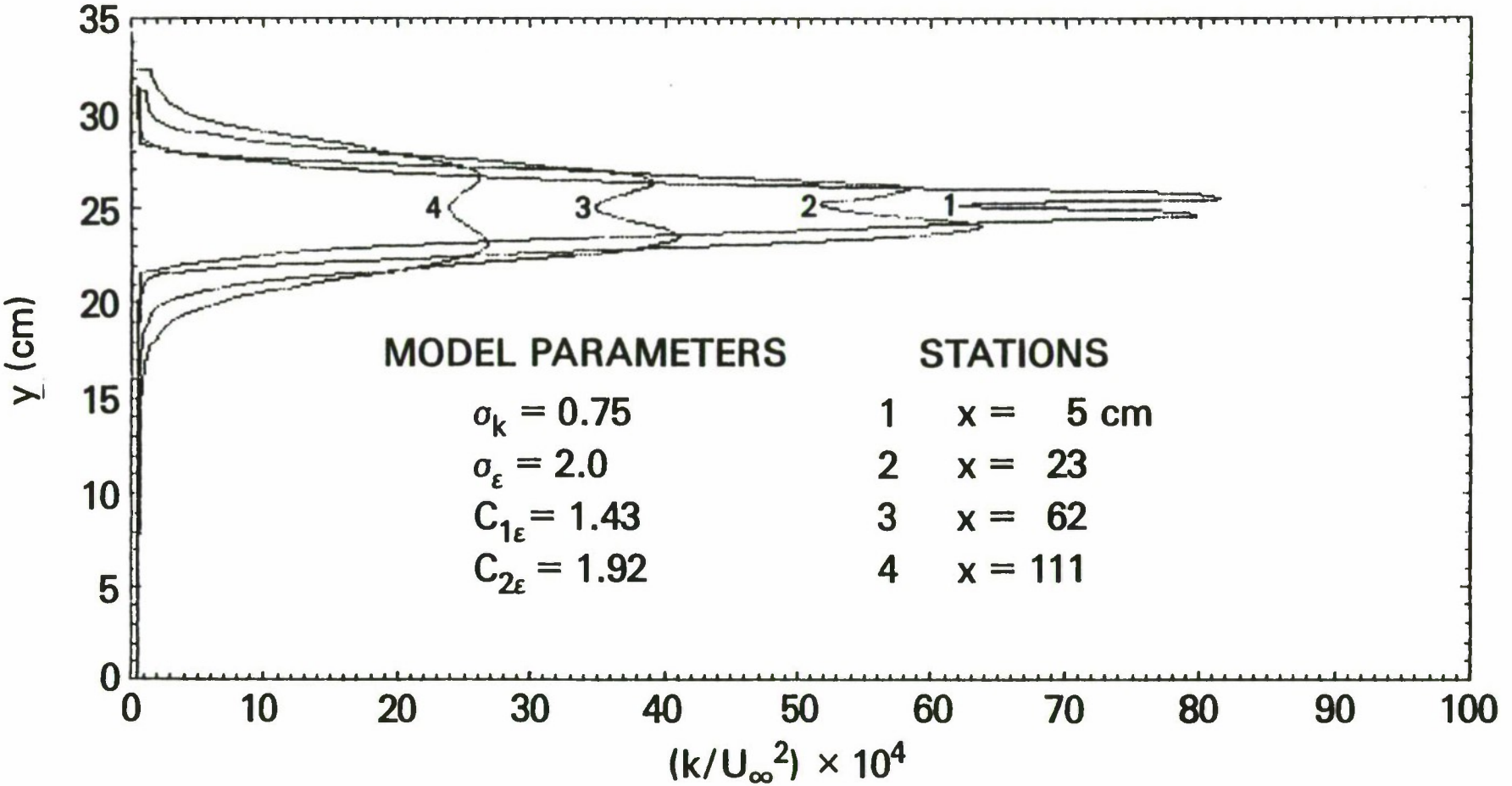

Figure 16 Turbulence kinetic energy profiles for infinite fluid with $\sigma_k = .75$ $\sigma_\varepsilon = 2.0$.

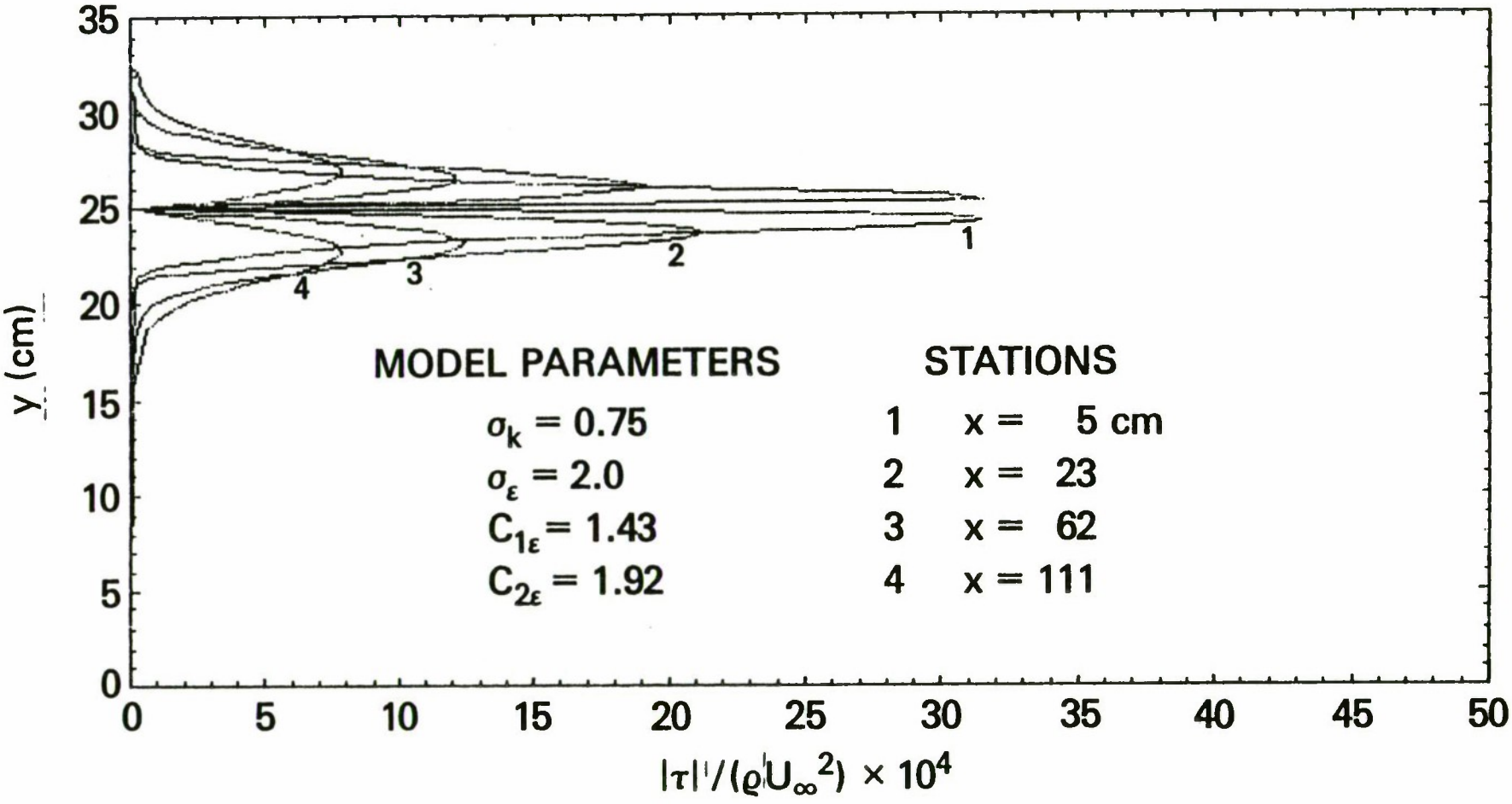

Figure 17 Turbulent shear stress profiles for infinite fluid with $\sigma_k = .75$ $\sigma_\varepsilon = 2.0$.

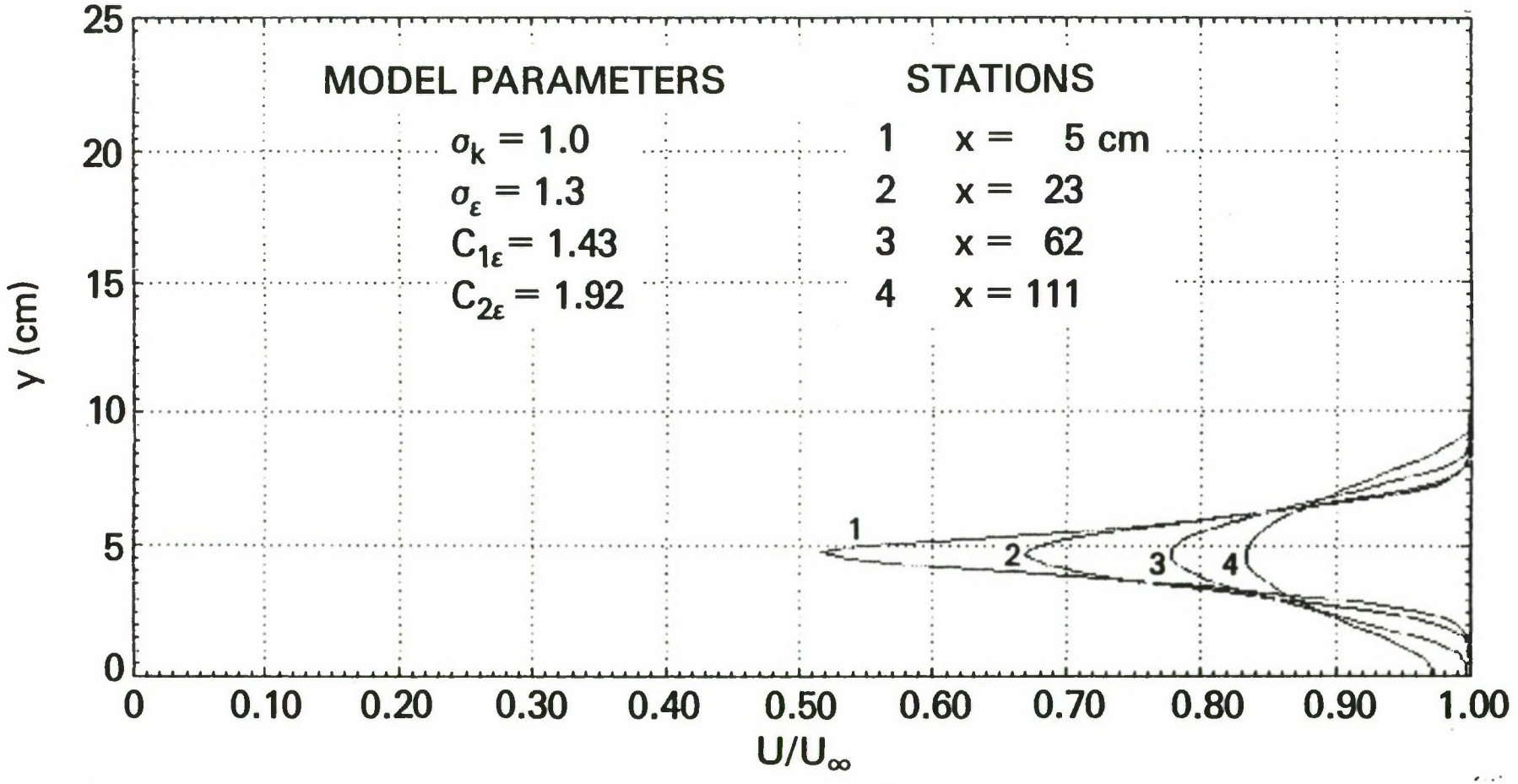

Figure 18 Velocity profiles for finite fluid with reference parameters and symmetric free surface boundary conditions.

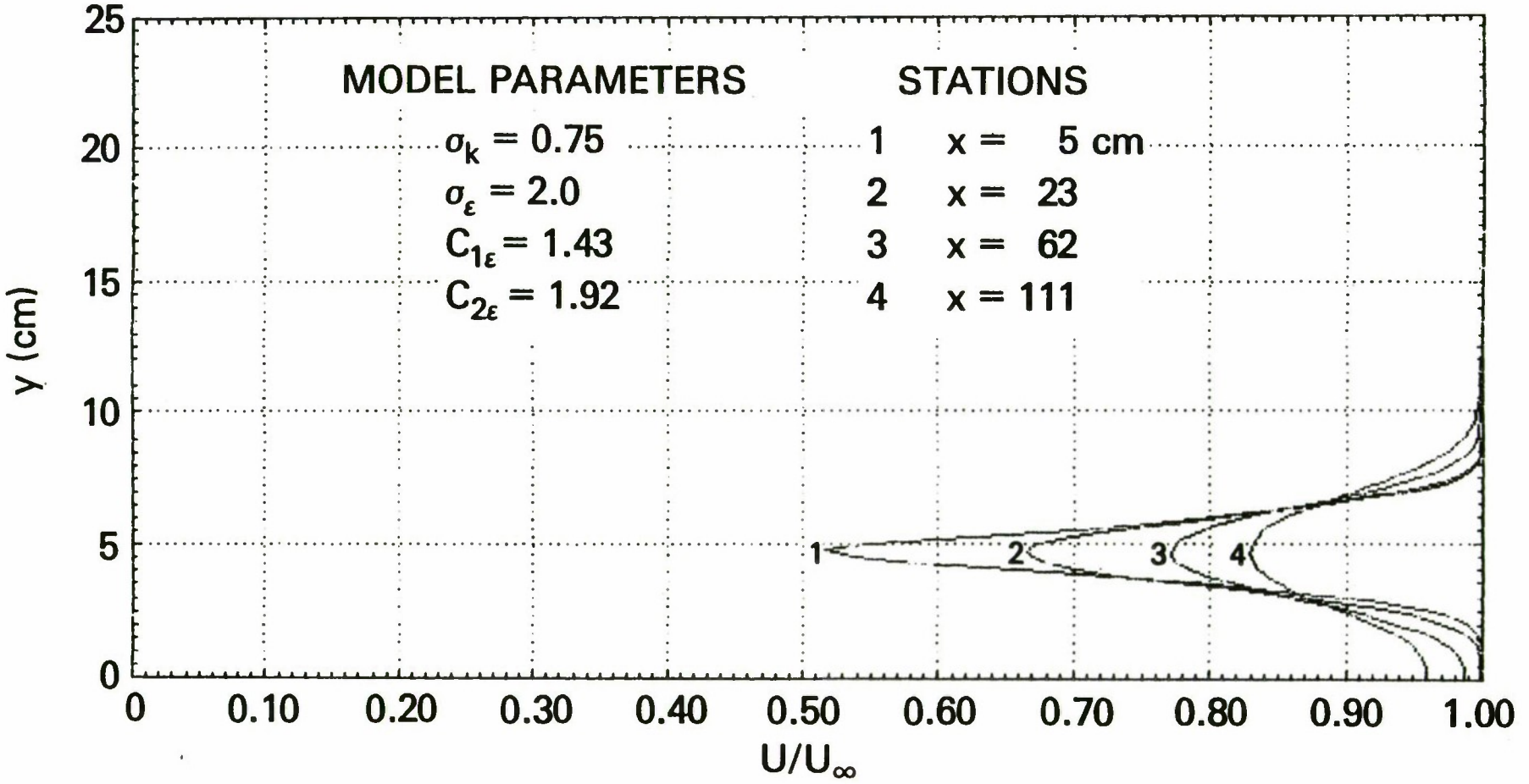

Figure 19 Velocity profiles for finite fluid with σ_k = .75 σ_ε = 2.0 and symmetric free surface boundary conditions.

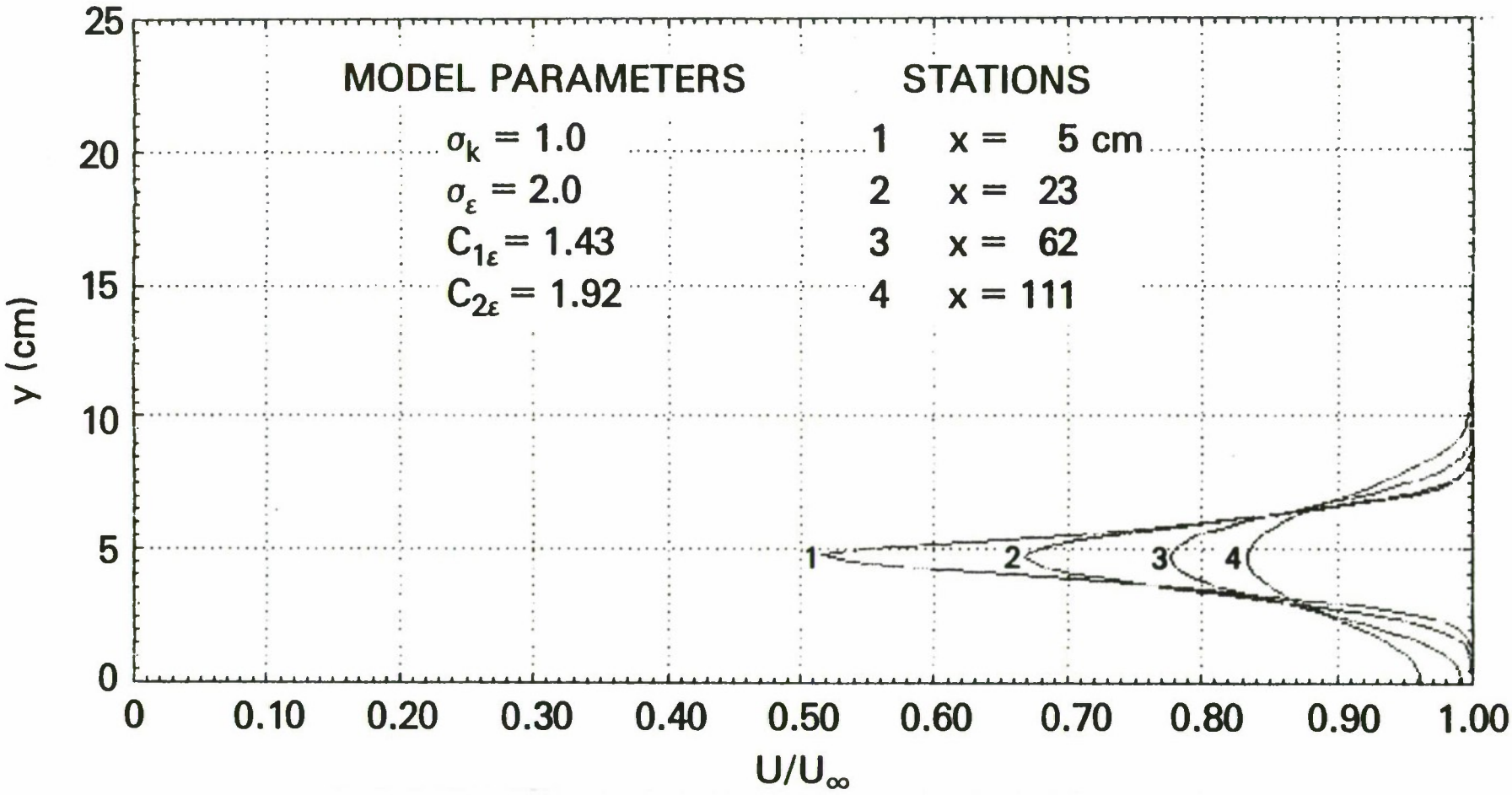

Figure 20 Velocity profiles for finite fluid with $\sigma_k = 1.0$ $\sigma_\varepsilon = 2.0$ and symmetric free surface boundary conditions.

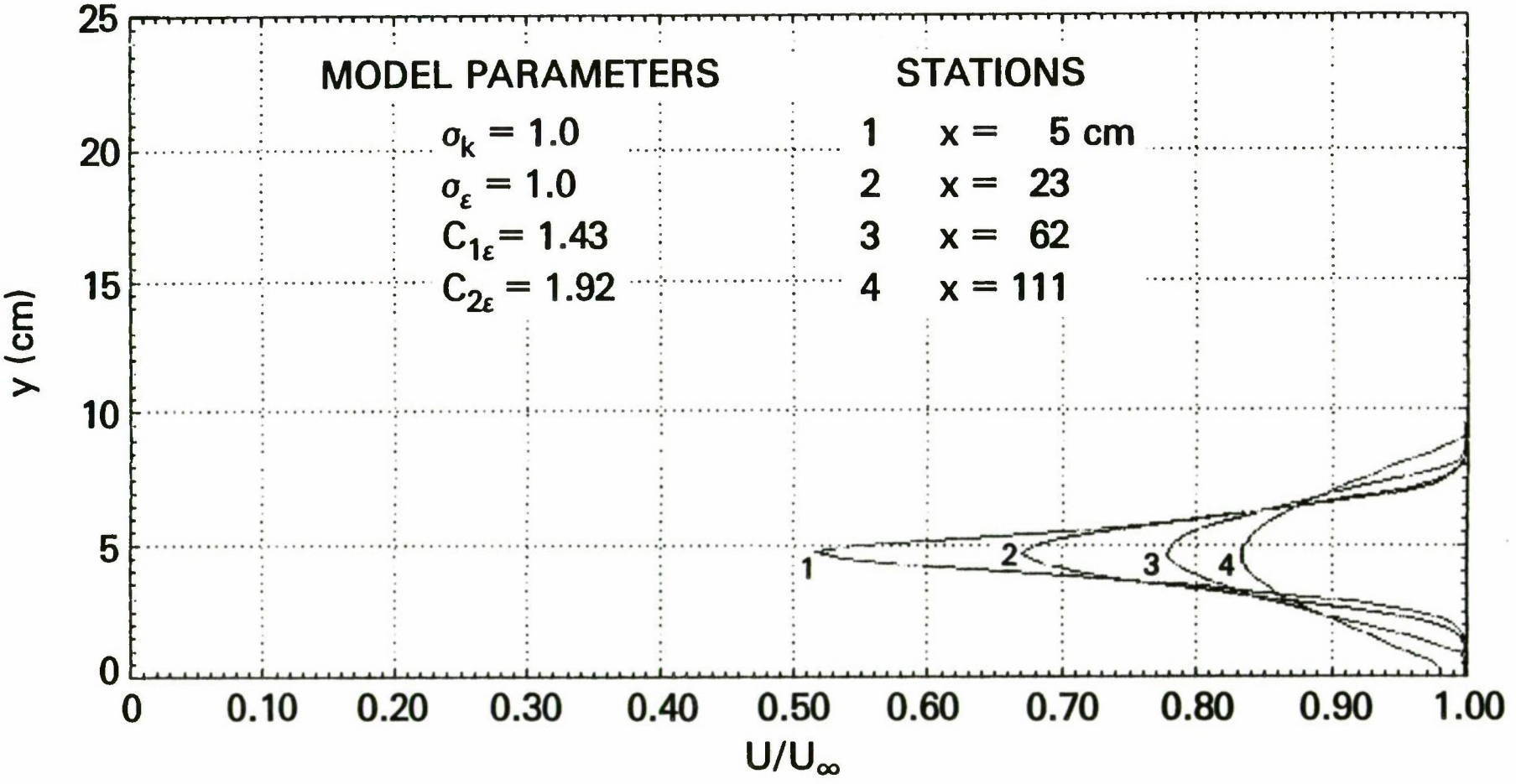

Figure 21 Velocity profiles for finite fluid with σ_k = 1.0 σ_ε = 1.0 and symmetric free surface boundary conditions.

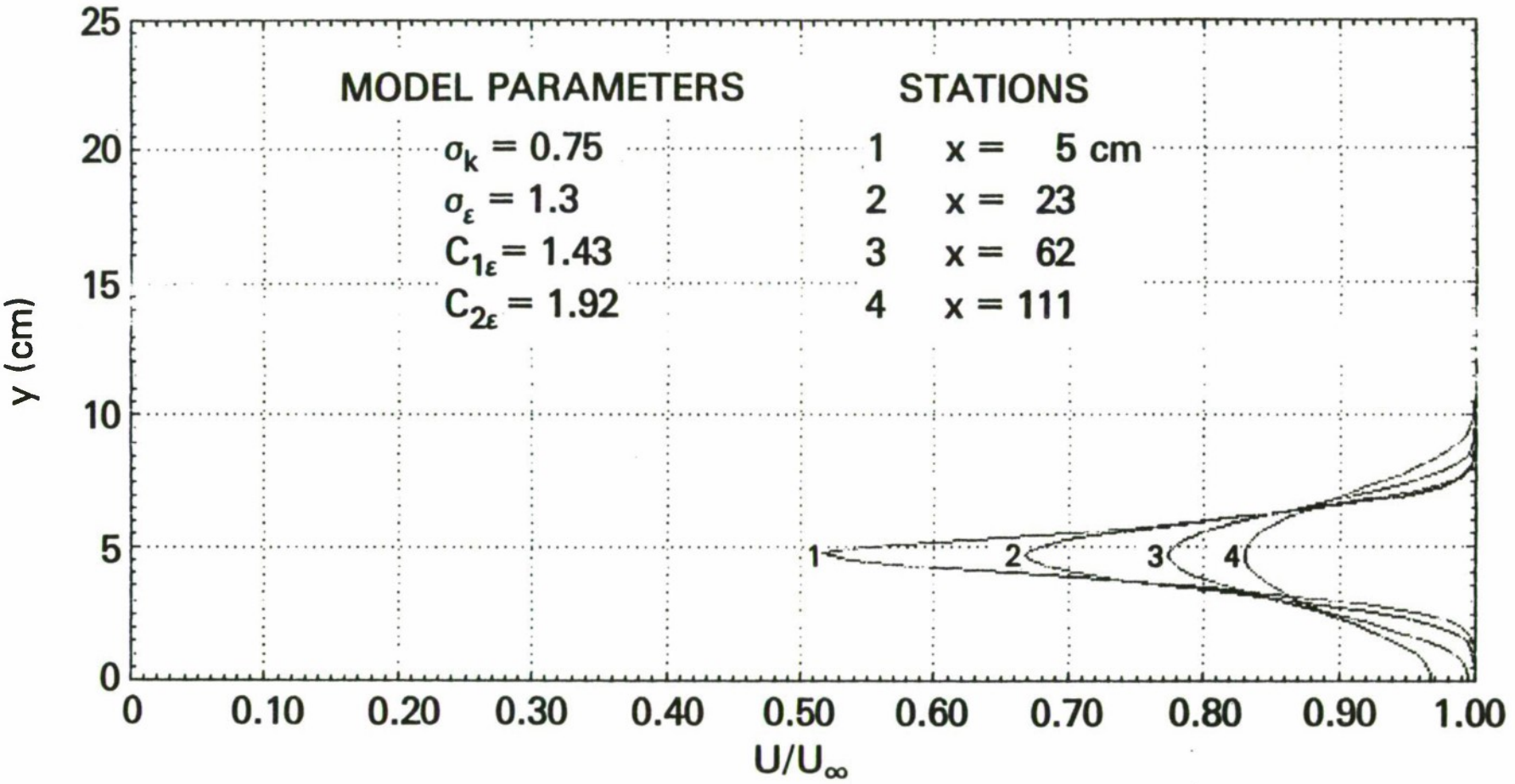

Figure 22 Velocity profiles for finite fluid with $\sigma_k = .75$ $\sigma_\varepsilon = 1.287$ and symmetric free surface boundary conditions.

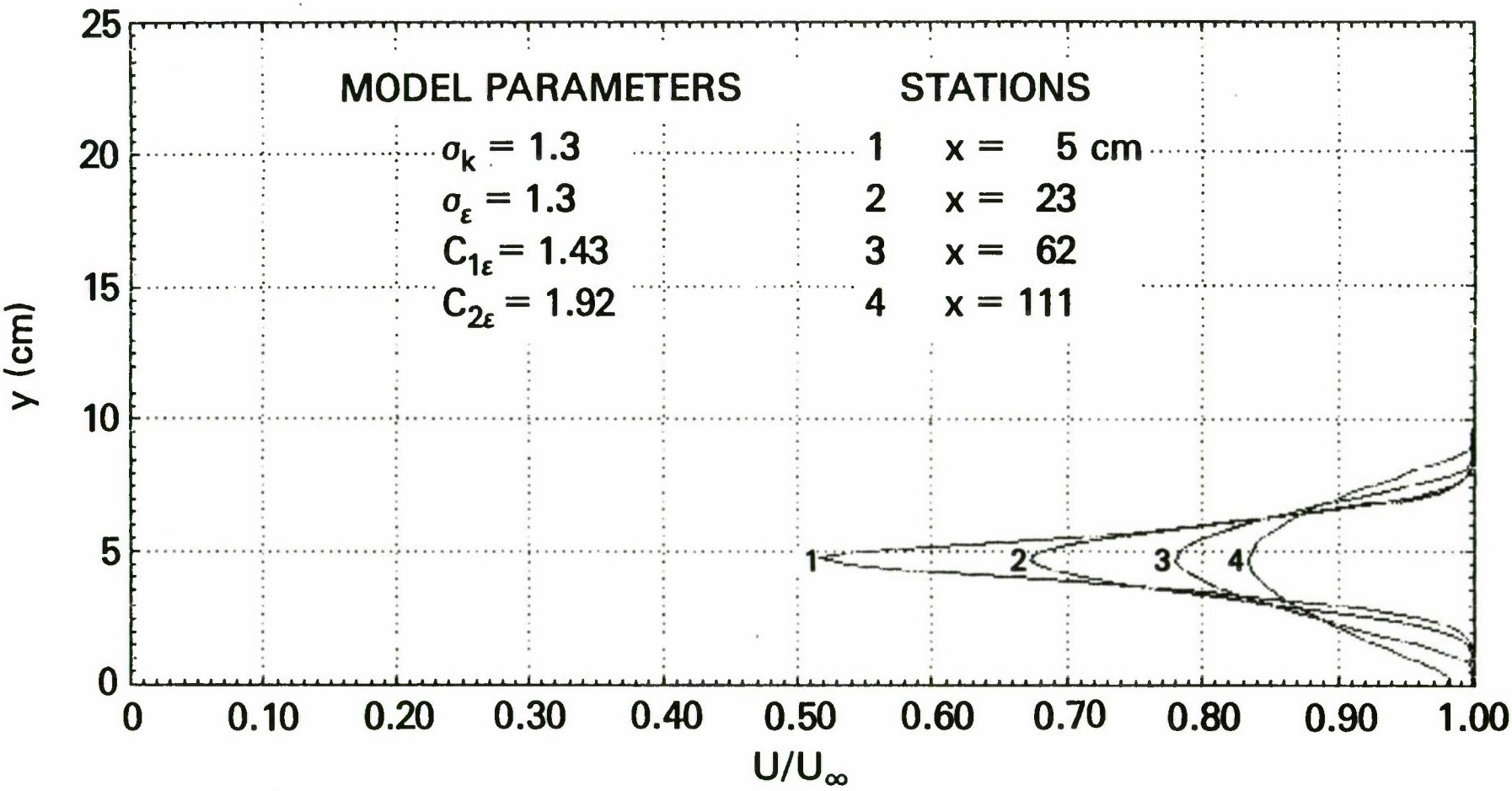

Figure 23 Velocity profiles for finite fluid with σ_k = 1.287 σ_ε = 1.287 and symmetric free surface boundary conditions.

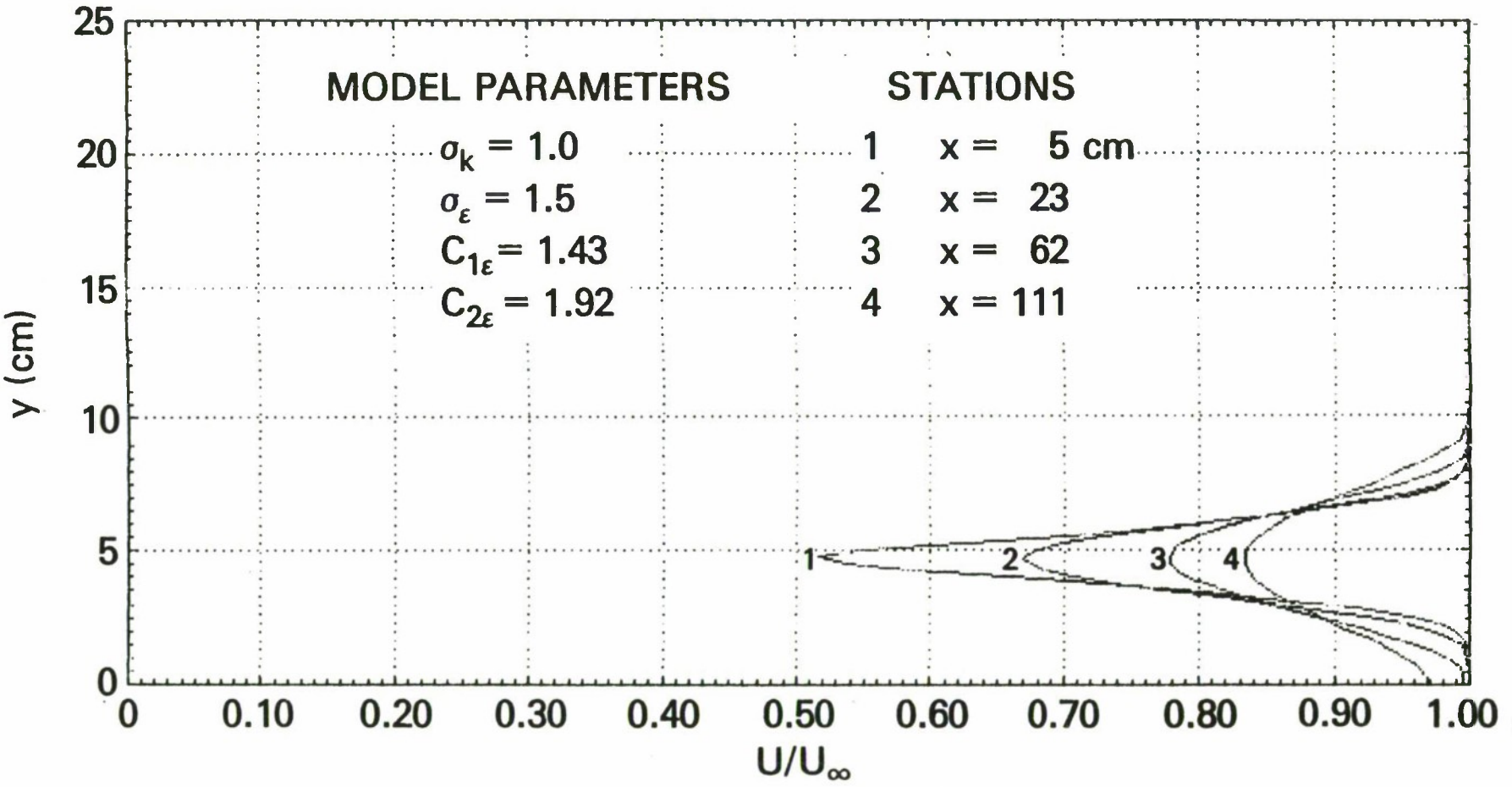

Figure 24 Velocity profiles for finite fluid with σ_k = 1.0 σ_ε = 1.5 and symmetric free surface boundary conditions.

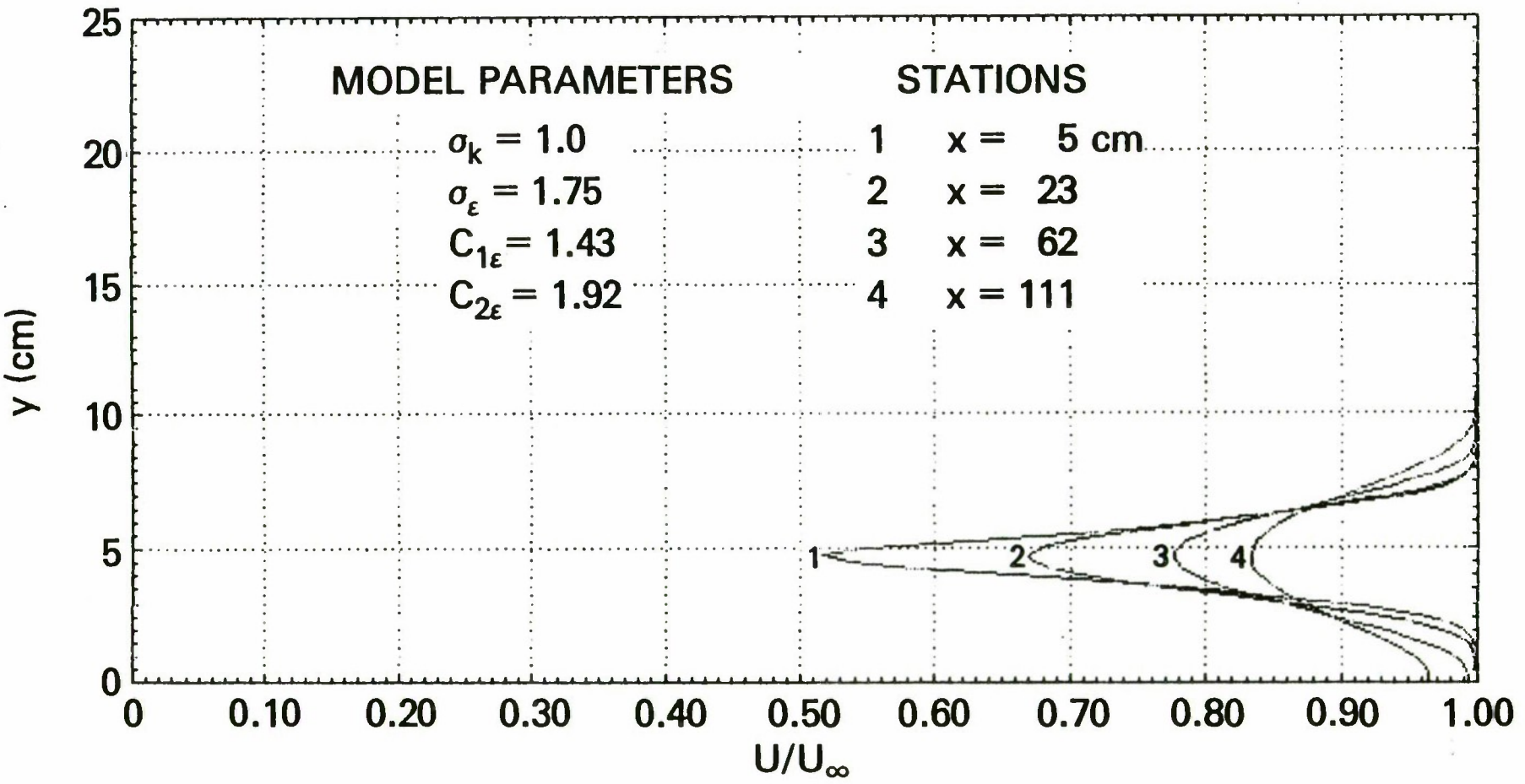

Figure 25 Velocity profile for finite fluid with $\sigma_k = 1.0$ $\sigma_\varepsilon = 1.75$ and symmetric free surface boundary conditions.

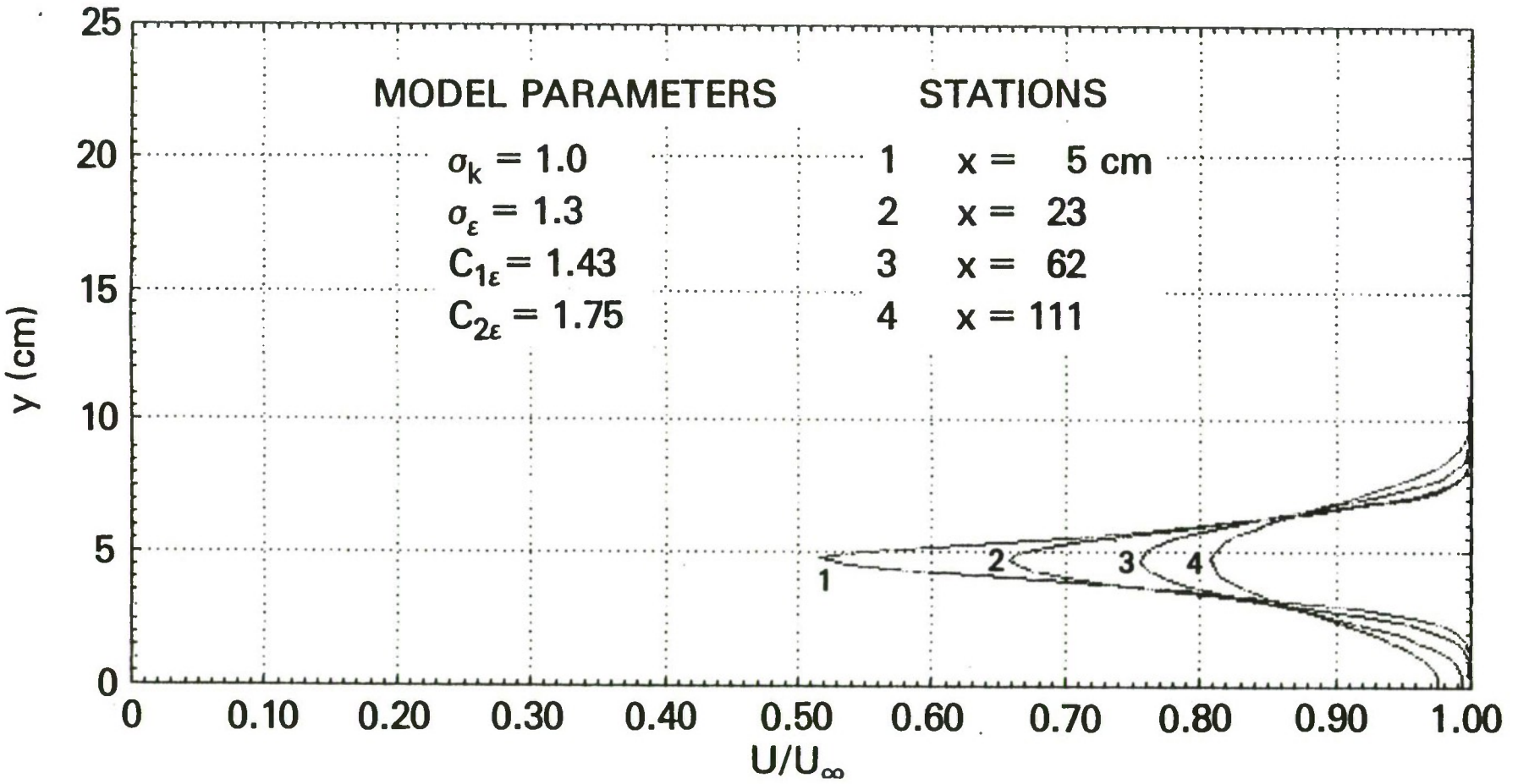

Figure 26. Velocity profiles for finite fluid with $C_{1\varepsilon}$ = 1.43 $C_{2\varepsilon}$ = 1.75 and symmetric free surface boundary conditions.

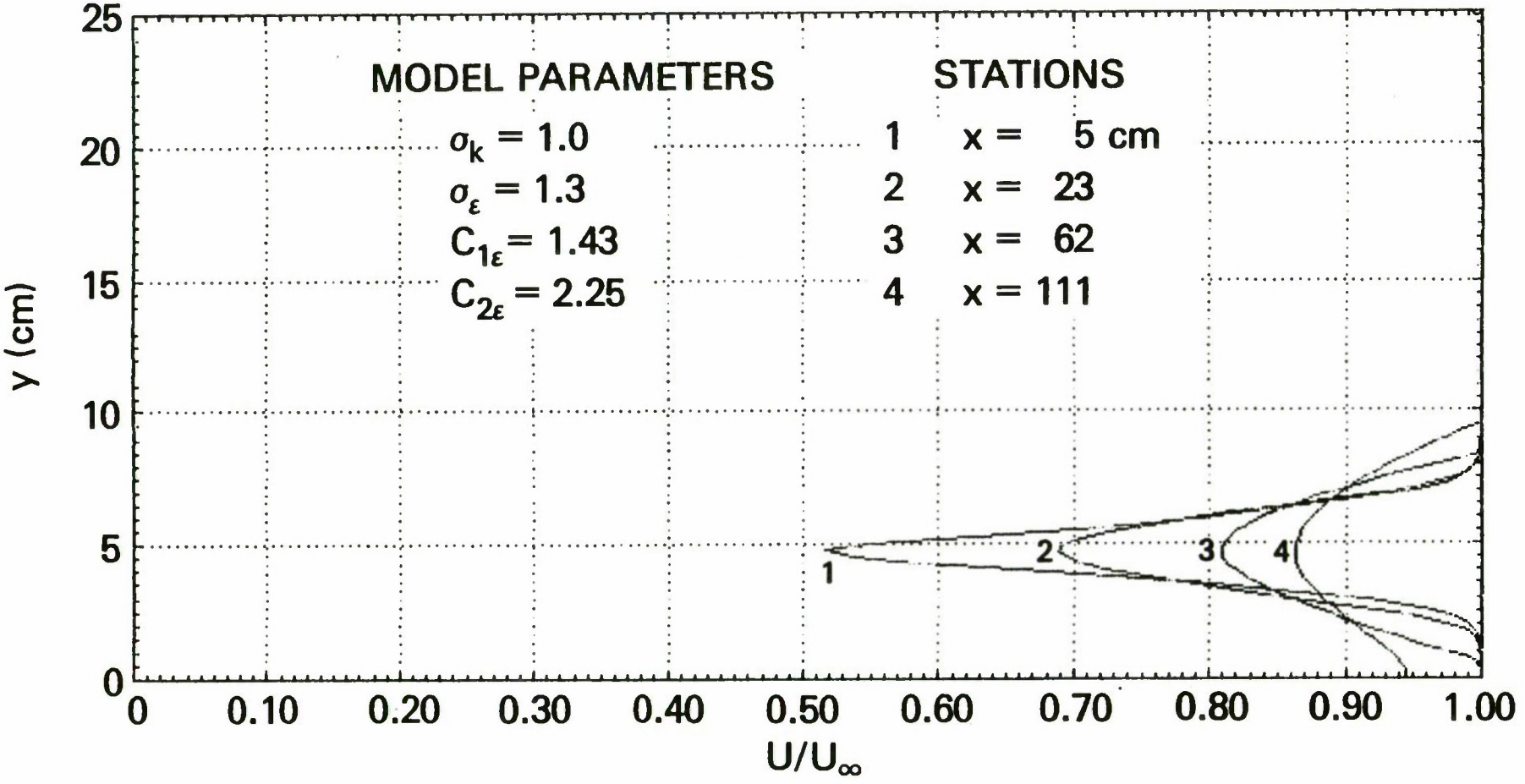

Figure 27 Velocity profiles for finite fluid with $C_{1\varepsilon}$ = 1.43 $C_{2\varepsilon}$ = 2.25 and symmetric free surface boundary conditions.

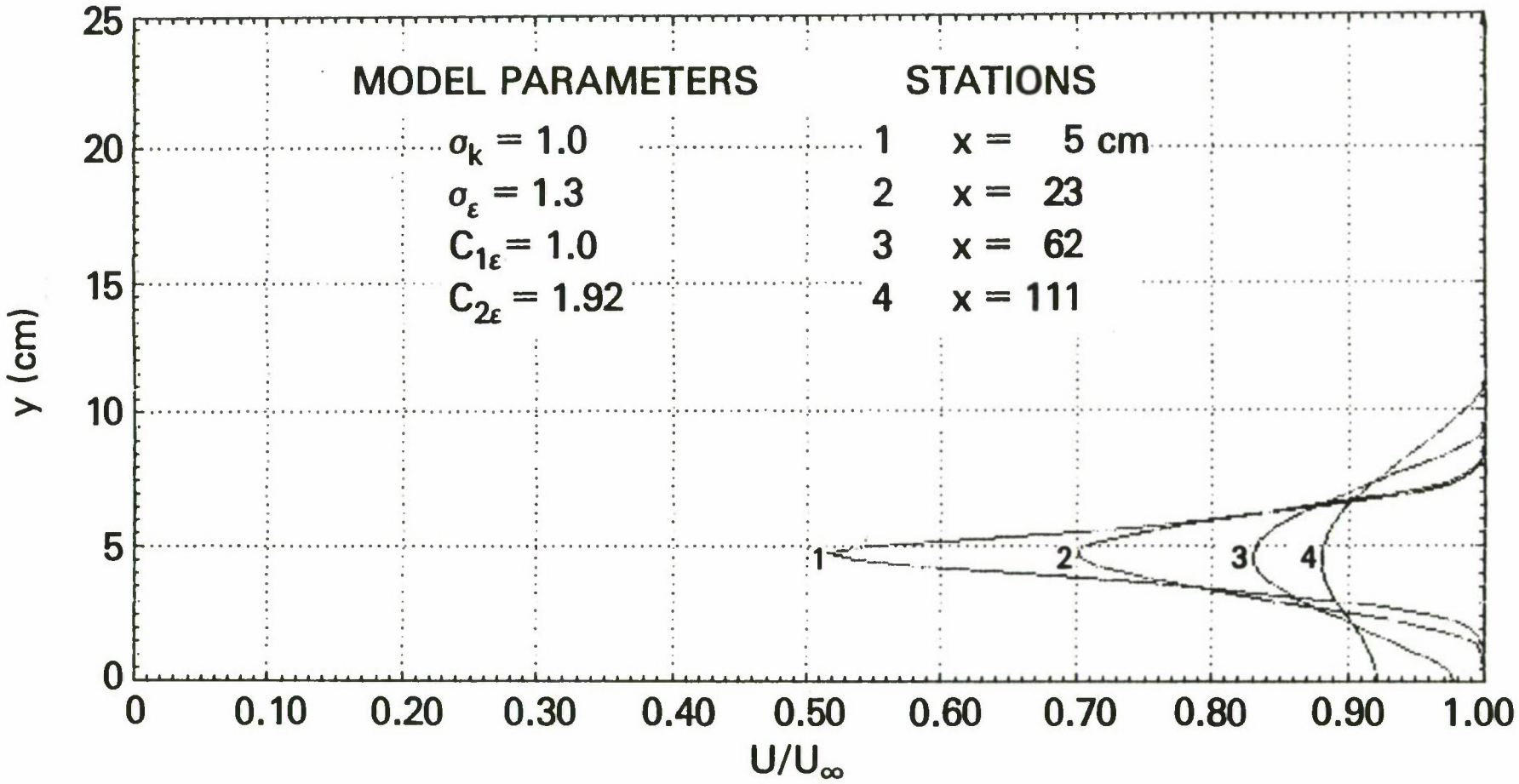

Figure 28 Velocity profiles for finite fluid with $C_{1\varepsilon}$ = 1.0 $C_{2\varepsilon}$ = 1.92 and symmetric free surface boundary conditions.

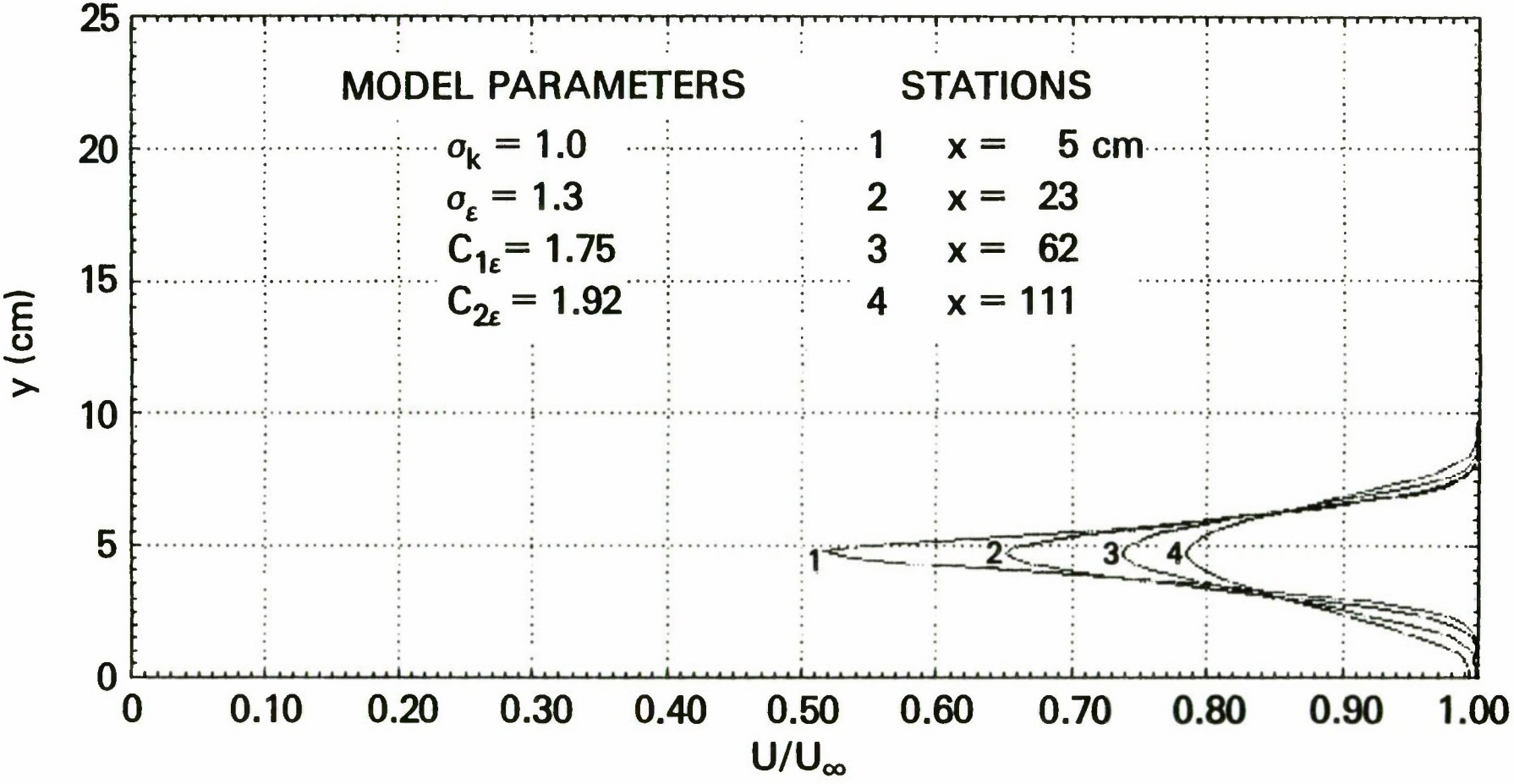

Figure 29 Velocity profiles for finite fluid with $C_{1\varepsilon}$ = 1.75 $C_{2\varepsilon}$ = 1.92 and symmetric free surface boundary conditions.

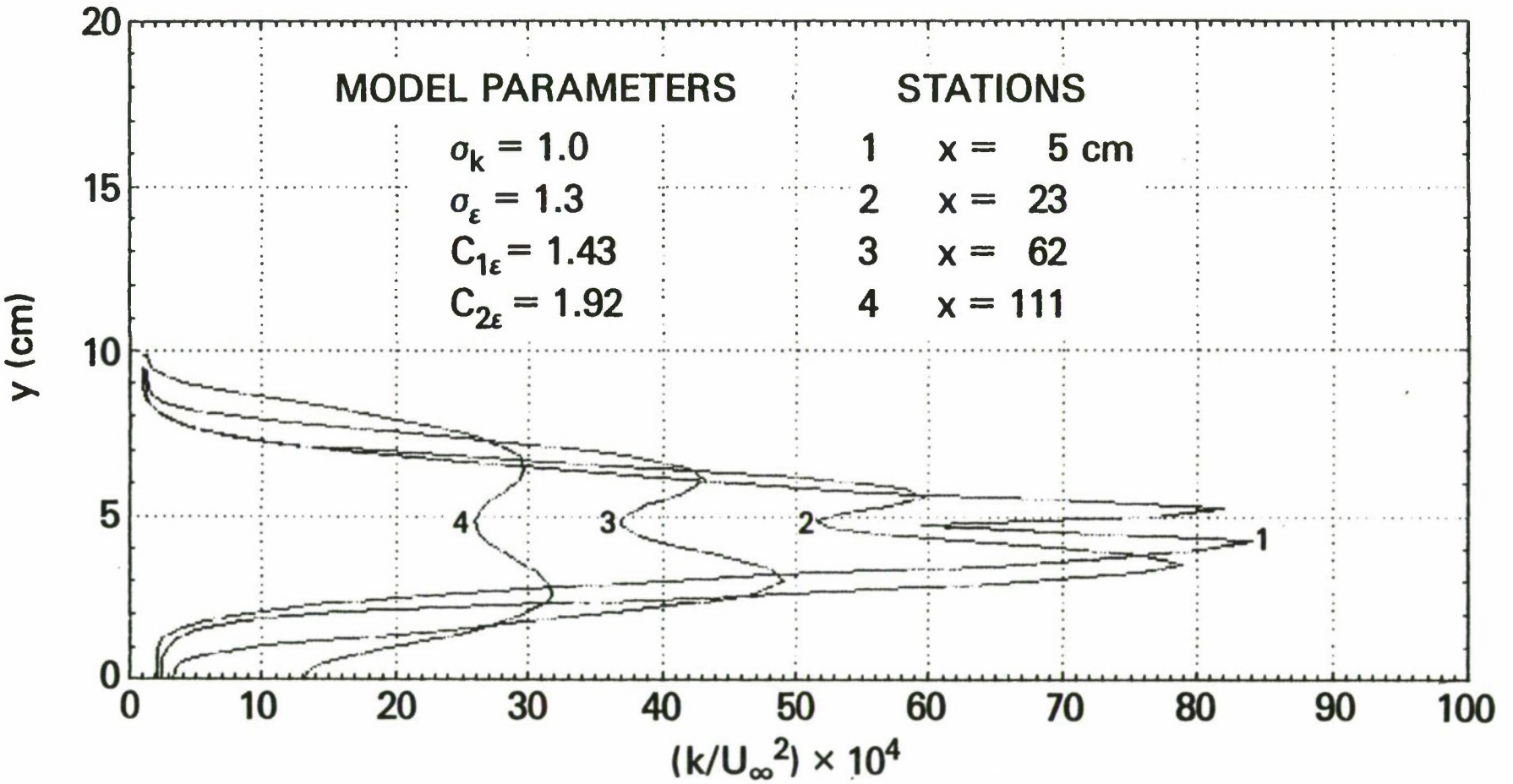

Figure 30 Turbulence kinetic energy profiles for finite fluid with reference parameters and symmetric free surface boundary conditions.

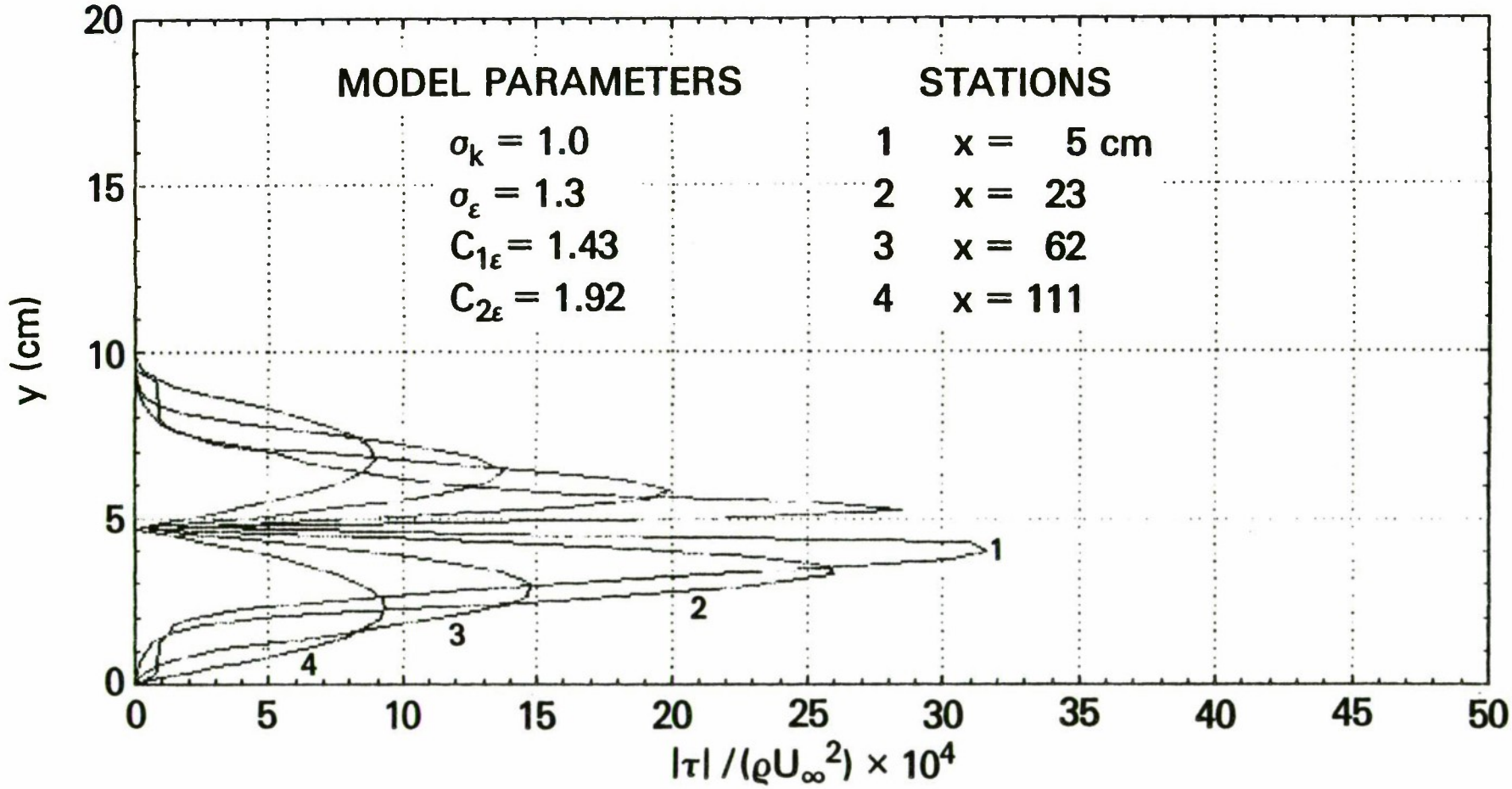

Figure 31 Turbulent shear stress profiles for finite fluid with reference parameters and symmetric free surface boundary conditions.

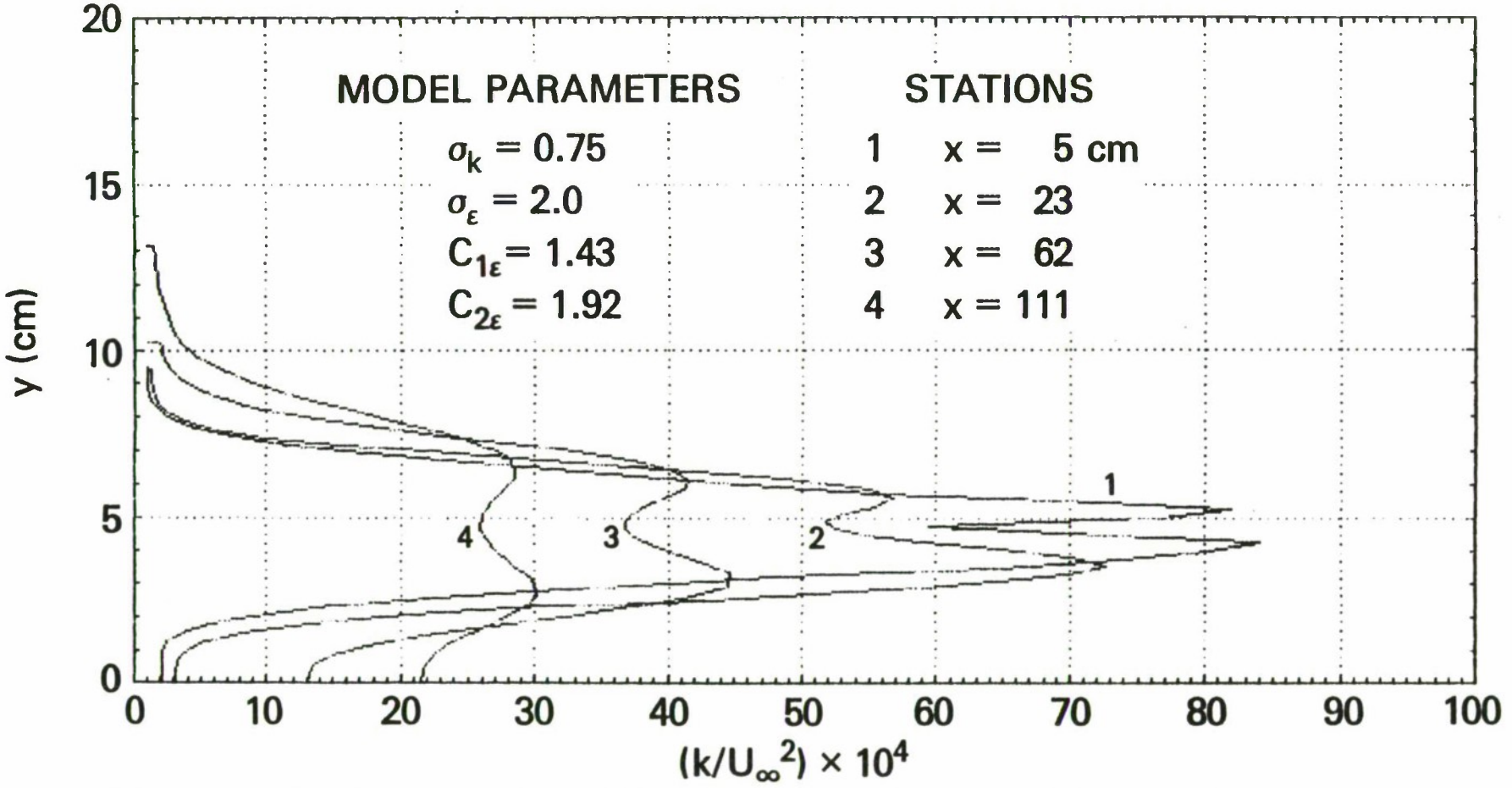

Figure 32 Turbulence kinetic energy profiles for finite fluid with $\sigma_k = .75$ $\sigma_\varepsilon = 2.0$ and symmetric free surface boundary conditions.

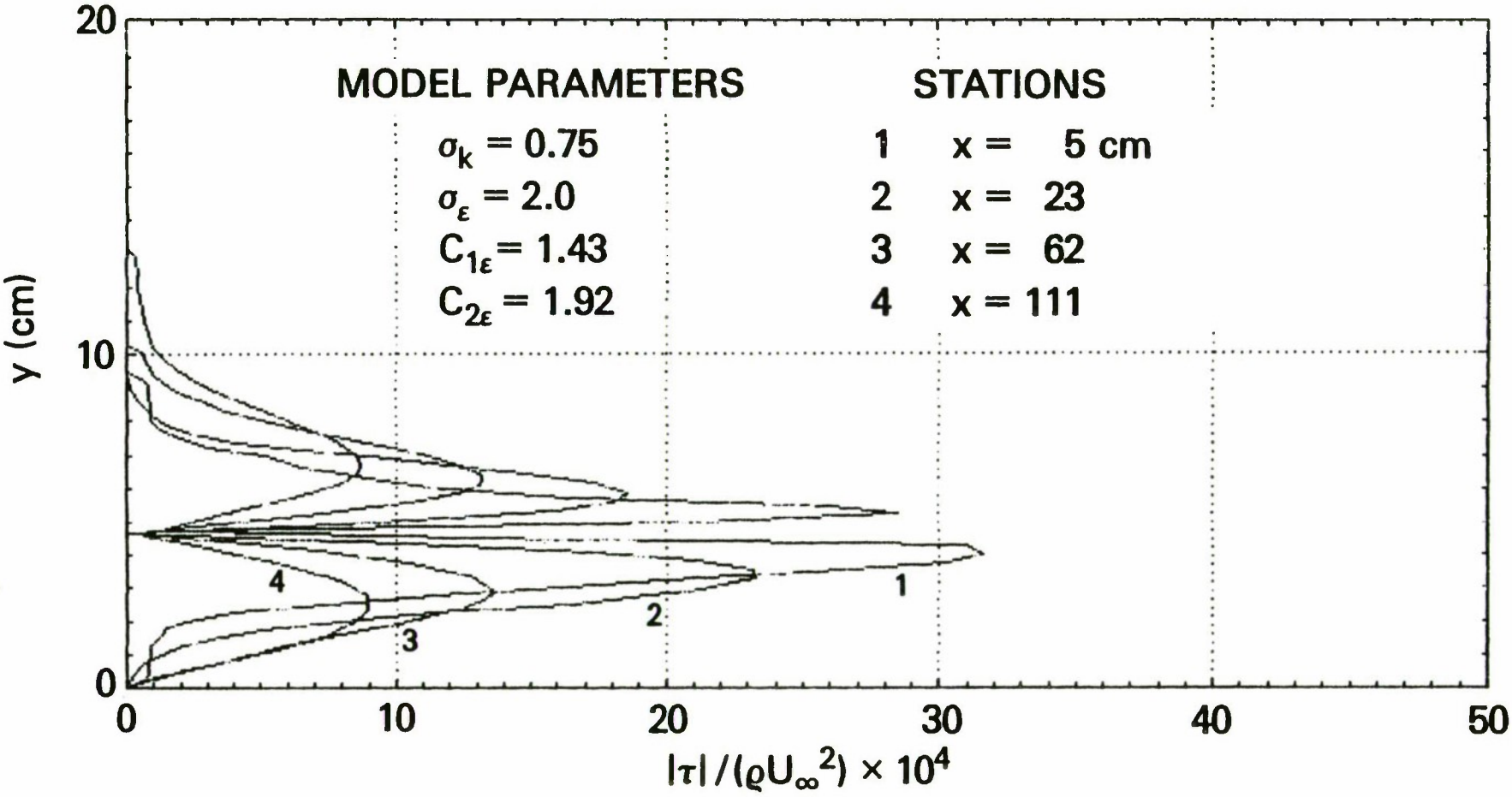

Figure 33 Turbulent shear stress profiles for finite fluid with $\sigma_k = .75$ $\sigma_\varepsilon = 2.0$ and symmetric free surface boundary conditions.

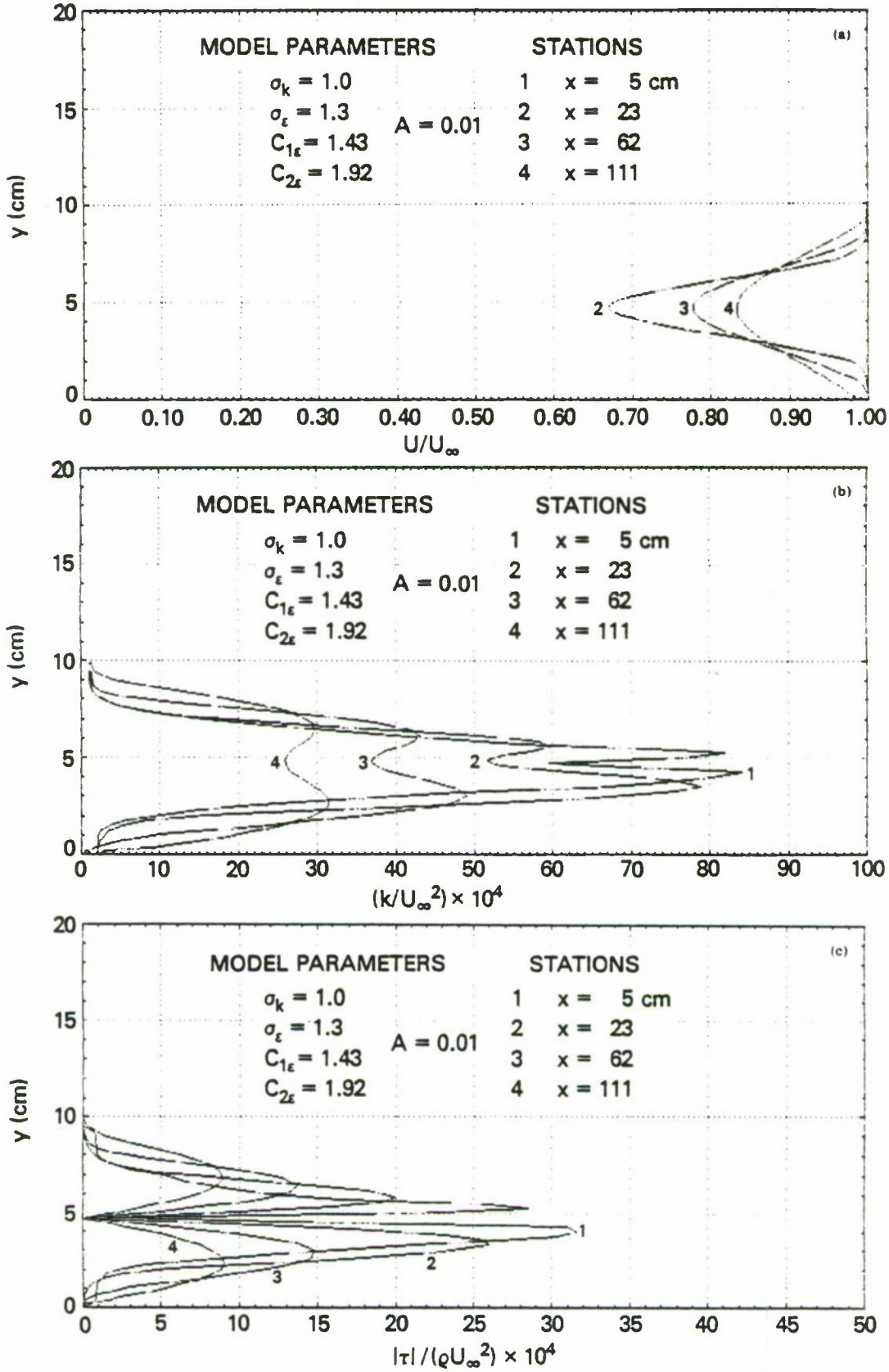

Figure 34 Finite fluid profiles for A = .01 (non symmetric boundary condition for ε) with reference parameters

a - velocity

b - turbulence kinetic energy

c - turbulent shear stress.

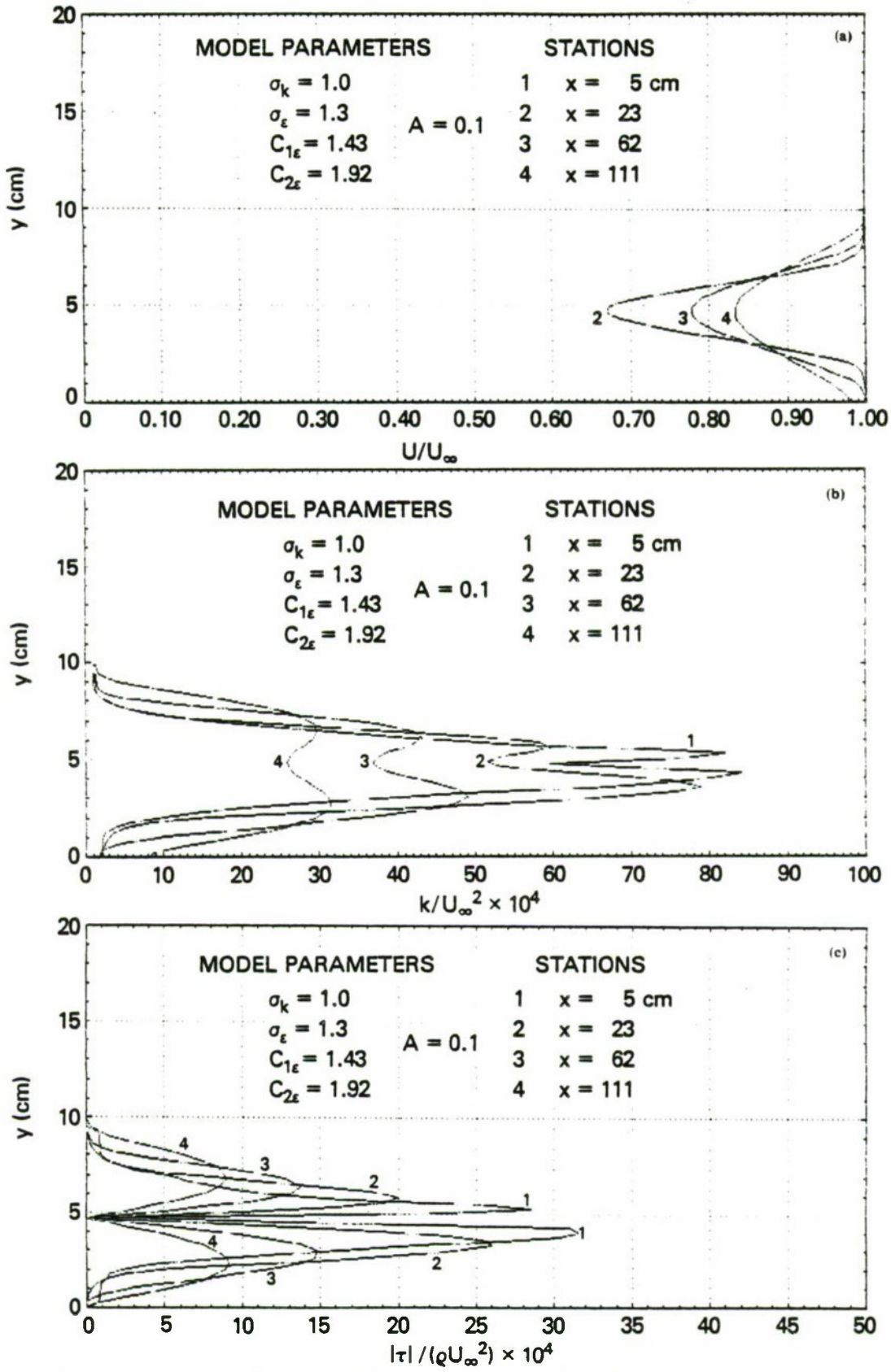

Figure 35 Finite fluid profiles for A = 0.1 (non symmetric boundary condition for ε) with reference parameters

a - velocity

b - turbulence kinetic energy

c - turbulent shear stress.

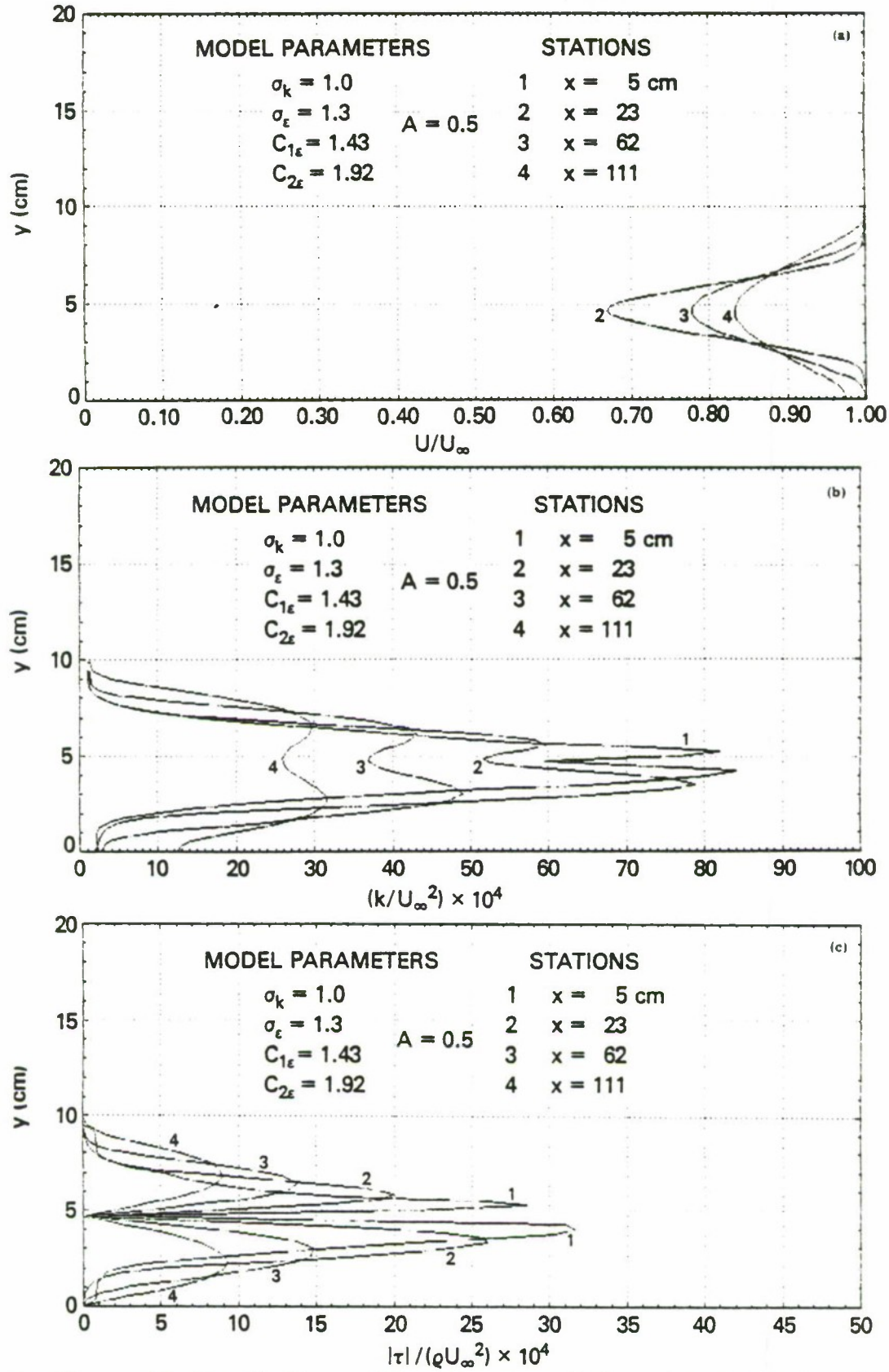

Figure 36 Finite fluid profiles for A = .5 (non symmetric boundary condition for ε) with reference parameters

a - velocity

b - turbulence kinetic energy

c - turbulent shear stress

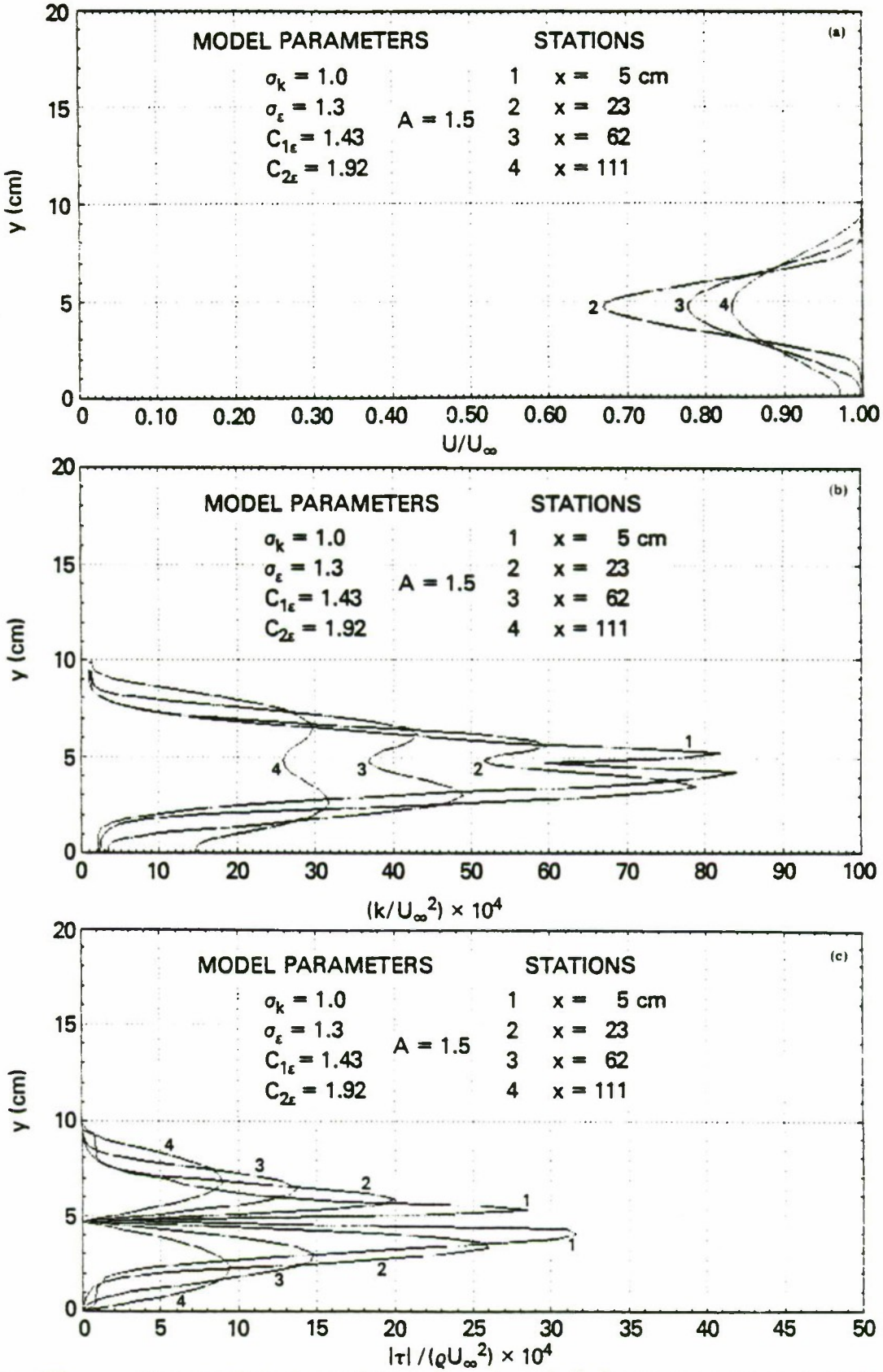

Figure 37 Finite fluid profiles for A = 1.5 (non symmetric boundary condition for ε) with reference parameters

a - velocity

b - turbulence kinetic energy

c - turbulent shear stress.

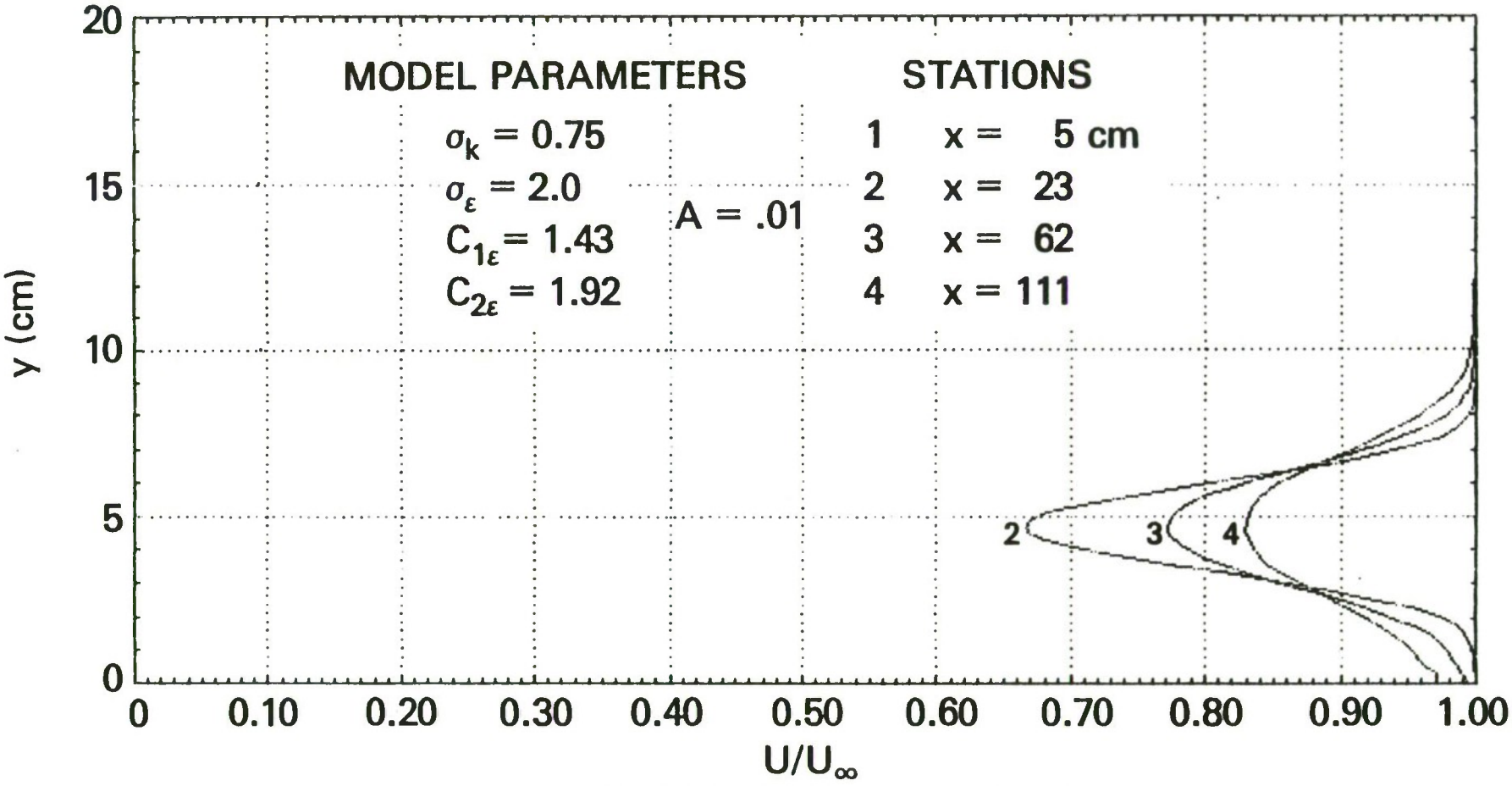

Figure 38 Finite fluid velocity profiles for
A = .01 σ_k = .75 σ_ε = 2.0

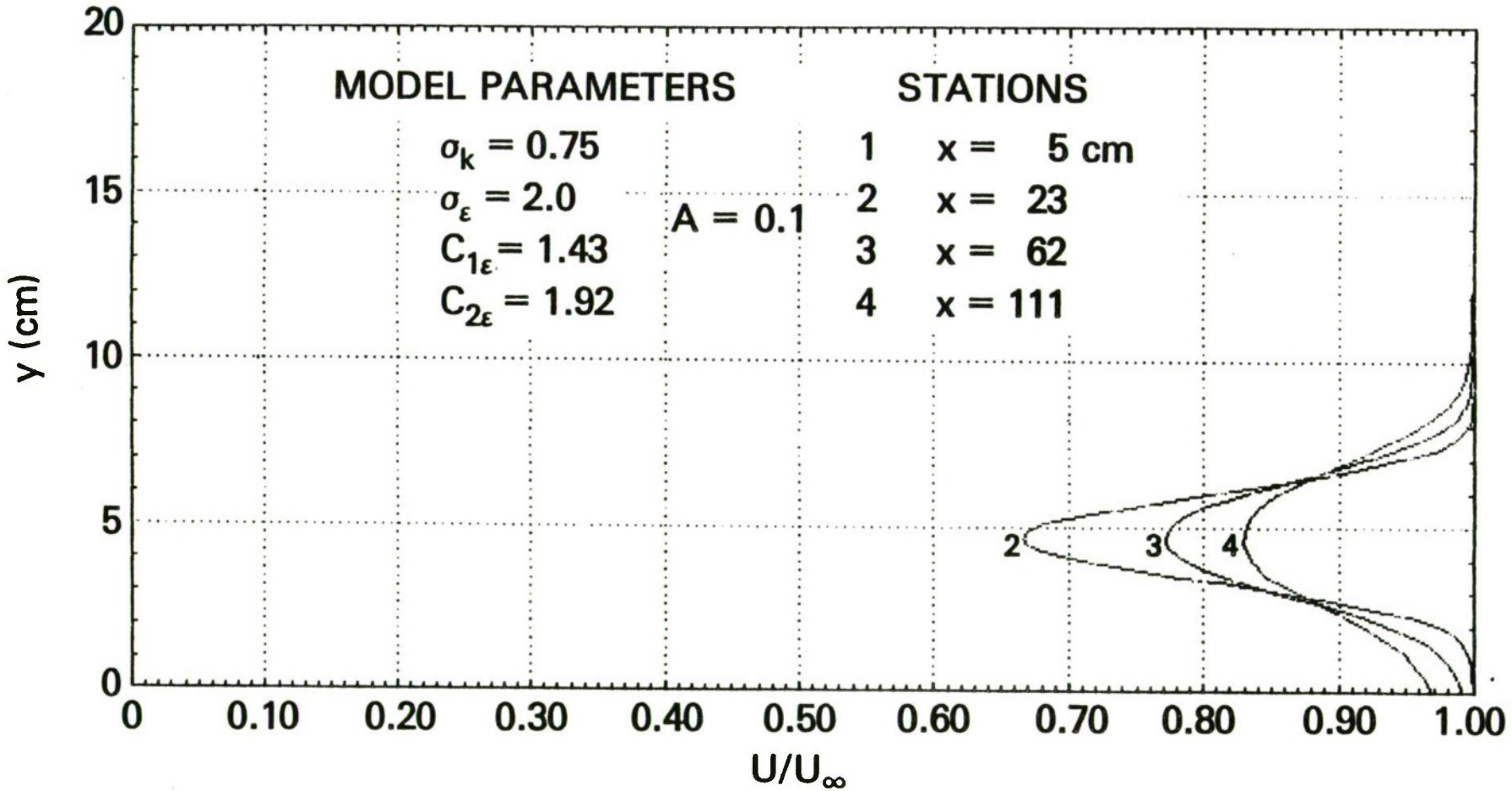

Figure 39 Finite fluid velocity profiles for A = 0.1 σ_k = .75 σ_ε = 2.0

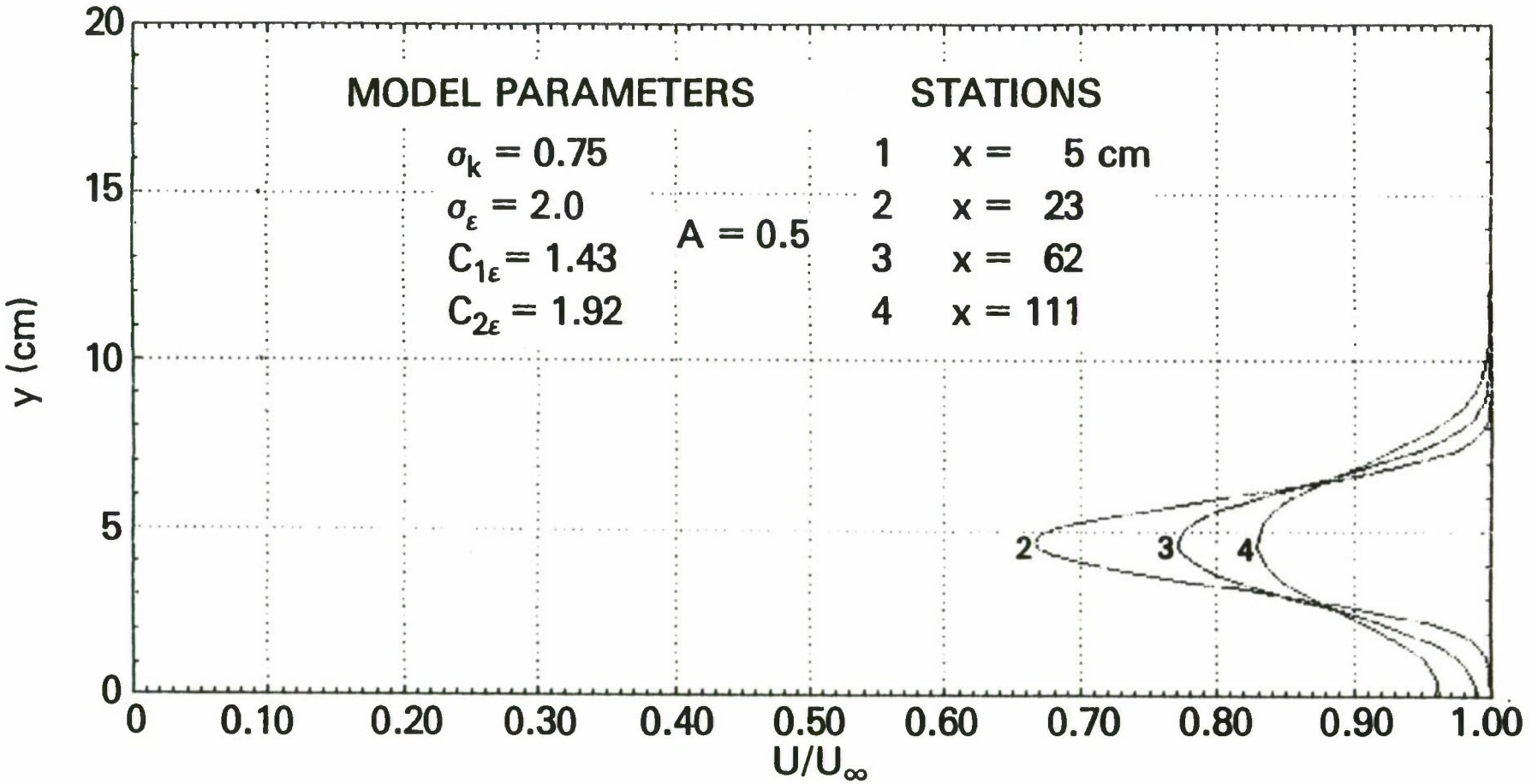

Figure 40 Finite fluid velocity profiles for
A = .5 σ_k = .75 σ_ε = 2.0

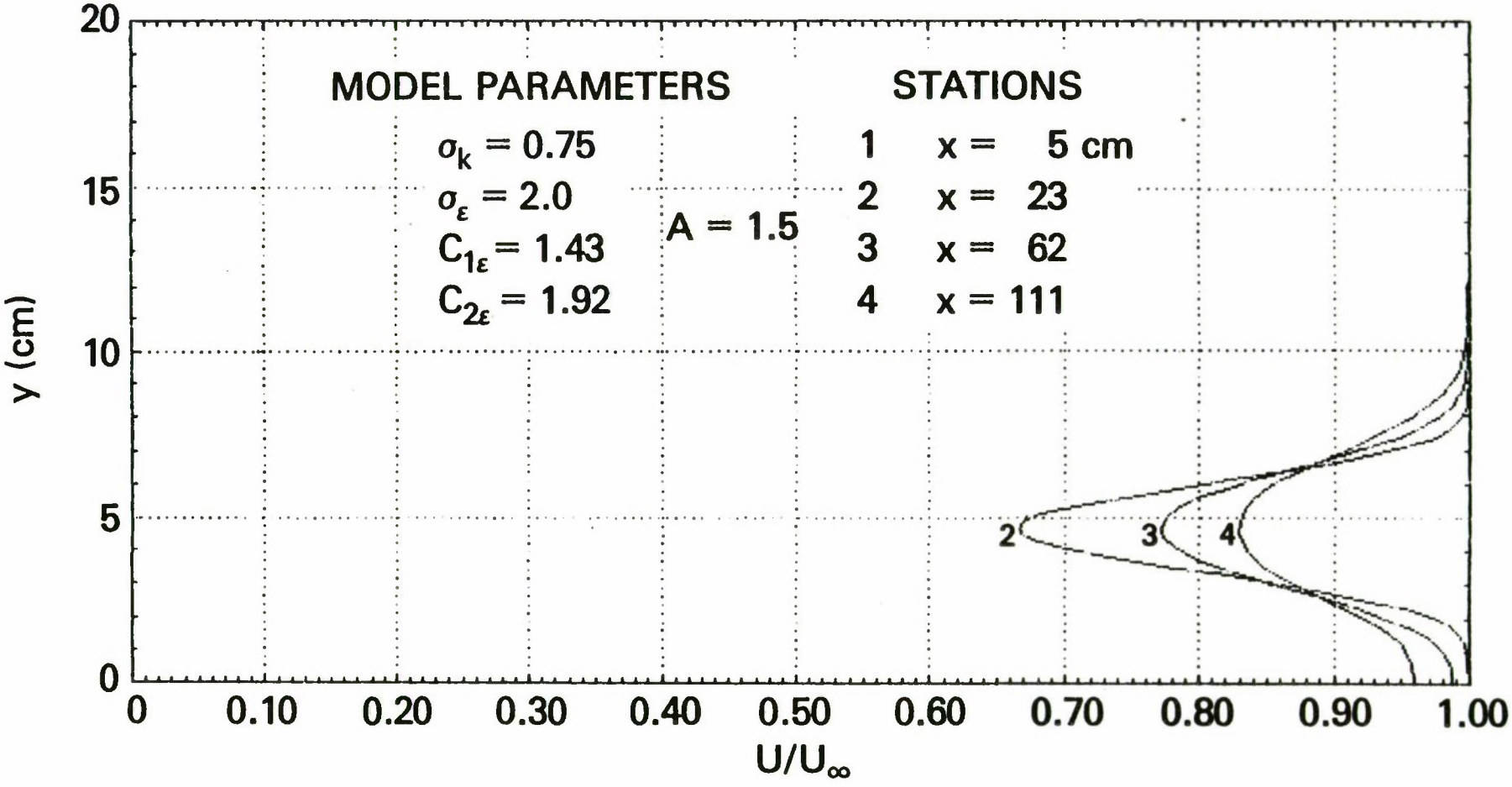

Figure 41 Finite fluid velocity profiles for
A = 1.5 σ_k = .75 σ_ε = 2.0

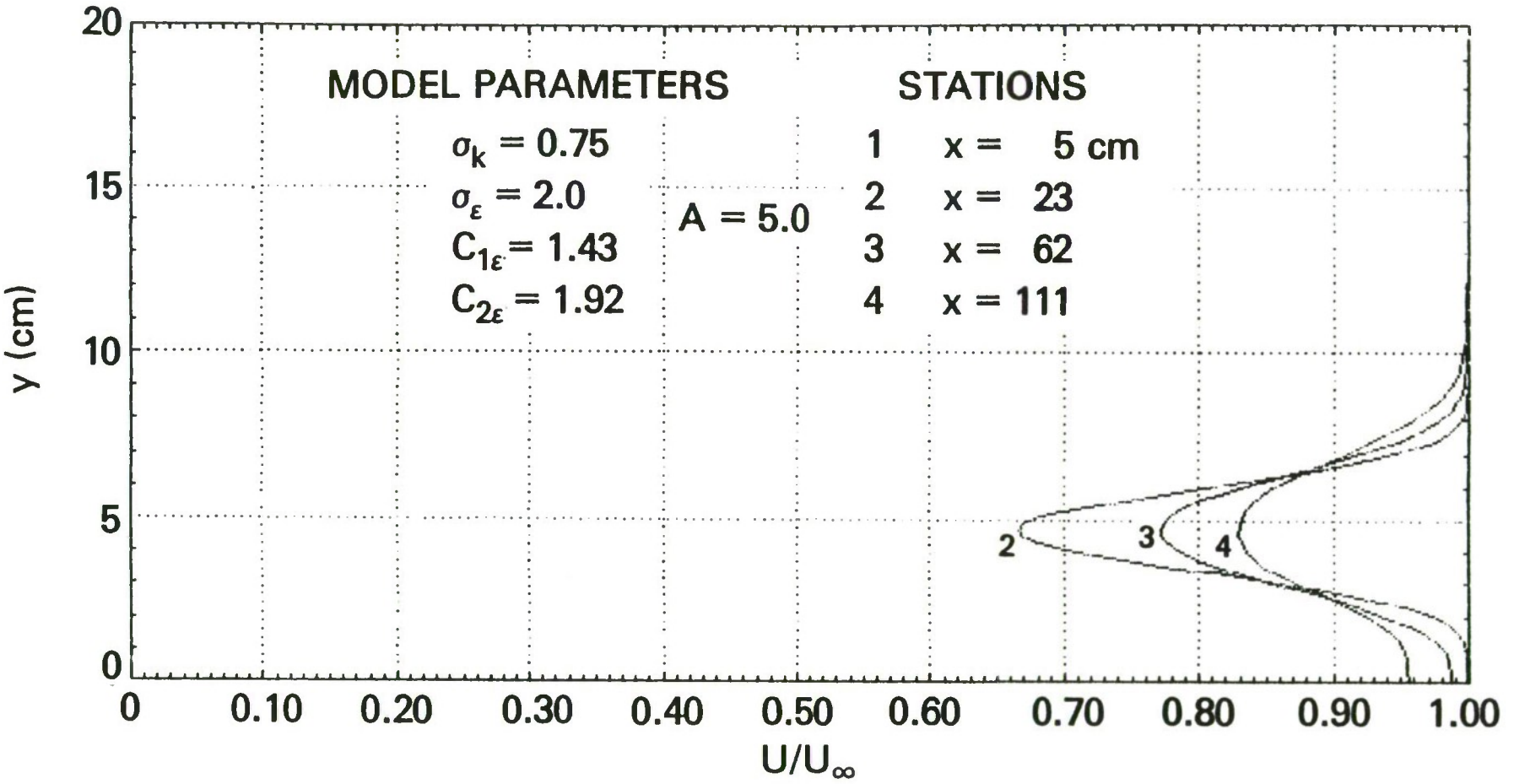

Figure 42 Finite fluid velocity rpfiles for
A = 5.0 σ_k = .75 σ_ε = 2.0

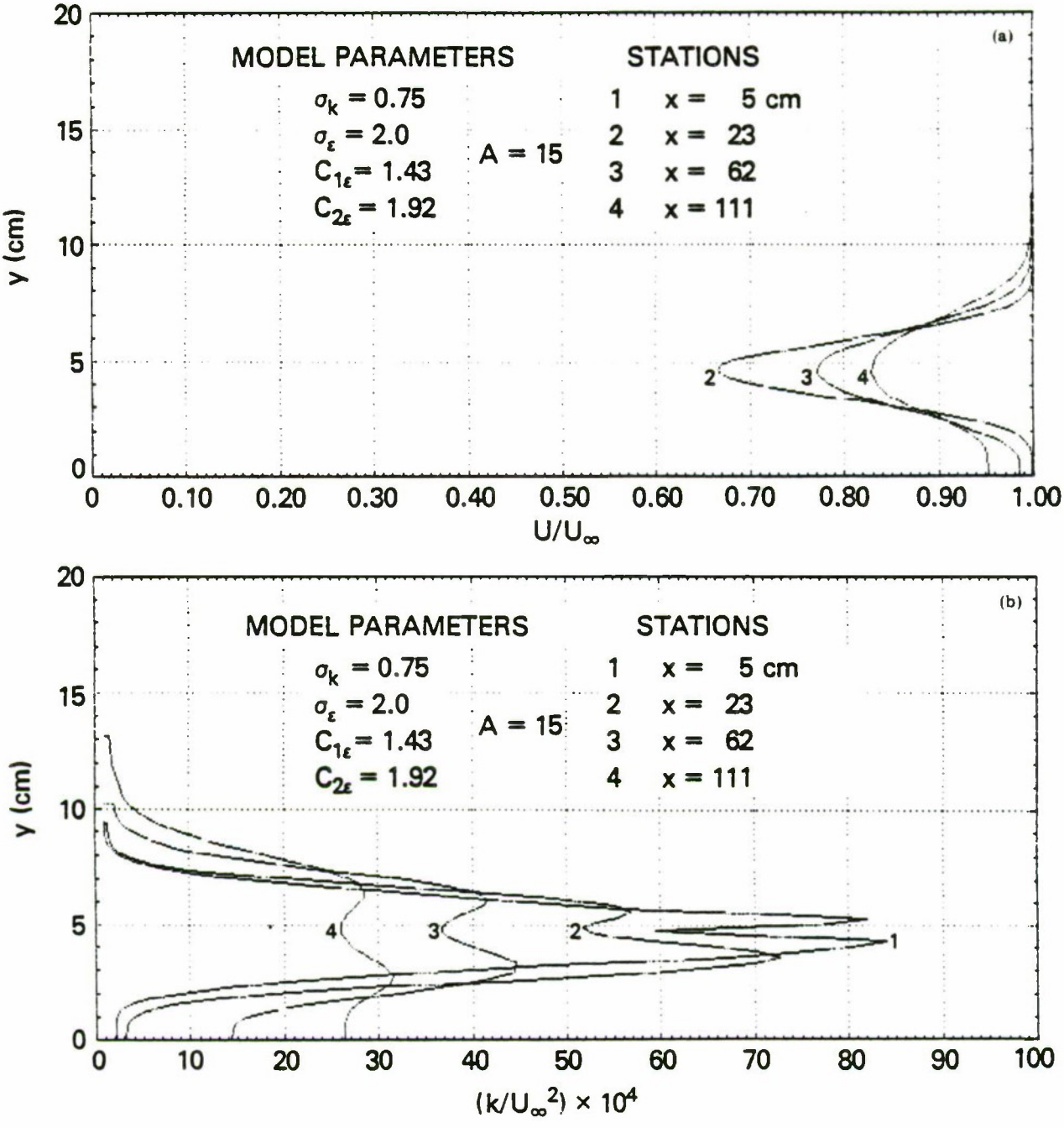

Figure 43 Finite fluid profiles for

A = 15 σ_k = .75 σ_ε = 2.0

a - velocity

b - turbulence kinetic energy

APPENDIX A. Modeling of the Reynolds Stress Equation

Before we proceed with the generation of an algebraic stress model from the Reynolds stress equation certain terms in that equation need to be modeled. Rewriting equation (2.6) in symbolic form with the viscous diffusion term neglected as indicated earlier we have

$$\frac{\partial \overline{u_i u_j}}{\partial t} + \bar{U}_k \frac{\partial \overline{u_i u_j}}{\partial x_k} = -\frac{\partial}{\partial x_k}\left(\overline{u_i u_j u_k}\right) - \frac{1}{\rho}\left(\frac{\partial \overline{u_j p}}{\partial x_i} + \frac{\partial \overline{u_i p}}{\partial x_j}\right)$$

$$+ P_{ij} + \pi_{ij} - \varepsilon_{ij} \qquad \text{(A.1)}$$

where the stress production term P_{ij} is given by

$$P_{ij} = -\overline{u_i u_k}\,\frac{\partial \bar{U}_j}{\partial x_k} - \overline{u_j u_k}\,\frac{\partial \bar{U}_i}{\partial x_k}\,.$$

The pressure strain is given by π_{ij} as

$$\pi_{ij} = \overline{\frac{p}{\rho}\left(\frac{\partial u_i}{\partial x_j} + \frac{\partial u_j}{\partial x_i}\right)}$$

and ε_{ij} is the viscous dissipation term

$$\varepsilon_{ij} = 2\nu\,\overline{\frac{\partial u_i}{\partial x_k}\,\frac{\partial u_j}{\partial x_k}}.$$

Of these three terms, P_{ij} is exact while π_{ij} and ε_{ij} must be modeled. The dissipation ε_{ij} occurs on the smallest scale of turbulence so that at the

large Reynolds numbers anticipated the turbulence is expected to be isotropic (11). Therefore ε_{ij} is usually modeled as

$$\varepsilon_{ij} = \frac{2}{3} \varepsilon \delta_{ij}. \tag{A.2}$$

The pressure strain term π_{ij} has been shown by Rotta (17) and Lumley (12) to contribute to two processes one involving only fluctuating velocities and the other involving the interaction of fluctuating velocities with the mean strain. These are denoted by $\pi_{ij,1}$ and $\pi_{ij,2}$ respectively. Following Rotta (17) $\pi_{ij,1}$ is usually taken to be proportional to the local anisotropy of the turbulence. That is

$$\pi_{ij,1} = - C_1 \frac{\varepsilon}{k} \left(\overline{u_i u_j} - \frac{2}{3} k \delta_{ij} \right) \tag{A.3}$$

For $\pi_{ij,2}$ we take the model of Launder, Reece, and Rodi (18)

$$\begin{aligned} \pi_{ij,2} = & - \alpha \left(P_{ij} - \frac{2}{3} P \delta_{ij} \right) \\ & - \gamma \left(\frac{\partial U_i}{\partial x_j} + \frac{\partial U_j}{\partial x_i} \right) k \\ & - \beta \left(D_{ij} - \frac{2}{3} P \delta_{ij} \right) \end{aligned} \tag{A.4}$$

where $D_{ij} \equiv - \left(\overline{u_i u_k} \frac{\partial U_k}{\partial x_j} + \overline{u_j u_k} \frac{\partial U_k}{\partial x_i} \right)$ and $P \equiv \frac{1}{2} P_{ii}$.

Launder, et al (18) further found that in general the first term above is dominant and therefore recommended

$$\pi_{ij,2} = -\alpha \left(P_{ij} - \frac{2}{3} P\delta_{ij}\right) \tag{A.5}$$

which relates $\pi_{ij,2}$ to the anisotropy of the turbulence production P_{ij}. Further, they introduced wall proximity effects into the pressure-strain model by taking the model coefficients to be functions of distance from the walls. Daly and Harlow (19) and Shir (8) introduced an additional proximity term, $\pi_{ij,s}$ to the pressure strain, π_{ij}. Following Shir (8) we take

$$\pi_{ij,s} = C_1' \frac{\varepsilon}{k} \left(\overline{u_k u_\ell}\, n_k n_\ell\, \delta_{ij} - \frac{3}{2}\, \overline{u_k u_i}\, n_k n_j - \frac{3}{2}\, \overline{u_k u_j}\, n_k n_i\right) f \tag{A.6}$$

where f is a surface damping function which decays with increasing distance from the surface and n_k is a unit normal to the surface. The effect of $\pi_{ij,s}$ is seen to reduce the normal fluctuations relative to those transverse while conserving turbulent kinetic energy. Conservation of k is guaranteed since the trace of $\pi_{ij,s}$ vanishes. Therefore in the vicinity of the surface $\pi_{ij,s}$ retards the normal turbulent fluctuations and distributes them adiabatically among the transverse fluctuations. This represents the free surface damping effect eluded to earlier which has been observed experimentally in the vicinity of a free surface. Therefore, $\pi_{ij,s}$ has

recently been employed to model free surface proximity by Naot and Rodi (6) and Celik, Hossain, and Rodi (9) in applications to open channel flows.

We will not describe models for the other terms of the Reynolds stress equation as they will not be needed in the remainder of the work to follow. Having incorporated the major physics associated with near free surface flows in the modeling of the pressure strain term we now generate the desired algebraic stress model.

APPENDIX B. The Algebraic Stress Model

If we examine the Reynolds stress equation (2.6) we note that derivatives of the dependent variables appear in the time rate of change, convective and diffusion terms. If these terms could be expressed as algebraic forms of the dependent variable $\overline{u_i u_j}$ and lower order correlations, the differential equations would become algebraic and therefore the local behavior of the Reynolds stress could be approximately determined without the computational load of propagating a modeled differential equation. Various procedures have been utilized to generate algebraic stress models. Of these the most general one is due to Rodi (20). Rodi assumes that the sum of the transport terms (rate of change, convection and diffusion) for $\overline{u_i u_j}$ is proportional to that for the turbulent kinetic energy, k. We note that the sum of the transport terms for k is given from equation (2.9) as $P-\epsilon$. Therefore we have from equation (A.1) with the inclusion of the surface proximity term, $\pi_{ij,s}$ from equation (A.6)

$$P_{ij} + \pi_{ij} + \pi_{ij,s} - \epsilon_{ij} = \frac{\overline{u_i u_j}}{k}\left(P-\epsilon\right) \tag{B.1}$$

where the proportionality factor has been taken to be $\overline{u_i u_j}/k$. This equation is seen to yield an identity if we take its trace and Rodi (21) suggests that it represents a good approximation when the variation of $\overline{u_i u_j}/k$ is small compared to the variation of $\overline{u_i u_j}$. Equation (B.1) provides the desired algebraic stress model after substitution of the modeled forms of π_{ij}, $\pi_{ij,s}$ and ε_{ij} from equations (A.3), (A.4) or (A.5), (A.2) and (A.6).

Before we proceed with these substitutions a few comments are in order with respect to the general algebraic stress equation above. For flows that evolve very slowly it is often justifiable to neglect the time rate of change and transport of $\overline{u_i u_j}$. This then is equivalent to setting $P = \varepsilon$ in equation (B.1). Sometimes this is done for the off-diagonal stress components only with the normal components evaluated with the full algebraic equation $P \neq \varepsilon$ (9) because of their close relationship to k.

When convection and diffusion are neglected completely, corresponding to $P=\varepsilon$ in equation (B.1), and after substitution of the modeled terms for π_{ij}, $\pi_{ij,s}$ and ε_{ij} from equations (A.2), (A.4) and (A.6), the following equation results

$$(1-\alpha)\, P_{ij} - \beta\, D_{ij} - \gamma\, k \left(\frac{\partial U_i}{\partial x_j} + \frac{\partial U_j}{\partial x_i}\right) + \frac{2}{3} P\, (\alpha + \beta)\, \delta_{ij}$$

$$- \frac{\varepsilon}{k} \left[C_1 \left(\overline{u_i u_j}\right) + \frac{2}{3} \left(1 - C_1\right) \delta_{ij} k\right] \qquad \text{(B.2)}$$

$$+ C_1' \frac{\varepsilon}{k} \left(\overline{u_n^2}\, \delta_{ij} - \frac{3}{2}\, \overline{u_n u_i}\, \delta_{nj} - \frac{3}{2}\, \overline{u_n u_j}\, \delta_{ni}\right) f = 0$$

where as defined previously,

$$D_{ij} = -\left(\overline{u_i u_k}\,\frac{\partial \bar{U}_k}{\partial x_j} + \overline{u_j u_k}\,\frac{\partial \bar{U}_k}{\partial x_i}\right)$$

The last term of equation (B.2) is recognized as Shir's (8) model applied to the free-surface proximity. The variable u_n in that term represents the fluctuating velocity component normal to the free surface.

The algebraic stress relation given above has been developed for a general turbulent flow field in the vicinity of a free surface. Further simplifications can be made if we introduce some of the specialized features of the wake application to be pursued here. First, we anticipate the flow field to be predominantly in the x direction, so that the velocity components in the y and z direction are expected to be much smaller and in fact of secondary nature (unidirectional flow). In addition, with respect to a ship-fixed coordinate system, the basic flow is expected to be steady. Then the asymptotic analysis of Skop (1) shows for large Reynolds number that diffusion in the x direction will be negligible compared to that in the y and z directions. That is to say, we anticipate a parabolic flow-field description will be valid. In addition, this characteristic renders the k and ε equations (2.8) and (2.9) parabolic also. This is certainly to be desired so that a marching technique can be applied to generate the solution and no iteration will be required.

If we introduce the assumption of unidirectional flow, $\bar{U}_i = U(y,z)\,\vec{e}_x$ where y is perpendicular to the free surface into the stress relations, we

obtain the following algebraic modeling equations for the various Reynolds stress components (16):

$$\frac{\varepsilon}{k}\left(C_1 + 2C_1' f\right)\overline{v^2} = \frac{2}{3}\left(\alpha - \frac{\beta}{2}\right) P + \frac{2}{3}\left(C_1 - 1\right)\varepsilon$$

$$+ \beta\left[\overline{uv}\,\frac{\partial U}{\partial y} - \overline{uw}\,\frac{\partial U}{\partial z}\right] \qquad (B.3)$$

$$\frac{\varepsilon}{k} C_1 \overline{w^2} = C_1' f \frac{\varepsilon}{k}\overline{v^2} + \frac{2}{3}\left(\alpha - \frac{\beta}{2}\right) P + \frac{2}{3}\left(C_1 - 1\right)\varepsilon$$

$$- \beta\left[\overline{uv}\,\frac{\partial U}{\partial y} - \overline{uw}\,\frac{\partial U}{\partial z}\right] \qquad (B.4)$$

$$\frac{\varepsilon}{k}\left(C_1 + \frac{3}{2} C_1' f\right)\overline{uv} = -\left[(1-\alpha)\left(\overline{v^2} + \overline{vw}\tan\psi\right)\right.$$

$$\left. - \beta\overline{u^2} + \gamma k\right]\frac{\partial U}{\partial y} \qquad (B.5)$$

$$\frac{\varepsilon}{k} C_1 \overline{uw} = -\left[(1-\alpha)\left(\overline{w^2} + \overline{vw}\cot\psi\right) - \beta\overline{u^2} + \gamma k\right]\frac{\partial U}{\partial z} \qquad (B.6)$$

and

$$\frac{\varepsilon}{k}\left(C_1 + \frac{3}{2} C_1' f\right)\overline{vw} = \beta\left(\overline{uv}\,\frac{\partial U}{\partial z} + \overline{uw}\,\frac{\partial U}{\partial y}\right) \qquad (B.7)$$

where $\tan\psi \equiv \left(\frac{\partial U}{\partial z}\right) / \left(\frac{\partial U}{\partial y}\right)$ and therefore $\tan\psi$ characterizes somewhat the dimensionality of the basic flow. That is, for two-dimensional flow

where $\frac{\partial}{\partial z} = 0$, $\tan \psi = 0$. The two-dimensional plane wake which is of interest is considered below.

Naot and Rodi (16) developed an iterative procedure to solve these equations for the stress components for fixed values of the k-ϵ parameters and $\tan \psi$, and they have evaluated the variation of the stress components with the surface proximity $C_1' f$ and the inclination angle ψ. For all inclination angles they demonstrate that these equations provide for the damping of the normal fluctuations and the enhancement of the transverse components as we approach the free surface. Additionally, the Reynolds shear stress component $\overline{uv}$ is shown to be damped as the free surface is approached. For computational purposes, they suggest the following approximations for the turbulent shear stresses accurate to ten percent:

$$- \overline{uv} = C_\mu \frac{k^2}{\varepsilon} \left(\frac{C_1}{C_1 + \frac{3}{2} C_1' f}\right) \left(\frac{C_1}{C_1 + 2C_1' f}\right) \frac{\partial U}{\partial y} \tag{B.8}$$

and

$$- \overline{uw} = C_\mu \frac{k^2}{\varepsilon} \frac{\left(C_1 + \frac{5}{2} C_1' f\right)}{\left(C_1 + 2C_1' f\right)} \frac{\partial U}{\partial z} \tag{B.9}$$

where $C_\mu = 0.09$. These are in the form of eddy viscosity relations with the effective eddy viscosity a function of free surface proximity. Note that at remote locations from the free surface $f \to 0$ and we recover the standard eddy viscosity relations

$$\nu_t = C_\mu \frac{k^2}{\varepsilon}$$

for both stress components. As we approach the free surface, f increases and the effective eddy viscosity decreases. Different eddy viscosities are predicted for the vertical and transverse transport of momentum $\overline{uv}$ and $\overline{uw}$ because of the surface proximity effect.

The two equations (B.8) and (B.9) for $\overline{uv}$ and $\overline{uw}$ are complemented by equations (B.3) (B.4) and (B.7) for $\overline{v^2}$, $\overline{w^2}$ and $\overline{vw}$ to form an algebraic stress model including free surface effects. However, the surface proximity function f still must be defined.

The surface proximity function is taken to be dependent upon (ℓ/y), where ℓ is the local dissipation length scale of the turbulent motion at the point considered and y is the distance of this point from the free surface. Most authors have assumed linear variations of f with ℓ/y, e.g. Launder (22), Gibson and Launder (23) and Celik et al (9), in applications to both wall proximity and free-surface proximity for open-channel flows. Naot and Rodi (6) have taken quadratic variations for $f(\ell/y)$. A general form for f can therefore be written as

$$f = \frac{1}{\left(\frac{y}{\ell} + C_f\right)^n}, \tag{B.10}$$

where n = 1,2 depending upon whether a linear or quadratic dependence is to be utilized and C_f is a constant which is to be specified.

In the open-channel applications, free-surface proximity effects have been included in addition to simultaneous wall proximity effects. In our present application to the far wake problem, the walls which may have been responsible for generating the wake are so remote from the region of

interest that they need not be included. Our application therefore considers the free surface proximity only. Once a choice has been made for n in equation (B.10), the surface proximity effect is characterized by two constants C_1' and C_f.

1. Two-Dimensional Flow

The algebraic stress model equations given above have been developed for uni-directional three-dimensional flow. For a two-dimensional, uni-directional flow such as the NRL flat plate experiments (25), the equations are simplified as are the computational demands to generate turbulent flow field predictions. The geometry is illustrated in Fig. 1.

For two-dimensional planar flow we can neglect all variations in the z direction. That is, $\frac{\partial}{\partial z} = 0$ and also the Reynolds shear stress components $\overline{uw}$ and $\overline{vw}$ are zero. We must, however, include the normal stress component $\overline{w^2}$ since this will not be zero. The required algebraic stress relations therefore become

$$\frac{\varepsilon}{k}\left(C_1 + 2C_1' f\right)\overline{v^2} = \frac{2}{3}\left(\alpha - \frac{\beta}{2}\right) P + \frac{2}{3}\left(C_1 - 1\right)\varepsilon + \beta\,\overline{uv}\,\frac{\partial U}{\partial y}, \tag{B.11}$$

$$\frac{\varepsilon}{k} C_1 \overline{w^2} = C_1' f \frac{\varepsilon}{k}\overline{v^2} + \frac{2}{3}\left(\alpha - \frac{\beta}{2}\right) P + \frac{2}{3}\left(C_1 - 1\right)\varepsilon - \beta\left[\overline{uv}\,\frac{\partial U}{\partial y}\right], \tag{B.12}$$

and

$$\frac{\varepsilon}{k}\left(C_1+\frac{3}{2}C_1'f\right)\overline{uv} = -\left[(1-\alpha)\left(\overline{v^2}\right) - \beta\overline{u^2} + \gamma k\right]\frac{\partial U}{\partial y}\,. \tag{B.13}$$

We recognize that the last terms in equations (B.11) and (B.12) are proportional to the turbulence production P for two-dimensional unidirectional flow,

$$P = \overline{uv}\ \frac{\partial U}{\partial y}. \tag{B.14}$$

Substituting (B.14) into (B.11) and (B.12) and making the local equilibrium assumption $P = \varepsilon$ and $2k = \overline{u^2} + \overline{v^2} + \overline{w^2}$, the following solution is obtained:

$$\overline{uv} = -\frac{k^2}{\varepsilon}\frac{2}{3}\left(\frac{1}{C_1+\frac{3}{2}C_1'f}\right)\left\{\frac{(1-\alpha+\beta)(\alpha-2\beta+C_1-1)}{(C_1+2C_1'f)}\right.$$

$$+\frac{\beta}{C_1}\left[\frac{C_1'f}{C_1+2C_1'f}(\alpha-2\beta+C_1-1)+\alpha+\beta+C_1-1\right]$$

$$\left.-(3\beta+\gamma)\right\}\frac{\partial U}{\partial y}\,, \tag{B.15}$$

$$\frac{\overline{v^2}}{k} = \frac{2}{3}\frac{1}{C_1+2C_1'f}\ [\alpha-2\beta+C_1-1]\,, \tag{B.16}$$

and

$$\frac{\overline{w^2}}{k} = \frac{2}{3C_1}\left\{\frac{C_1'f}{C_1+2C_1'f}\left[\alpha-2\beta+C_1-1\right] + \alpha+\beta+C_1-1\right\} . \tag{B.17}$$

For the case $\beta = \gamma = 0$ often employed in these models as a consequence of utilizing the dominant behavior for $\pi_{ij,2}$ given in equation (3.5), these results simplify further to yield

$$\overline{uv} = -\frac{k^2}{\varepsilon}\frac{2}{3}\frac{1}{C_1+\frac{3}{2}C_1'f}\frac{(1-\alpha)(\alpha+C_1-1)}{(C_1+2C_1'f)}\frac{\partial U}{\partial y} \tag{B.18}$$

$$\frac{\overline{v^2}}{k} = \frac{2}{3}\frac{1}{C_1+2C_1'f}(\alpha+C_1-1) \tag{B.19}$$

and

$$\frac{\overline{w^2}}{k} = \frac{2}{3C_1}(\alpha+C_1-1)\left\{\frac{C_1'f}{C_1+2C_1'f}+1\right\} \tag{B.20}$$

Equation (B.18) is seen to be very similar to the approximation of Naot and Rodi (16) given previously by equation (B.8). It represents an eddy viscosity formulation for the Reynolds shear stress with the surface proximity behaving identically to that of equation (B.8). The surface damping of the normal stress $\overline{v^2}$ and the enhancement of $\overline{w^2}$ is apparent from equations (B.19) and (B.20). We can make a complete connection of Equation (B.18) with Equation (B.8) by defining in (B.18)

$$\frac{2}{3}\,\frac{(1-\alpha)(\alpha+C_1-1)}{C_1^{\,2}} \equiv C_\mu$$

This yields

$$\overline{uv} = -C_\mu \frac{k^2}{\varepsilon}\left(\frac{C_1}{C_1+2C_1'f}\right)\left(\frac{C_1}{C_1+\frac{3}{2}C_1'f}\right)\frac{\partial U}{\partial y}. \qquad (B.21)$$

Note that in Equation (B.21) in the limit $f \to 0$ we recover the standard eddy viscosity formulation. That is, Eq. (B.21) behaves as a standard eddy viscosity in the absence of surface proximity effects. The surface proximity effects are seen to reduce the eddy viscosity as the free surface is approached. Equation (B.21) is seen to be sufficient to close the turbulence problem for the two-dimensional case. In its given form, it provides for two additional parameters $\left(\frac{C_1'}{C_1}\right)$ and C_f. C_f is necessary to define the surface proximity function f. Therefore combining this with the k and ε equations (2.8) and (2.9) which were seen to contain five constants, our complete turbulence model including free-surface proximity effects possesses seven constants or adjustable parameters.